Stanford Geothermal Program
Interdisciplinary Research in
Engineering and Earth Sciences
STANFORD UNIVERSITY
Stanford, California

SGP-TR-87

CLOSED CHAMBER WELL TEST ANALYSIS BY SUPERPOSITION OF THE CONSTANT PRESSURE CUMULATIVE INFLUX SOLUTION TO THE RADIAL DIFFUSIVITY EQUATION

By

Jeffrey F. Simmons

February 1985

Financial support was provided through the Stanford Geothermal Program under Department of Energy Contract No. DE-AT03-80SF11459 and by the Department of Petroleum Engineering, Stanford University

1: ABSTRACT

A computer Program was developed to model the closed chamber test. Superposition of the constant pressure cumulative influx solution was utilized to avoid the problems associated with direct solution of the governing partial differential equations.

The model was tested for the ability to generate a slug test response and then used to illustrate the difference between the slug test and closed chamber test.

A sensitivity study was conducted by varying tool and reservoir parameters from a control basecase. Unlike the slug test, initial fluid level, initial chamber gas pressure, and produced fluid gravity greatly influence the closed chamber pressure response. As a result, the slug test dimensionless group t_D / C_D is ineffective in collapsing the closed chamber curves. Assuming ideal chamber gas behavior did to not significantly influence the closed chamber pressure response.

The developed superposition model was used to generate dimensionless type curves for a particular tool and reservoir situation. A log-log plot of p_D versus t_D, analogous to the late time slug test format of Ramey et. al (1975), yields the greatest sensitivity to skin analysis.

CONTENTS

2: INTRODUCTION

2.1 General Description

Closed chamber well testing is common in the petroleum industry today in the guise of backsurge perforation cleaning. In oil producing regions of the world where sand control is required, backsurging is often performed prior to gravel packing of the productive interval as a means of cleaning debris from the perforations. First introduced in the U.S. Gulf Coast, backsurging has proven successful in providing more productive completions.

The backsurge operation utilizes a work string composed of two remote controlled valves, a temporary packer, and a pressure recorder suspended on a tail pipe as shown in Figure 2.1. The assembly is run into the wellbore with the enclosed chamber formed between the valves. Initially the chamber is occupied by air or nitrogen at essentially atmospheric pressure. As the packer is set, the completion fluid overbalance is removed, and the pressure below the packer becomes equal to the static reservoir pressure.

The backsurge is performed by either mechanically or hydraulically, (via annulus pressure), opening the lower valve. At the instant the lower valve is opened the formation is exposed to a minimum pressure equal to the initial chamber pressure plus the hydrostatic pressure of the fluid column between the lower valve and the perforations. The resulting surge of fluid into the wellbore tends to clean any residual perforation debris from the sand face. Upon completion of the backsurge the upper valve is opened, the packer released, and the produced

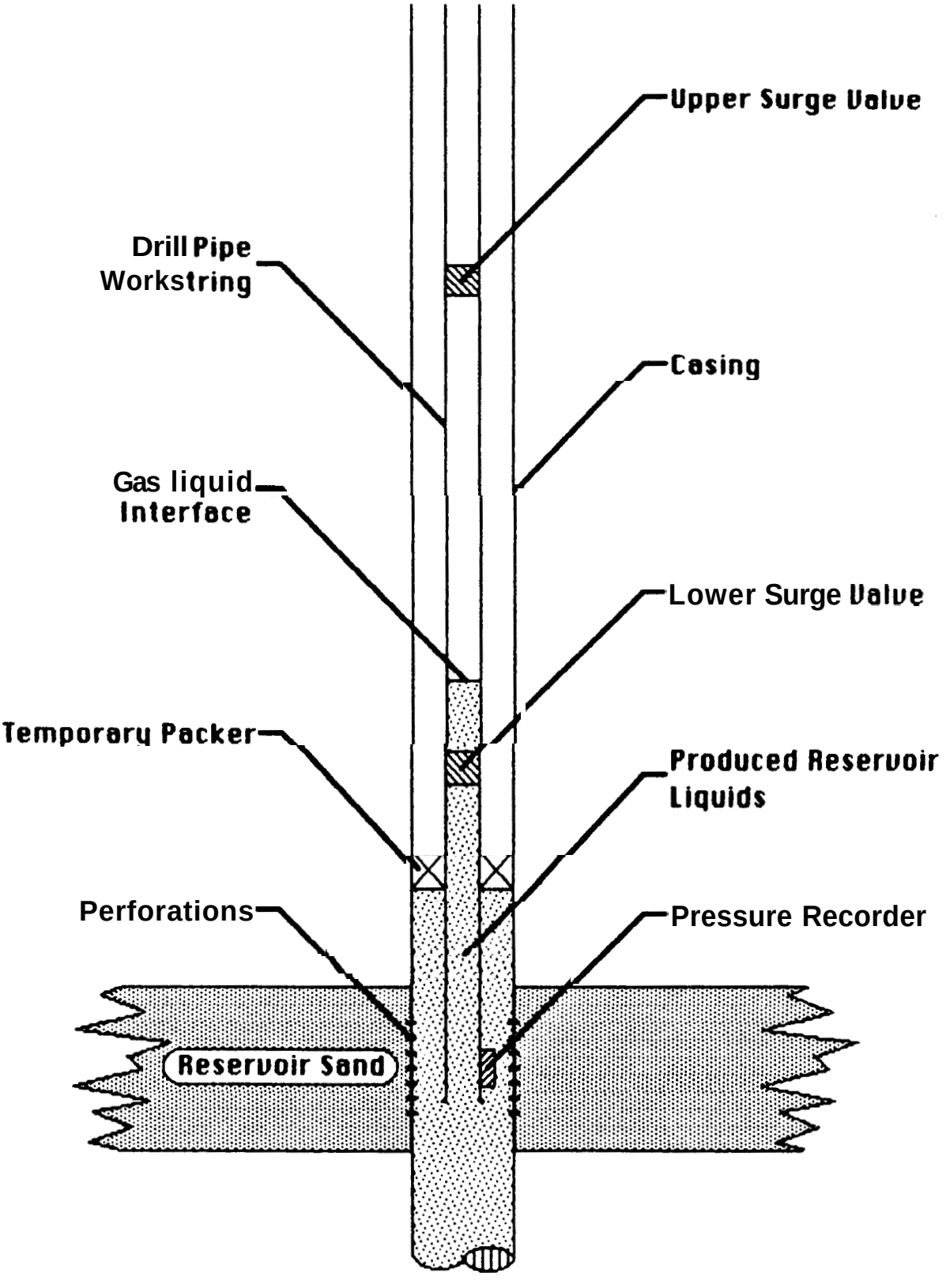

Figure 2.1 Mechanical Sketch of Backsurge Equipment

fluids are reverse circulated out of the wellbore.

The pressure response form the backsurge is commonly recorded with an Amerada Hess type recorder to verify that a successful draw down was achieved. A typical pressure response from a successful backsurge is presented in Figure 2.2.

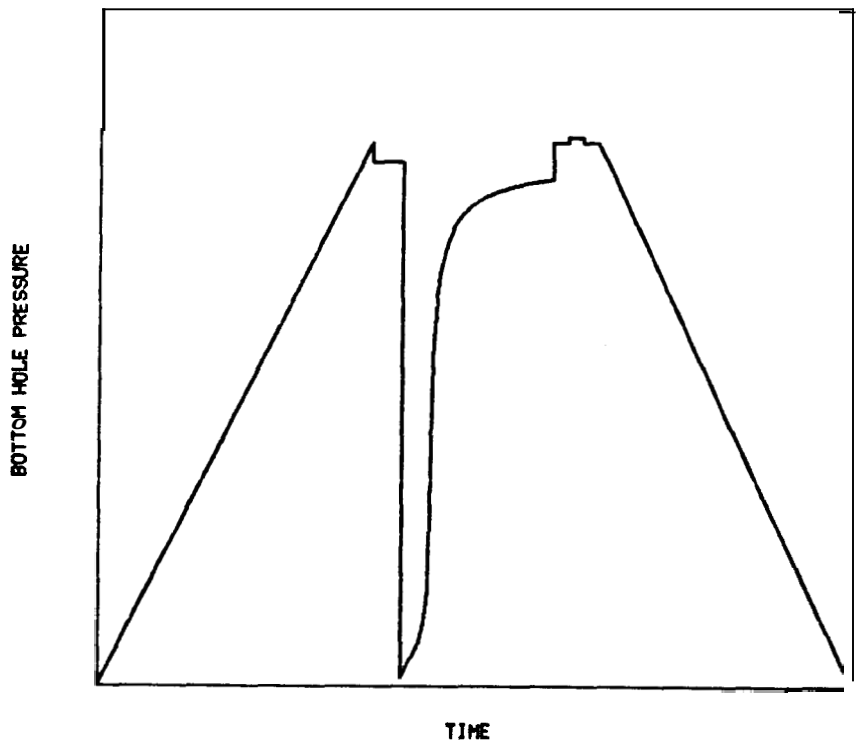

Figure 2.28 Typical Pressure Response

As the tool assembly is run into the well, the pressure bomb records the increase in hydrostatic pressure. Setting the packer relieves the completion fluid overbalance, and the bottom hole pressure becomes equal to the static reservoir pressure. When the lower surge valve is opened the draw down is obtained, and fluids are produced. As the fluid level rises, the bottom hole pressure approaches the static reservoir pressure. The packer is then released, returning the bottom hole pressure to an overbalance. Reverse circulation of produced fluids causes a momentary pressure increase prior to pulling the tool assembly out of the well.

A reduced ineffective draw down results when either a valve, the packer or drill pipe fail to seal. If an acceptable draw down was achieved during the operation, the pressure data is often utilized only as a measure of the initial reservoir pressure.

Permeability and Skin **Analysis**

The intent of this report is to present a method of analyzing backsurge pressure data to determine oil reservoir parameters of permeability and Hurst skin effect. Knowledge of these parameters will yield greater efficiency of field development. Closed chamber well testing provides a safer method of obtaining permeabiltity and skin values in areas often considered unsuitable for conventional drill stem analysis, No surface pressure build up occurs during a closed chamber test as often does a conventional drill stem test. Conventional drill stem tests are seldom utilized in geopressured offshore oil fields for fear of well control problems.

The closed chamber well test is a more generalized form of the drill stem test known as the slug test. Analogous to the slug test, a closed chamber well test begins with the instantaneous removal of a volume of liquid from the wellbore. The resulting decrease in bottom hole pressure causes an immediate influx of reservoir fluids. As the removed fluid volume is replaced the bottom hole pressure increases due to the hydrostatic pressure of the rising liquid column. For the closed chamber test, the additional upper valve results in a compressing gas volume on top of the rising fluid level. The effect is to produce continuous changing well bore storage through out the test. Because of the gas compression, the bottom hole pressure increases much faster than in the case of the slug test. In both cases the ever increasing back pressure on the formation continually decreases the flow rate at the sand face until the bottom hole pressure reaches the static reservoir pressure.

Permeability and skin analysis of the slug test by type curve match has proven a valid solution technique. Yet attempts to analyze closed chamber well test data by type curve matching with published slug test dimensionless solutions are often impossible. Because the slug test assumption of constant wellbore storage is greatly violated, as the gas compression becomes significant, late time closed chamber pressure data deviates from the equivalent slug test response.

The deviation is often so severe that two thirds of a closed chamber test response must be neglected in order to match the early time response with the slug test of the correct transmissibility. In the rare case of a closed chamber test of a low pressured formation using a long chamber containing low initial chamber pressure, a large portion of the pressure response would be analogous to the slug test and suitable for analysis by slug test type curve match. But, in general, such an approach in inappropriate and may yield erroneous results.

2.2 PREVIOUS WORK

Slug Test

A detailed derivation of the slug test solution, including skin effect, was presented in 1972 by Ramey and Agarwal. The method of solution by Laplace transformation was similar to the solution of the heat transfer problem of a cylinder with a heat resistance (skin effect). Solution to the heat transfer problem was presented by Jaeger in 1956. The slug test solution was obtained by neglecting momentum, friction, phase change, and wellbore fluid compressibility changes.

In 1975, Ramey, Agarwal, and Martin reduced the slug test solution to a set of dimensionless curves using the concept of effective wellbore radius. Although somewhat empirical, the correlation effectively collapsed the slug test data using the parameter $C_D e^{2S}$. Slug test analysis is obteined by type curve matching with

the collapsed set of curves.

Closed Chamber **Test**

Alexander, in **1977** suggested analysis of closed chamber well test data as a qualitative method of designing conventional drill stem tests. Alexander proposed conducting a closed chamber well test initially to determine the produced fluid properties and expected flow rates of new wells. The closed chamber test results would then be used in the design of the conventional drill stem test equipment and to determine the necessary flow period of the test.

In **1980** Shinohara presented a detailed analytic solution to the closed chamber test problem. The inner boundary condition for the radial diffusivity equation was derived by applying a momentum balance to the rising fluid level within the well bore. A dimensionless solution was obtained by assuming the gas column length insignificant compared to the initial fluid column height. With this assumption, and assuming ideal chamber gas behavior, variations **of** the slug test dimensionless variables may be derived, resulting in a nondimensional diffusivity equation. The resulting partial differential equations were found to **be** nonlinear an unsuitable **for** solution by Laplace transformation. Solution was obtained numeri**cally** using a finite difference scheme. Although momentum effects were considered in the formulation, wellbore friction, phase change, and compressibility of the wellbore fluids were considered negligible.

Saldana, in **1983,** presented a detailed study of a generalized drill stem test formulation including friction and momentum effects. A general equation was proposed to analyze various test scenarios. **For** each test situation the general equation coefficients were defined to adapt the generalized equation. A closed chamber well test was considered by substituting specific coefficients. **As** with Shinohara's approach, ideal gas behavior was assumed to facilitate the use of dimensionless variables. **It** is not clear what other assumptions were required to

obtain the numerical solutions offered for several examples.

3: PROPOSED SOLUTION METHOD

3.1 Overview and Assumptions

Even with the assumption of ideal gas behavior, previous solutions of the closed chamber well test problem by Shinohara and Saldana, have resulted in non-linear partial differential equations. The non-linearity results from the continuous changing well bore storage present through out the test caused by the compressing column of gas above the rising fluid level interface. Numerical techniques have been required to evaluate the pressure response governed by the non-linear partial differential equations.

The method of closed chamber well test analysis presented in this report utilizes superposition to avoid the limitations required when solving the diffusivity equation in the presence of changing well bore storage. Analysis by superposition makes possible the inclusion of non-ideal chamber gas behavior and places no restrictions on the well bore geometry. Because the approach is not analytic, a dimensionless general solution is not presented. But because fewer restriction are required for solution, the influence of independent test parameters can be studied as a guide to future analysis.

Many assumptions are still required in the superposition formulation which follows. To avoid ambiguity, the limitations of the proposed model are presented first in the development. It is assumed that:

1) No phase change occurs between the produced liquids and the chamber gas. Furthermore it is assumed that all solution gas remains dissolved in the liquid phase during the test period.

2) Wellbore liquids are considered incompressible. The chamber gas compressibility is assumed much greater than the produced liquid compressibility.

3) Momentum effects are not considered in the model.

4) Friction effects are not considered in the model.

6) Critical flow does not impede the flow rate during the test period.

6) Only liquid is produced from the reservoir during the test.

7) Throughout the test period, the reservoir behaves as an infinite homogeneous radial system of constant thickness.

8) Total formation compressibility is constant and independent of pressure.

9) Gradient of pressure with respect to depth can be neglected in the gas column.

10) Gradient of temperature with respect to depth can be neglected in the gas column.

3.2: Constant Pressure Cumulative Influx

Governing Equations

The closed chamber well test solution is obtained by superposition of the cumulative influx, constant draw down, infinite reservoir solution to the radial diffusivity equation. In radial coordinates the dimensionless diffusivity equation is given by:

$$\frac{\partial^2 p_{f_D}}{\partial r_D^2} + \frac{1}{r_D}\frac{\partial p_{f_D}}{\partial r_D} = \frac{\partial p_{f_D}}{\partial t_D} \tag{3.1}$$

Where the dimensionless time and radius are defined as:

$$t_D = \frac{kt}{\varphi \mu C_t r_w^{\,2}} \tag{3.2}$$

$$r_D = \frac{r}{r_w} \tag{3.3}$$

For a constant pressure inner boundary, dimensionless pressure is defined as:

$$p_D = \frac{P_i - P_{wf}}{P_i - P_o} \tag{3.4}$$

And dimensionless flow rate into the well bore is:

$$q_D = \frac{qB\mu}{2\pi kh(p_i - p_{wf})} \tag{3.5}$$

Using Darcy's law, dimensionless flow rate into the well bore can be written in terms of the other dimensionless variables:

$$q_D = -\left[\frac{\partial p_{f_D}}{\partial r_D}\right]_{r_D=1} \tag{3.6}$$

Dimensionless cumulative influx is defined as:

$$Q_D = \frac{Q}{2\pi\varphi h C_t r_w^2 (p_i - p_{wf})} \tag{3.7}$$

Initial and Boundary Conditions

The reservoir is considered at static equilibrium prior to the onset of constant pressure draw down. At $t = 0$, $p = p_i$ at all r. In terms of dimensionless variables:

$$p_{f_D}(r_D, t_D = 0) = 0 \tag{3.8}$$

At the outer boundary, the reservoir is considered to behave as if infinite during the test:

$$\lim_{r_D \to \infty} p_D(r_D, t_D) = 0 \tag{3.9}$$

Additional pressure drop at the sand face due to damage or stimulation is considered with the van Everdingen and Hurst dimensionless skin factor:

$$p_{wf} = \left(p_f - rS \left(\frac{\partial p_f}{\partial r} \right) \right)_{r = r_w} \tag{3.10}$$

In dimensionless terms corresponding to the definitions given above:

$$p_{wf_D} = \left(p_{f_D} - S \left(\frac{\partial p_{f_D}}{\partial r_D} \right) \right)_{r_D = 1} \tag{3.11}$$

The Inner boundary is constant pressure. For all time greater than $t = 0$; $p_{wf} = p_o$. In dimensionless terms:

$$p_{wf_D}(r_D = 0, t_D > 0) = 1 \tag{3.12}$$

Which implies that:

$$p_{f_D} - S\left(\frac{\partial p_{f_D}}{\partial t_D}\right)_{r_D=1} = 1 \qquad (3.13)$$

Solution by Laplace Transformation

Solution of Equation 3.1 with the conditions of Equations 3.8, 3.9, and 3.13 is obtained by Laplace transformation. Through Laplace transformation, the equations are reduced to ordinary differential equations which can be solved analytically. The Laplace solution is a function of the Laplace variable "s" which replaces time in the transformation. Da Prat (1981) has presented the dimensionless Laplace flow rate solution:

$$\bar{q}_D = \frac{\sqrt{s}K_1(\sqrt{s})}{s\left(K_0(\sqrt{s}) + S\sqrt{s}K_1(\sqrt{s})\right)} \qquad (3.14)$$

Where K_0 and K_1 are modified Bessel functions of the second kind, zero and first order respectively. Da Prat (1981) has also integrated the dimensionless rate solution and given a simple relation between dimensionless rate and dimensionless cumulative influx in Laplace space:

$$\bar{Q}_D(s) = \frac{\bar{q}_D(s)}{s} \qquad (3.16)$$

Substitution of Equation 3.14 into Equation 3.15 yields:

$$\bar{Q}_D(s) = \frac{\sqrt{s}K_1(\sqrt{s})}{s^2\left(K_0(\sqrt{s}) + S\sqrt{s}K_1(\sqrt{s})\right)} \qquad (3.16)$$

An analytic inversion of Equation 3.16 has not been obtained. Evaluation of cumulative influx in the time domain requires numerical inversion with a method such as the Stehfest routine.

3.3 Superposition to Determine Cumulative Influx

Dimensionless cumulative influx for a constant pressure draw down can be evaluated by numerical inversion of Equation **3.16.** **To** relate dimensionless cumulative Influx to influx a constant of proportionality is defined:

$$\beta = 2\pi\varphi h C_t r_w^2 \qquad (3.17)$$

Then, for the case of constant pressure draw down:

$$Q(t) = \beta[p_i - p_{wf}]Q_D(t_D) \qquad (3.18)$$

Where t_D is calculated using the time the draw down **is** in effect.

Pressure Draw Down Variation

During a closed chamber well test, the flowing pressure at the sand face varies **as** the fluid level **rises** with in the well bore. Superposition of the constant pressure, cumulative influx solution allows the cumulative influx from a radial system to be calculated given a well bore pressure history.

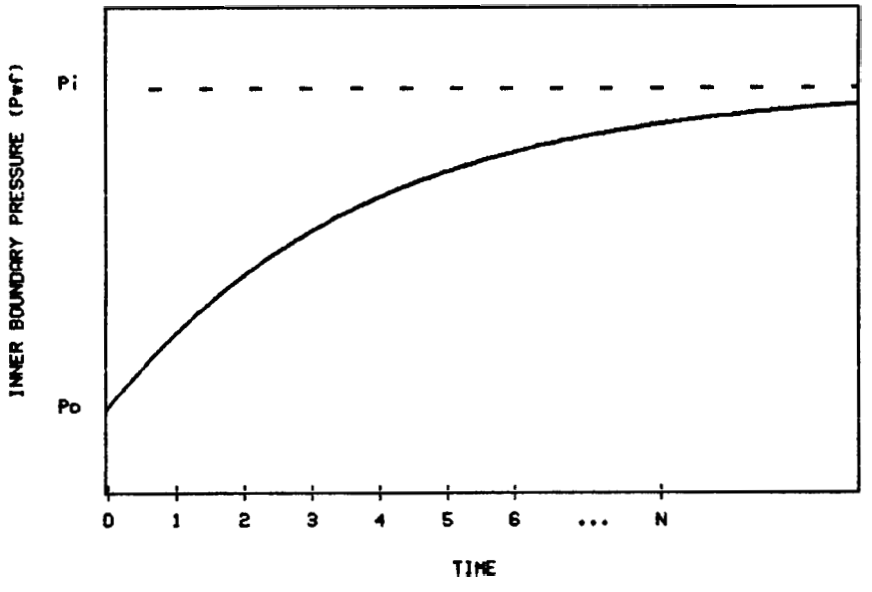

Figure 3.1: Variable Pressure Response

To perform the calculation the continuous pressure response is discretized into constant pressure intervals of short duration. Because the radial diffusivity equation is linear for a constant pressure inner boundary, the individual response to each constant pressure interval may be summed together to determine the net influx at a given time.

Consider the pressure response presented in Figure **3.1. The** time scale is discretized into equal time increments. **To** determine the influx after time increment **"N",** the draw down pressure response is represented as **a** series of step functions:

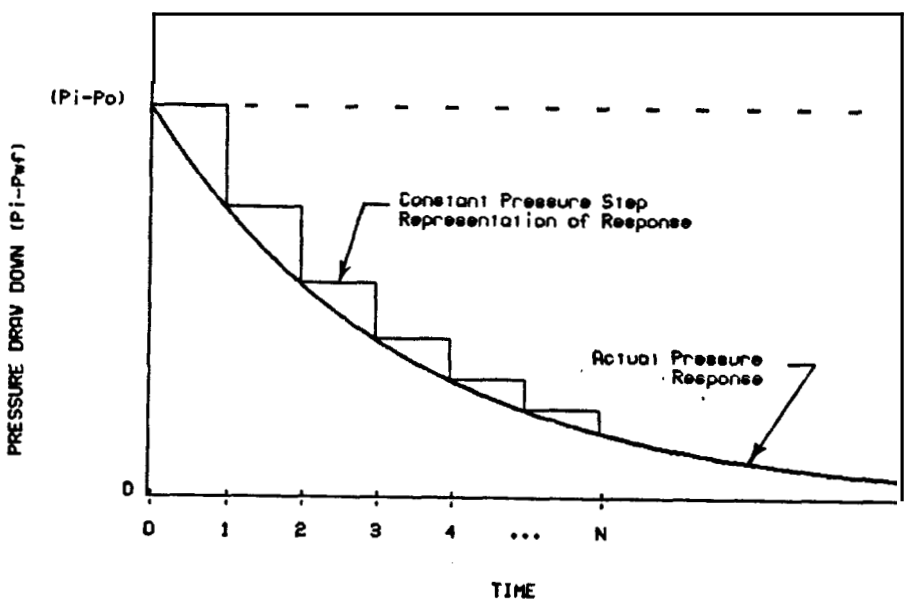

Figure 3.2: Constant Draw Down Representation

Because a forward looking calculation is required to model the closed chamber test response, the initial draw down at the beginning of each time step is assumed to remain constant over the time step interval. Accurate representation **of** the actual response requires that the time increment be small, such that the pressure change **per** time step **is** insignificant compared to the pressure.

Cumulative influx after time step "N" is calculated by superposing the effect of each time step. After time step "N", the pressure drop $[p_i - p_o]$ has been in effect for the total time. Successive pressure changes must be subtracted during the corresponding time in effect. Fluid produced after "N" time steps may be represented as:

$$N_p = \beta [p_i - p_o] Q_D(N\Delta t_D) - \beta \sum_{j=1}^{N-1} \left([p_j - p_{j-1}] Q_D([N-j]\Delta t_D) \right) \quad (3.19)$$

Where Δt_D is evaluated based on the time step Δt.

9.4 Calculation **of** the Closed Chamber Test Response

Using the concept of superposition as presented in the preceding section, cumulative fluid influx at given time can be calculated from a known pressure draw down history. With the assumption that the pressure change per time step is small, the superposition technique can be extented to calculate the fluid influx at one time step past the last pressure history value. Then knowing the cumulative influx, the bottom hole flowing pressure can be calculated from the well bore geometry and fluid properties. The pressure history is updated and the two step process repeated to generate the pressure response,

The chamber gas pressure can be calculated from the initial gas pressure assuming the type of compression. **If** the compression occurs rapidly with **out** time for significant heat transfer, the process could be treated as adiabatic. Annular fluids and the surrounding rock would tend to maintain an isothermal process if compression occurs slow enough to allow for heat dissipation. The actual process is probably somewhere between adiabatic and isothermal, with limited heat transfer during the test period. Subsequent sensitivity studies, presented in this report, have shown gas temperature variance does not significantly alter the bottom hole pressure calculation. For simplicity, isothermal gas compression is assumed.

Consider the well bore geometry **of** Figure 3.3. Assuming the chamber cross sectional area constant, with respect to depth, the chamber gas pressure can be calculated from the ideal **gas** law. For isothermal compression **of** a constant molar quantity of gas:

$$\frac{p_{ch} V_{ch}}{Z} = \frac{p_{ch_i} V_{ch_i}}{Z_i} \tag{3.20}$$

The chamber volume, V_{ch}, may be expressed as:

$$V_{ch} = A_{ch}[L_c - X] \tag{3.21}$$

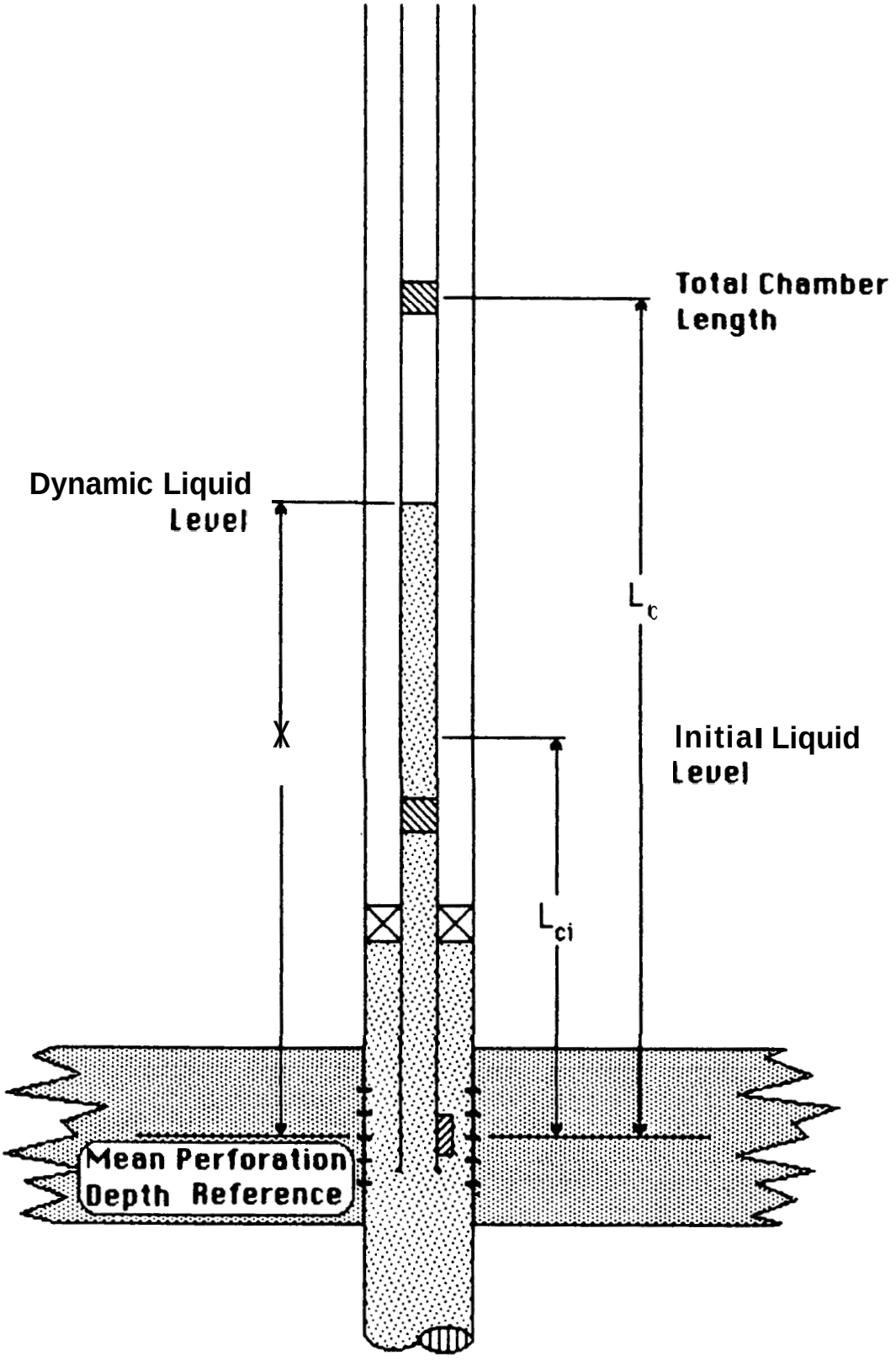

Figure 3.3 Geometry Defining Variables

Substituting Equation 3.21 into 3.20 and rearranging, yields an expression for chamber pressure as a function of fluid level X:

$$p_{ch} = \frac{p_{ch_i}[L_c - L_i]Z}{[L_c - X]Z_i} \tag{3.22}$$

The real gas Z factor was calculated, assuming hydrocarbon gas composition, using the Brill and Breggs correlation. Because Z is a function of p_{ch} the calculation of p_{ch} was iterative. Convergence was reached when the change in Z per iteration was less than 0.01 X.

The fluid level, X, can be calculated form the cumulative fluid influx:

$$X = L_i + \frac{N_p}{A_{ch}} \tag{3.23}$$

Assuming momentum and friction effects are insignificant within the well bore, the bottom hole pressure is equal to the chamber gas pressure plus the hydrostatic pressure of liquid column:

$$p_{wf} = p_{ch} + \rho_f g X \tag{3.24}$$

For a given value of fluid influx, Equations 3.22, 3.23, and, 3.24 allow calculation of the flowing well bore pressure. Thus the pressure at one time step past the known pressure history can be calculated from the fluid influx as calculated by Equation 3.19.

In retrospect, the pressure response is generated as follows:

1) Assume the flowing pressure during time step "N" is equal to the pressure at the start of the time step, "p_{N-1}".

2) Calculate the cumulative fluid influx at the end of time step "N" using Equation 3.19.

3) Calculate the fluid level at the end of time step "N" using Equation **3.23.**

4) Calculate the chamber pressure at the end of step "N" using Equation **3.22.** Iteration is necessary because Z is a function of p_{ch}.

6) Calculate the bottom hole pressure at the end of time step "N" using Equation **3.24.**

6) Update the pressure history, index, and return to step number **1).**

Figure **3.4** presents the computer flow chart of the superposition closed chamber model.

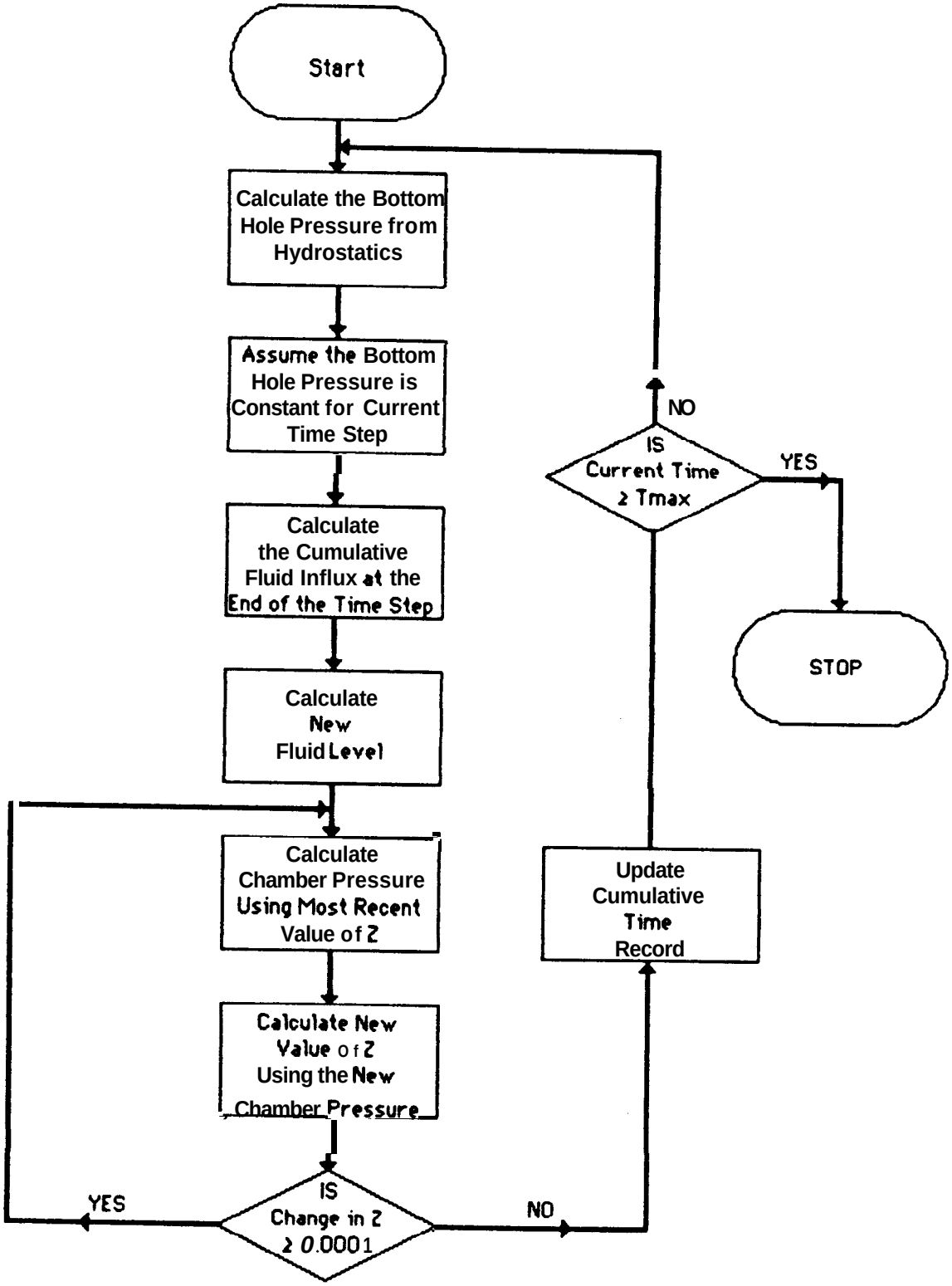

Figure 3.4 Computer Progrem Flow Chart

5.5 Type **Curve** Analysis

The algorithm proposed in the preceding section provides a method **of** generating the pressure response of a closed chamber test, for a given set of tool and reservoir parameters. Evaluation of unknown reservoir parameters requires application of **a** history matching technique. As previously discussed, type curve analysis has proven to be a practical method **of** slug test evaluation. **Closed** chamber test response data were therefore plotted on coordinate axes used by Ramey et. al. **(1**976) **for** slug test analysis.

Slug Test

In 1975, Ramey, Agarwal, and Martin proposed type curve plotting of slug test data on three coordinate systems. Dimensionless pressure was found to be a function of only two parameters: $C_D e^{2S}$ and t_D / C_D . Thus a single set of curves provides the general slug test solution. Each coordinate system emphasizes sensitivity to a particular time range of the data.

Analysis of field data is obtained by plotting dimensionless pressure versus time and type curve matching with the dimensionless solutions. Transmissibility is calculated from the time match. Skin effect is obtained by curve shape match with **a** dimensionless curve **of** constant $C_D e^{2S}$. To interpret the entire slug test response, three **plots** are requlred. Slug test type curves are presented in Figure **3.5, 3.6,** and 3.7.

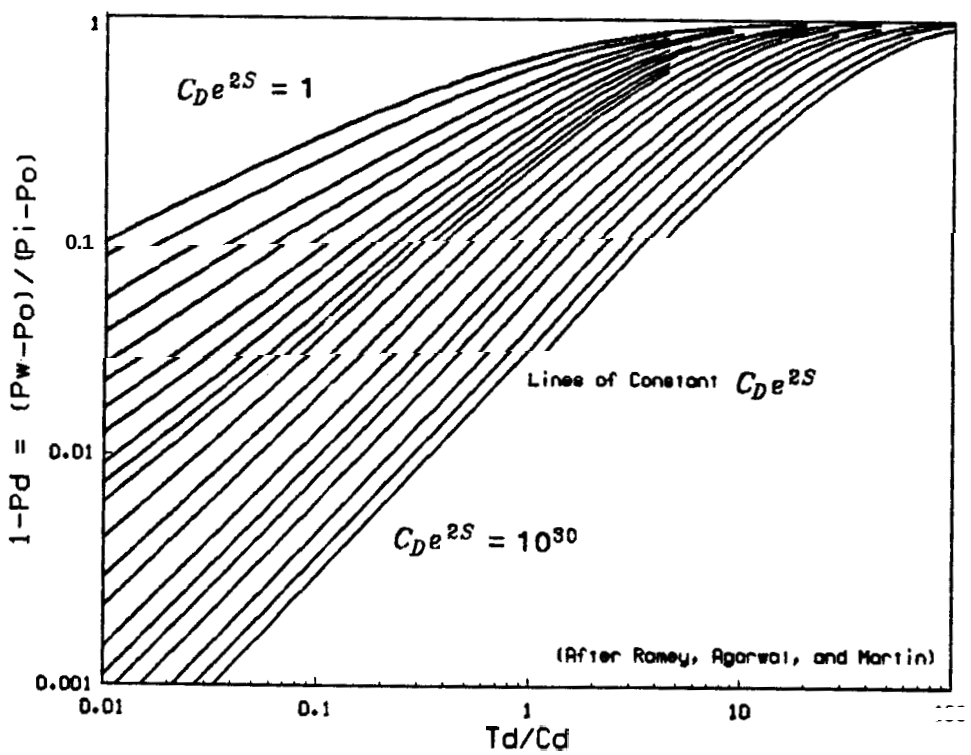

Figure 3.5: Early Time Slug *Test*

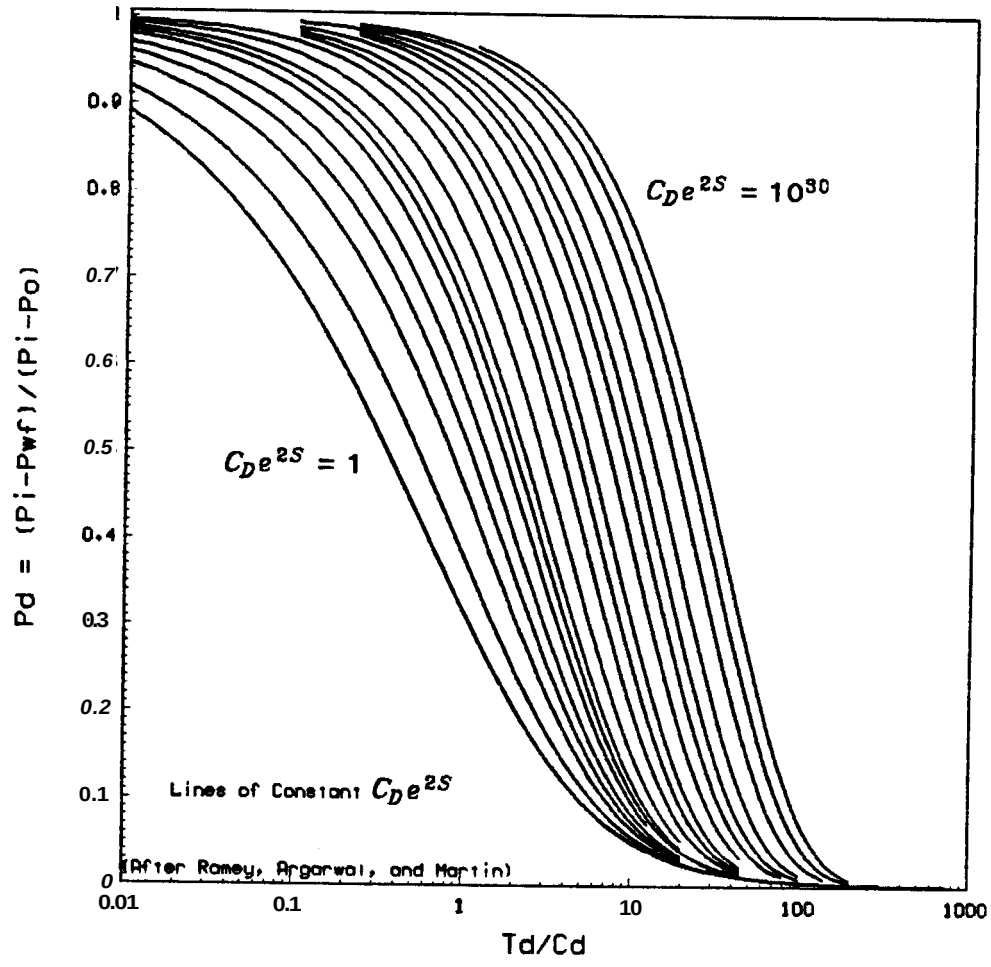

Figure 3.6: Middle Time Slug Test

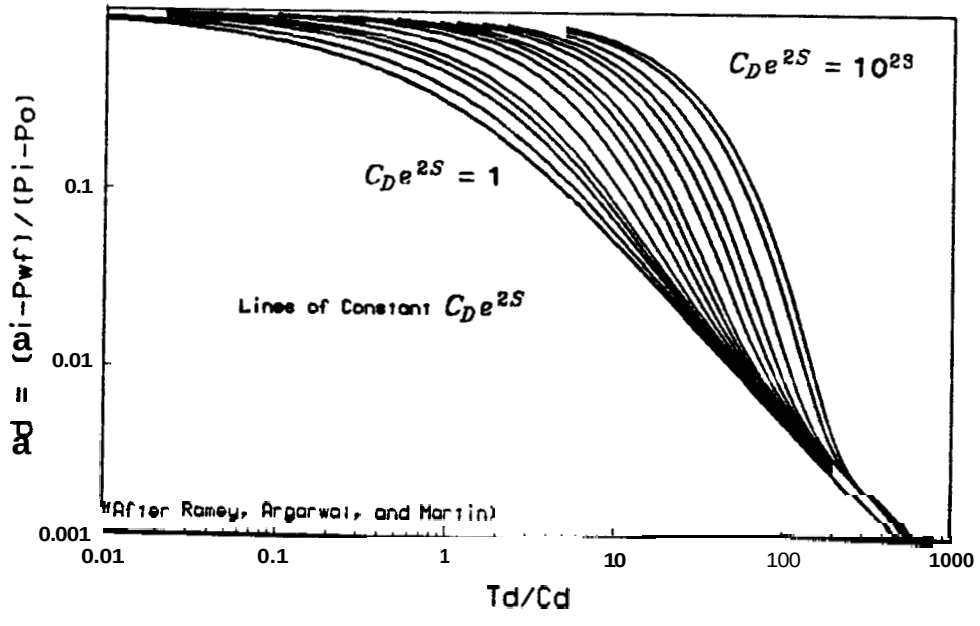

Figure 3.7: Late Time Slug Test

Closed **Chamber Test**

Using the model developed in Section **3.4,** closed chamber pressure response data can be generated for a wide variety of reservoir parameters and tool configurations. Because the closed chamber test is similar to the slug test, plotting closed chamber response data on the slug test coordinates is a logical extension of the type curve technique. Closed chamber field data could then be analyzed by type curve analysis, as shown to be effective for the slug test. But, **as** the sensitivity study presented in Section **6** indicates, closed chamber pressure response data cannot be reduced to a single set of general type curves using the slug test dimensionless groups. In order to correctly evaluate unknown transmissibility and skin effect, **it** is therefore important to understand the influence of each reservoir end tool parameter on the dimensionless plots.

For the closed chamber test, dimensionless pressure is not a function of only Initial $C_D e^{2S}$ and t_D / C_D because C_D is not constant throughout the test. Perhaps if C_D were evaluated at every pressure point the curves could be collapsed. But such **an** analysis would not be practical for evaluating field data. When C_D is evaluated using initial chamber pressure, variables such **as** initial chamber pressure and initial fluid height separate curves of equal skin effect. Thus there **is** no particular utility in choosing t_D / C_D as the abscissa.

Yet type curve matching **is still** an effective means to match the model parameters to actual field data. For a given set of tool parameters and estimated reservoir properties, the pressure response can be generated using the model and graphed in dimensionless p_D versus t_D format. The resulting dimensionless curve is independent of the assumed permeability. Type curve matching of field data can therefore be used to calculate field permeability from the time match, and skin effect from the curve shape.

The optimum dimensionless format for the closed chamber type curve would emphasize the influence of skin effect on curve shape, and minimize the effect of tool geometry. The greater the effect of skin effect on curve shape, the greater will be the resolution of the type curve when determining the wellbore skin effect. Using the traditional definition of t_D for the abscissa will eliminate the effect of other reservoir parameters, with the exception of sand thickness.

In order to determine which of the three slug test type curve formats would yield the greatest resolution to skin effect, pressure responses were generated for skin effect values of 0 to +8. The reservoir and tool parameters used in the superposition model are given in Table 6.1. Similar to the slug test formulation, negative values of skin must be represented by effective well bore radius.

Figures 3.8, 3.0, and 3.10 are dimensionless plots of the simulated pressure responses. Inspection of these three plots suggest that the late time format yields the greatest resolution to skin effect. When transmissibility is also an unknown, the time match would make it difficult to match the curve shape in Figures 3.8, and 3.0 because the curves are nearly similar in shape. It is therefore recommended that the late time format be used for the type curve match.

3.8 Typical Response

To better understand the closed chamber well test response, the time dependence of the variables was studied. Reservoir and tool parameters used in the closed chamber superposition model to generate the following plots are given in Table 6.1.

Figure 3.11 Illustrates how the fluid level rise occurs when the lower surge valve opens. Note that within 20 seconds the chamber is almost entirely filled with liquid. After 20 seconds the flow rate is essentially zero because a very small addition of fluid to the chamber results in a large gas pressure rise.

Figure 3.12 illustrates the rise in chamber gas pressure as the gas is isothermally compressed. The chamber gas pressure is responsible for the abrupt rise in the bottom hole flowing pressure. Fluid influx causes separation of the chamber pressure curve from the bottom hole pressure. In the absence of momentum and friction, the difference in the two curves is the hydrostatic pressure differential of the fluid column.

Figure 3.13 confirms that for the moderate reservoir pressure and temperature of table 6.1, the gas compressibility factor of the chamber gas does not significantly deviate from unity. This is expected at the moderate range of pseudo reduced temperature. For a reservoir temperature of 175 (F) the pseudo reduced temperature of the gas is approximately 1.7 for a hydrocarbon gas of 0.65 specific gravity relative to air.

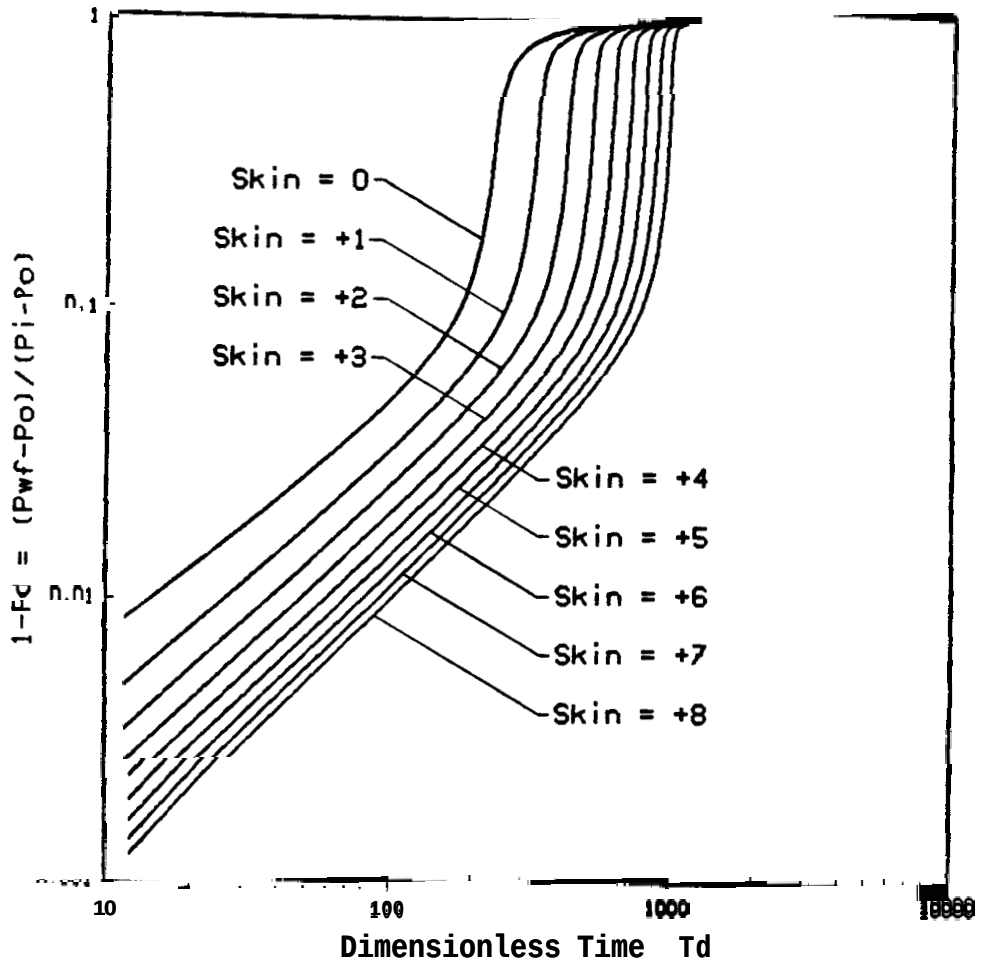

Figure 3.8: Closed Chamber Test (Early Time Format)

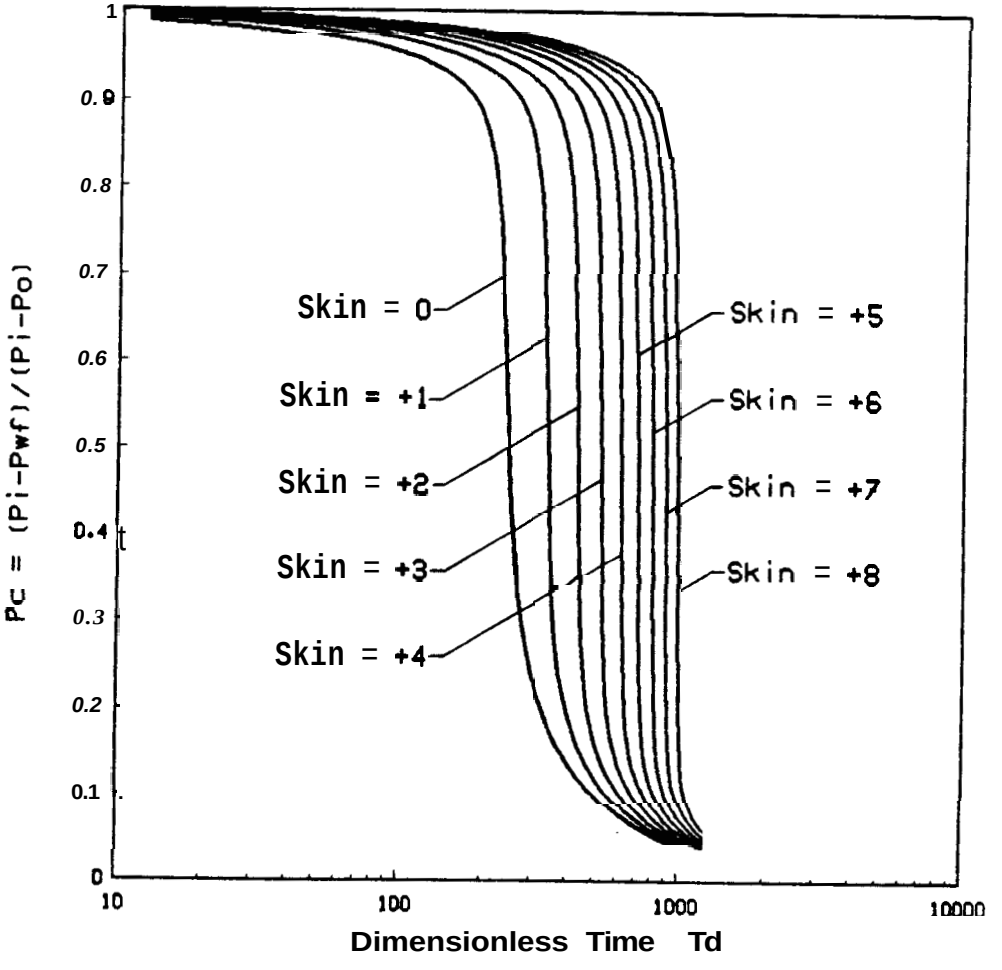

Figure 3.9: Closed Chamber Test (Middle Time Format)

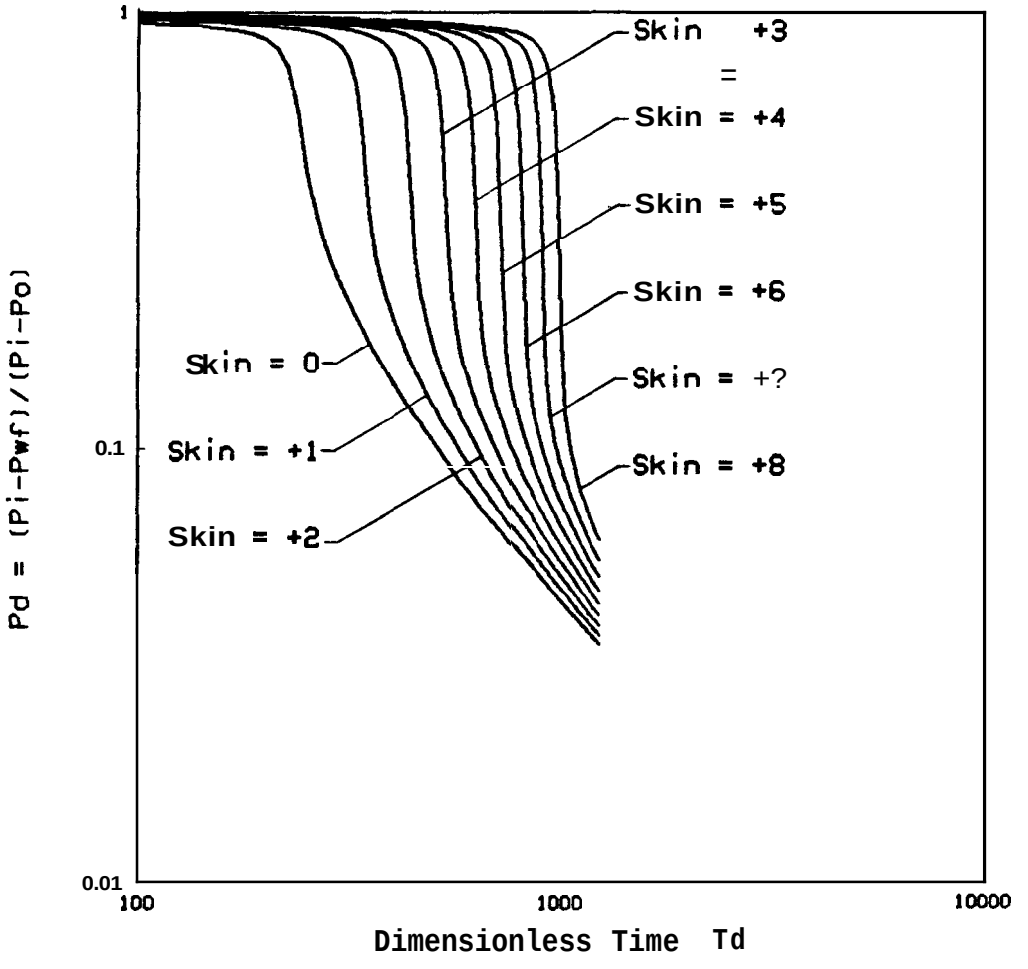

Figure 3.10: Closed Chamber Test (Late Time Format)

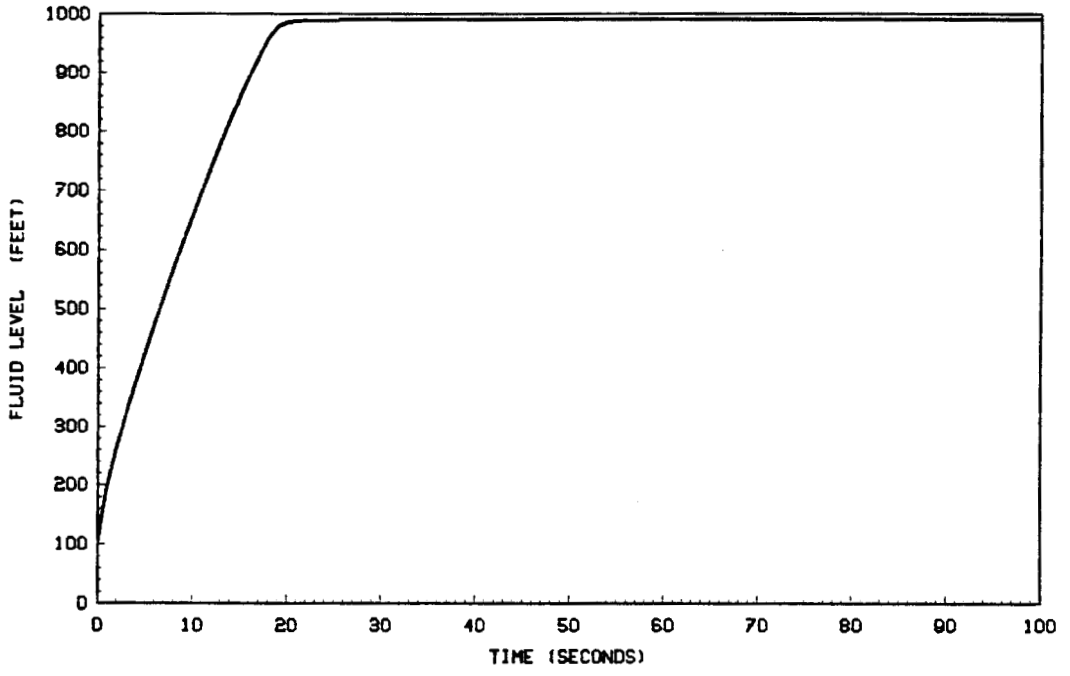

Figure 3.11 Fluid Level vs Time for Bosecose

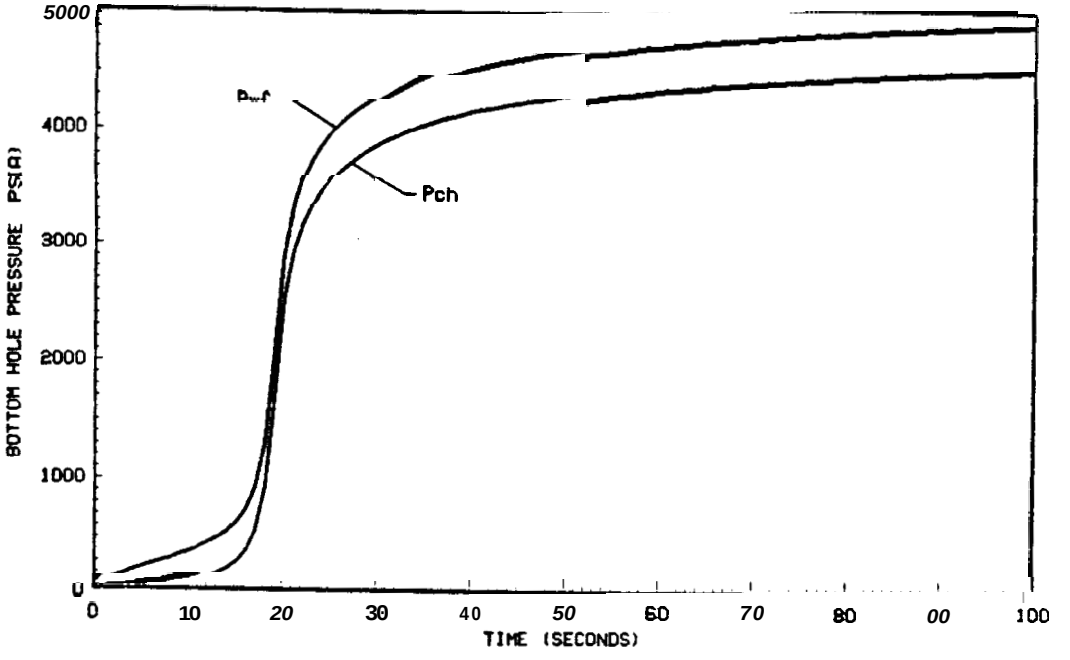

Figure 3.12 Pwf and Pch vs Time for Basecase

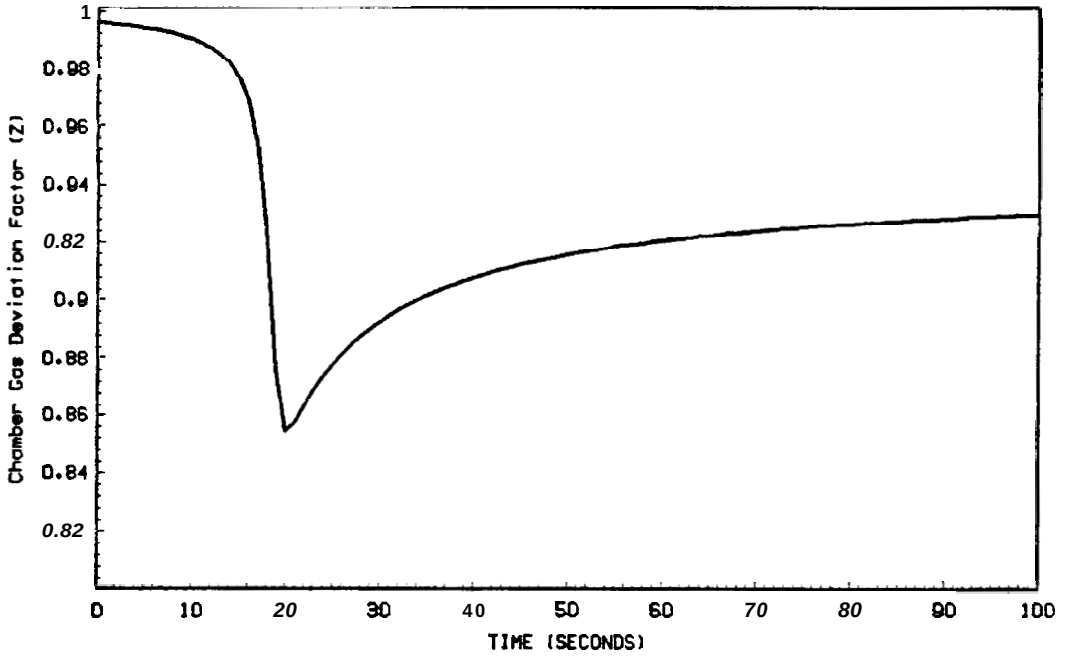

Figure 3.13 Chamber Cos Deviation Factor vs Time for Basecase

4: VERIFICATION OF CLOSED CHAMBER MODEL

4.1 Slug Test Duplication

A comparison of the slug test and closed chamber test tool geometry suggest that the slug test is a specialized case of the closed chamber test. Consider a special case of the closed chamber test where the upper surge valve is above the static fluid level and the initial chamber presure is 0 psia. Under these conditions, no gas compression will occur as the fluid level rises, and the closed chamber test becomes a slug test.

The proposed superposition model can therefore be tested by attempting to reproduce published slug test solutions obtained by analytical methods. As a test of the closed chamber model, slug test data were calculated using the superposition model for a value of $C_D e^{2S} = 10^{10}$ and compared to values obtained by Ramey, Agarwal, and Martian. Table 4.1 lists the reservoir and tool parameters selected, at random from typical values, used in the comparison test.

TABLE 4.1: SLUG TEST PARAMETERS USED IN COMPARISON TEST

Parameter	Value	
Static reservoir pressure	5000	psig
Fluid gravity	25	API
Fluid viscosity	1.25	CP
Porosity	27	X
Permeability	100	md
Skin	+8	
Total Compressibility	10×10^{-6}	psi^{-1}
Reservoir thickness	25	feet
Well diameter	10	Inches
Initial fluid height	0	feet
Chamber ID	2.441	inches

For the parameters of Table 4.1 C_D is calculated to be 1127.

The superposition model was run, using the parameters of Table 4.1, to produce a pressure history for the slug test. The comparison with previous slug test

solutions required calculation of dimensionless variables. Table 4.2 presents the comparison.

TABLE 4.2: COMPARISON OF SUPERPOSITION CALCULATED SLUG TEST

	Superposition p_D	Analytic p_D	Difference (%)
	0.990376	0.990324	0.005
	0.981496	0.981367	0.013
	0.956187	0.955945	0.025
	0.916555	0.916404	0.016
2.00	0.845057	0.844376	0.081
5.00	0.668265	0.667704	0.084
10.00	0.459848	0.458279	0.342
20.00	0.227461	0.226036	0.628

Where: $p_D = \frac{(p_i - p_{wf})}{(p_i - p_o)}$

And the analytic values are those of Ramey, Agarwal, and Martin (1976).

Comparison of slug test data, obtained using the superposition model, with published results, indicate the proposed model accurately duplicates Ramey's results obtained by numerical approximation of the integral solution to the slug test. Close agreement is expected because many of the assumptions of the slug test solution, including negligible friction and momentum effects, are also included in the superposition model.

The comparison supports the proposed superposition model but does not verify correct pressure response generation in the presence of compressing chamber gas. Yet the ability to generate slug test data, indicates correct modeling of reservoir behavior in the superposition model. The gas chamber pressure calculation is a simple addition as shown in Section 3.4.

4.2 Closed Chamber Variance **from Slug** Test

The influence of the upper surge valve on the pressure response can be illustrated by comparison with the superposition results of Section **4.1.** The superposition model was used to generate a pressure response for the parameters **of** Table **4.1** with the addition of an upper surge valve. A chamber length **of** 3000 (ft) and an initial chamber pressure of **14.7** (psia) were selected.

Figure **4.1** shows the pressure response for both the slug and closed chamber test. Figures **4.2, 4.3,** and **4.4** show the dimensionless comparison of the slug and closed chamber tests.

Figures **4.5, 4.6,** and **4.7 show** the dimensionless basecase response plotted **on** the slug test type curves of Ramey, Agarwal, and Martin **(1975).** Initially, the basecase behaves as a slug test, because at early time the chamber **gas** pressure does not rise significantly and the well bore storage is nearly constant. **As** the fluid level nears the upper surge valve, an abrupt change in storage occurs. The late time response again resembles a slug test but is shifted in time due to the decreased value of well bore storage governed by the chamber gas pressure. **On** logarithmic coordinates the shift in time of the late time response is proportional to the ratio of the initial to final well bore storage.

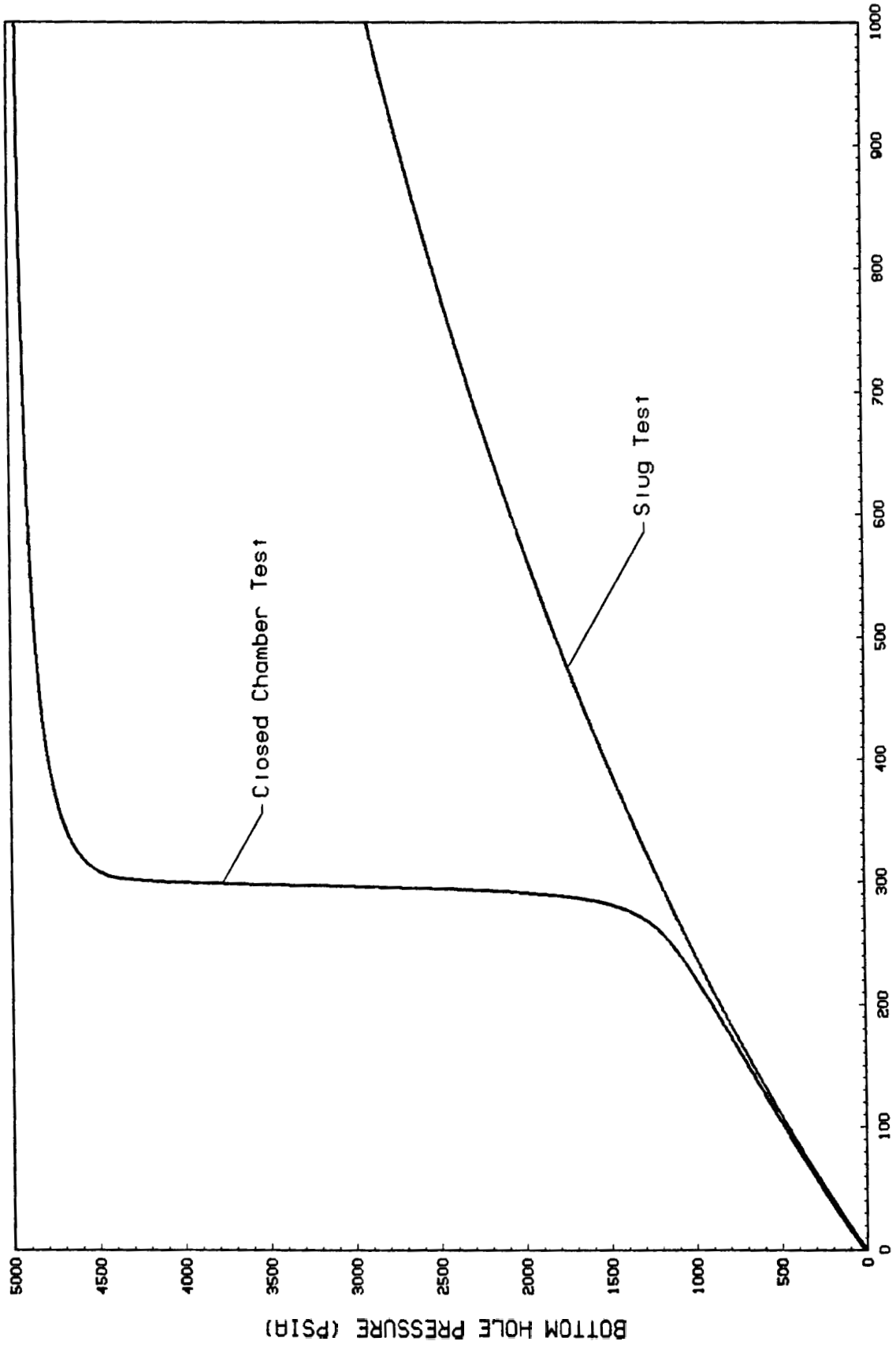

Figure 4.1 Pwf vs Time (Slug Test and Closed Chamber Test)

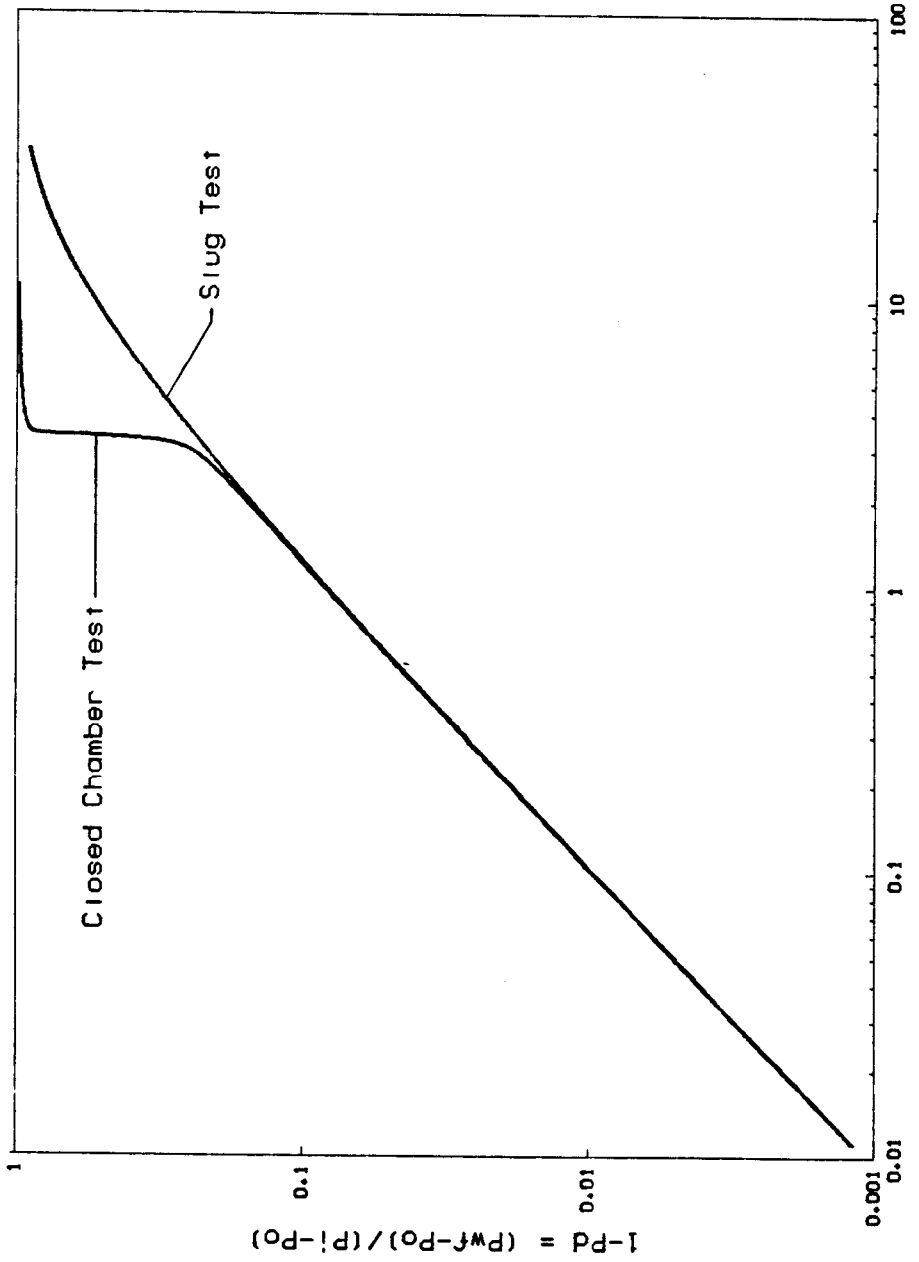

Figure 4.2 Early Time Dimensionless Plot (Slug Test and Closed Chamber Test)

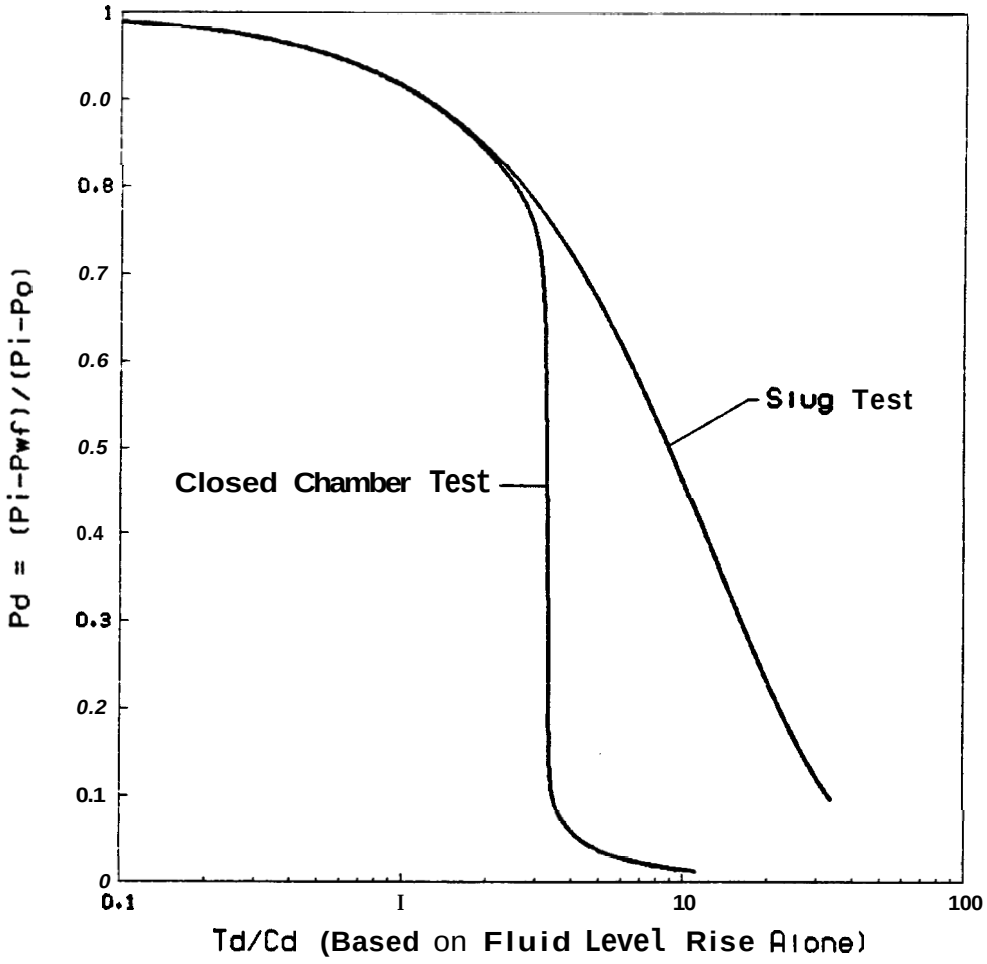

Figure 4.3 Middle Time Dimensionless Plot
(Slug Test ond Closed Chamber Test)

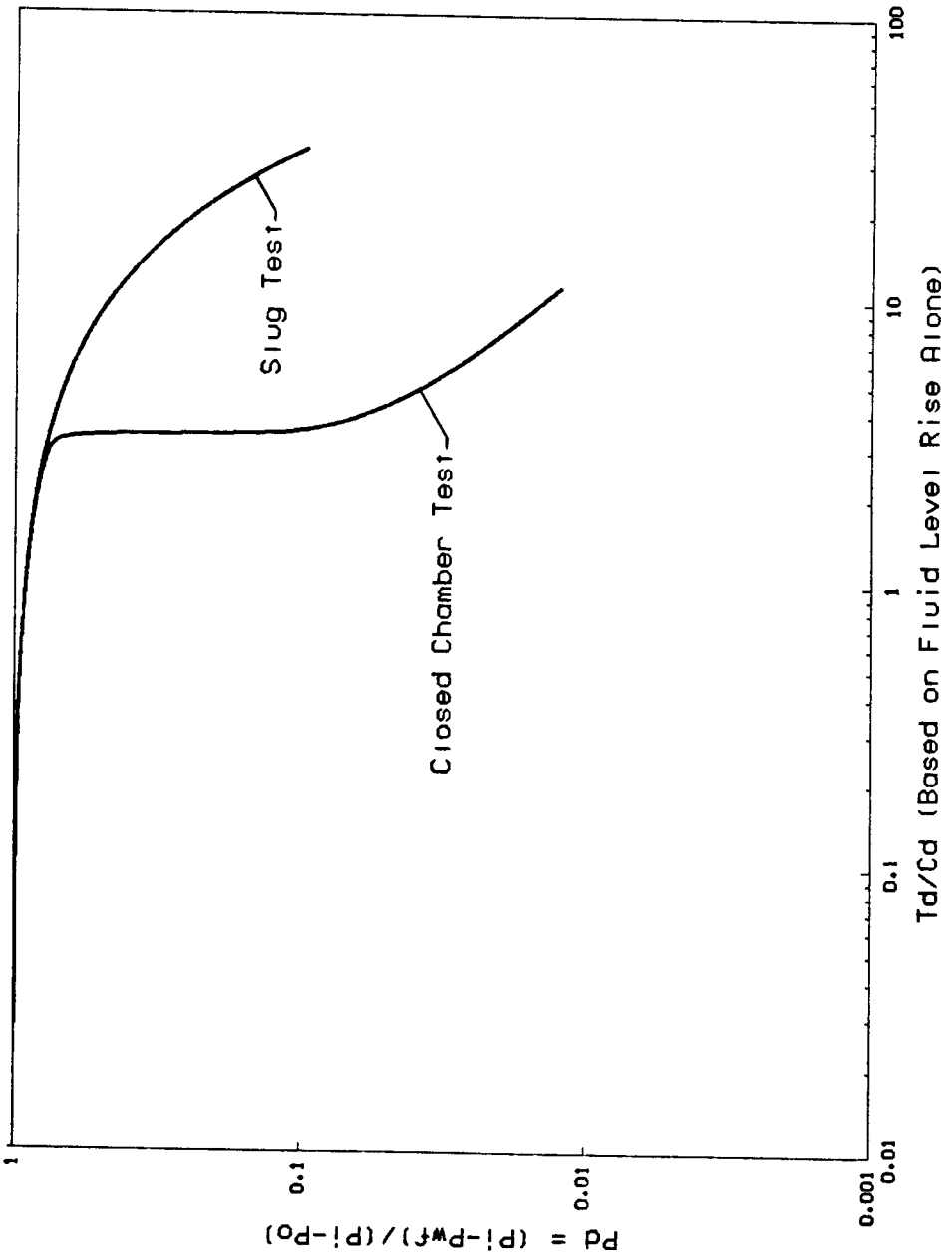

Figure 4.4 Late Time Dimensionless Plot (Slug Test and Closed Chamber Test)

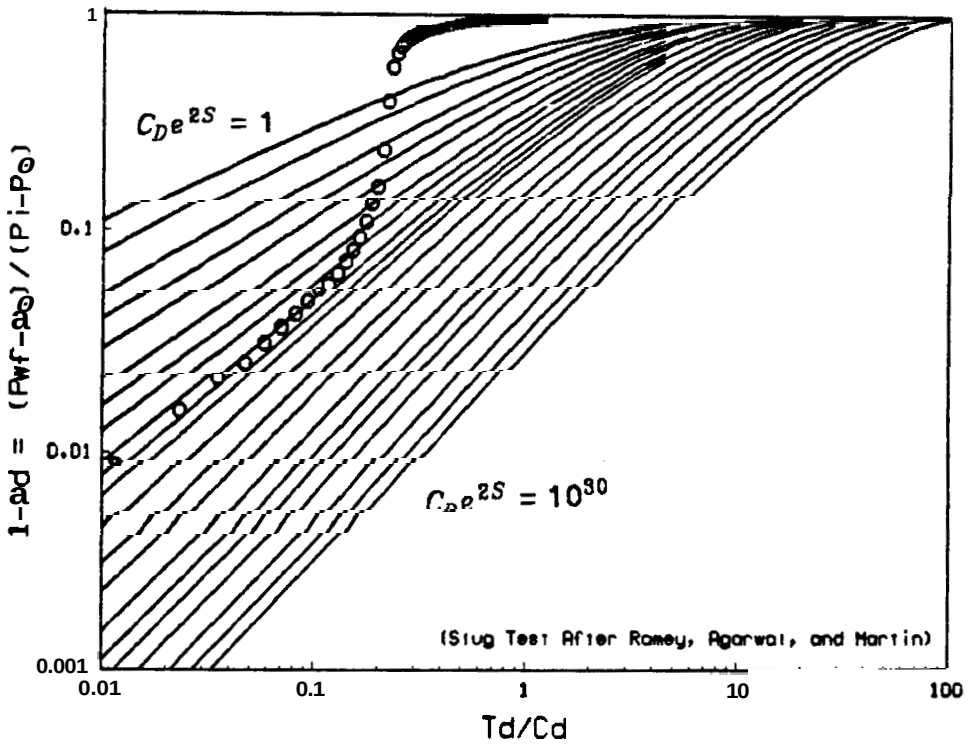

Figure 4.5: Basecase Plotted on Early Time Slug Test Type Curve

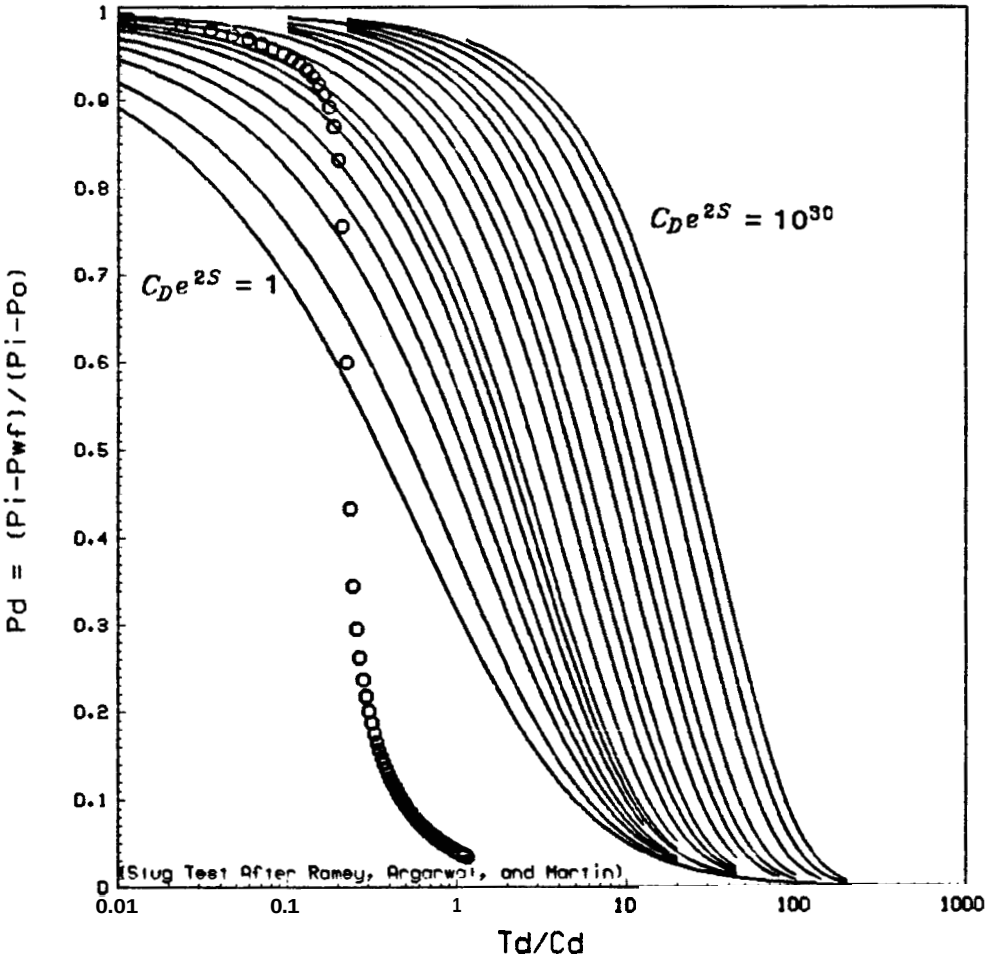

Figure 4.6: Bosecose Plotted on Middle Time Slug Test Type Curve

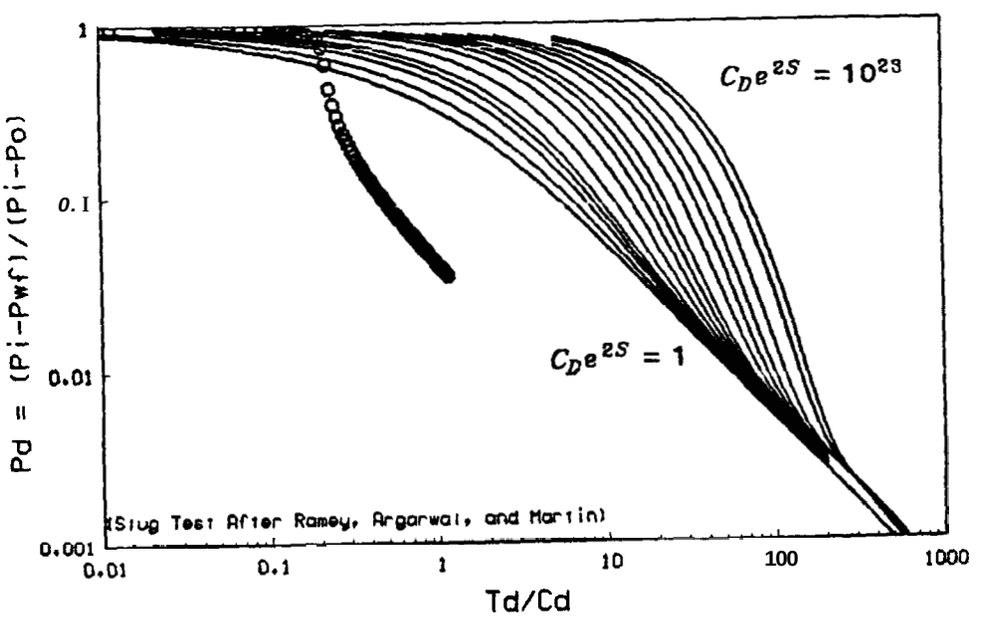

Figure 4.7: Bosecose Plotted on Late Time Slug Test Type Curve

5: NUMERICAL CONSIDERATIONS

6.1 Time Step Selection

As noted in the preceding section, the closed chamber test response is equivalent to the slug test response until the chamber gas pressure becomes significant compared to the static reservoir pressure. When the chamber gas pressure begins to effect the response, the bottom hole pressure rise is much more rapid. Numerical modeling of the closed chamber test requires selection of a time step size sufficiently small that the chamber pressure rise is accurately represented. The rate at which the pressure rise occurs is dependent upon the Initial chamber pressure, and the geometry which defines the relationship between fluid influx and compression ratio of the chamber gas.

Momentarily assume that the chamber gas behaves as an ideal gas. Also assume that the chamber gas compression is isothermal. Under these assumptions, the chamber gas pressure is equal to the initial chamber pressure times the volumetric compression ratio of the closed chamber. If the initial chamber pressure is small compared to the initial reservoir, as is often common when the initial chamber pressure is near atmospheric pressure, the chamber pressure will only approach the reservoir pressure when the volumetric compression ratio is very large. Simply stated, for a low initial chamber pressure, the chamber pressure will only effect the rate of influx when the fluid level is very near the upper surge valve.

Numerical problems occur if the time step size causes the fluid level to vary

excessively during one time step. When the time step is excessive, the effect is to cause the numerical model to over shoot the upper surge valve. This occurs because the model calculates the fluid influx during a time step assuming constant bottom hole pressure, as illustrated in Figure **3.3.** A forward looking routine **is** required to extend the calculation one step past the pressure history. The bottom hole pressure used during **a** time step was calculated using the chamber pressure at the end of the previous time increment. If at the beginning of the time step the fluid level is significantly below the upper surge valve, the assumption of constant bottom hole pressure during the time increment may cause calculation of fluid influx resulting in a fluid level at the end of the time step which is above the upper valve. **All** subsequent chamber pressure calculations **will** calculate a negative value using Equation **3.22,** and the fluid level rise will never feel the resistance of the gas compression.

Assuming isothermal, ideal **gas** compression, a simple estimate may be made of the maximum permissible time step. For an ideal gas, Equation **3.22** may be written **as:**

$$p_{ch} = p_{ch_i} \frac{[L_c - L_i]}{[L_c - X]} \tag{5.1}$$

To avoid fluid level over shoot of the upper surge valve, the maximum change in X per time step should not exceed the chamber volume at which the chamber pressure **is** sufficient to resist fluid influx. Neglecting the hydrostatic pressure differential of the fluid column, this occurs when the chamber pressure is equal to the initial static reservoir pressure. With these assumptions the following expression may be written:

$$\Delta X_{max} = [L_c - X]_{static} = \frac{p_{ch_i}}{p_i}[L_c - L_i] \tag{5.2}$$

Using dimensionless influx, ΔX_{max} can be related to time. For conservative estimation of the maximum permissible time step, assume the bottom hole pressure is equal to the initial chamber pressure after the lower surge valve opens. This assumption *is* consistent with neglecting the hydrostatic pressure differential of the liquid column. With this assumption Equation **3.19** may be written to give the influx during **a** single time step:

$$N_p = \beta[p_i - p_{ch_i}]\, Q_D(\Delta t_D) \tag{5.3}$$

For e single time step Equation **3.23** may be written as:

$$\Delta X = \frac{N_p}{A_{ch}} \tag{5.4}$$

Substituting Equation **5.3** into equation **5.4** yields:

$$\Delta X_{max} = \frac{\beta[p_i - p_{ch_i}]\, Q_D(\Delta t_D)}{A_{ch}} \tag{5.5}$$

Then equating Equations 6.2 and *5.5* and rearranging to solve for maximum dimensionless influx during a single time step:

$$Q_D(\Delta t_D)_{max} = \frac{A_{ch}}{\beta}\,\frac{p_{ch_i}}{p_i}\,\frac{[L_c - L_i]}{[p_i - p_{ch_i}]} \tag{5.6}$$

After calculating the maximum allowable value of dimensionless influx during a single time step, the maximum permissible value of Δt_D can be determined from tabulated values of Q_D for skin equals zero. As with other assumptions used in this development, using skin equals zero tables of dimensionless influx will result in e conservative value of the maximum time step. The maximum permissible time step is finally obtained from the dimensionless time step:

$$\Delta t_{max} = \frac{\varphi \mu C_t r_w^2 \Delta t_{D\,max}}{73.25(10^{-8})\, k_{max}} \tag{5.7}$$

Where Δt_{max} is expressed in seconds and k_{max} is the maximum expected average reservoir permeability expressed in millidarcys.

6.2 Improvements in Efficiency of Time Step

The time step requirements discussed in the preceding section often result in use of an extremely small time step. For example the sensitivity study examples presented in the next section required a time step of 0.01 seconds to avoid over shoot of the upper surge valve. When pressure data is desired over a reasonable interval of time the superposition routine can require unreasonable amounts of computer time. To obtain 100 seconds of pressure data for the sensitivity study, of Section 6, about one hour of run time was required on the Petroleum Engineering department's VAX 11/750 computer.

The period during which a small time step is required is only a fraction of the total test duration. To increase the efficiency of the superposition routine a scheme could be developed utilizing a variable time step. This would allow use of e larger time increment during the flow period when the chamber pressure is insignificant compared to reservoir pressure. As the fluid level approaches the upper surge valve the time step would have to be reduced to avoid over shoot of the upper surge valve. After the chamber pressure increases to near the reservoir pressure, the time step could be increased to a larger value again because the rate of pressure change with respect to time becomes small as the flow rate decreases. Time step size could be controlled by monitoring the derivative of chamber pressure with respect ot time and maintaining the rate of pressure change below some preset value.

The amount of numerical calculation could be greatly reduced by such a scheme. The reduction is much greater than proportional to the number of time increments deleted, because at each time step the superposition routine requires subtraction of all previous pressure changes. A variable time step model could increase the efficiency of the superposition model by an order of magnitude.

Evaluation of cumulative fluid influx at a point in time by superposition requires that the dimensionless influx be evaluated for all combinations of the previous time steps. Thus if the time step is allowed to vary continuously new dimensionless influx values would have to be calculated for each pressure change in the entire pressure history, at every time step. This requirement would negate the benefit of varying the time increment size.

The recalculation requirement can be circumvented if all time steps are a multiple of some small basic unit of time. The basic unit of time increment should be equal to the maximum permissible time step during the period of rapid chamber pressure rise as predicted by Equation 5.7. By utilizing a multiple time step increment the amount of superposition required could be significantly reduced without the need to recalculate dimensionless influx values at each time step. The only additional required calculation, over the constant time step model, would be the need to keep a record of the cumulative time each pressure change has been in effect and update the record at each time increment.

Although a variable time step superposition model is not presented in this report, a simple model was developed and shown to produce pressure response data much more efficiently than the constant time increment model presented. Many problems were encountered in developing a method of adjusting the number of time increments per time step. When the time step size was not reduced quickly enough, as the fluid level neared the upper surge valve, the model became unstable and produced oscillating pressure values. Continued development of a variable time step superposition model will be necessary to quickly generate closed chamber well test type curves as needed to analyze field data.

6: SENSITIVITY STUDY

General Description

Plotting of the closed chamber pressure response on slug test dimensionless coordinates indicates that many tool and reservoir parameters influence the dimensionless curve shape. The influence of tool and reservoir parameters should be understood, if traditional slug test type curve format is to be used in closed chamber test analysis. Such information is needed to predict the accuracy of measurement required to define a closed chamber test. Furthermore, knowledge of the influence of each input parameter will facilitate choosing realistic assumptions for future analytic approaches to the closed chamber test solution. Many of the tool parameters can be selected for a particular test situation. Knowing the influence of each tool parameter would allow the tool assembly to be designed for maximum sensitivity to unknown reservoir parameters.

Input Parameter sensitivity was therefore investigated using the superposition closed chamber computer model. Isolation of each parameter was obtained by creating a control basecase. Sensitivity analysis was then performed by varying a single parameter over a typical range. The basecase values were selected at random from what are believed to be typical values. Table 6.1 lists the basecase parameters.

TABLE 6.1 : BASE CASE CLOSED CHAMBER TEST PARAMETERS

Parameter	Value	
Static Reservoir Pressure	5000	psig
Fluid Gravity	25	API
Fluid viscosity	1.25	CP
Porosity	27	%
Permeability	100	md
Skin	0	
Total Compressibility	10×10^{-6}	psi^{-1}
Reservoir Thickness	25	feet
Well Diameter	10	inches
Initial Fluid Height	100	feet
Chamber ID	2.441	inches
Total Chamber Length	1000	feet
Chamber Gas Temperature	175	F
Chamber Gas Gravity	0.65	(to air)
Initial Chamber Pressure	30	psig
Total Test Time	100	seconds
Time Step	0.01	seconds
initial Dimensionless Storage	1070	

6.1: Effect of Produced Fluid Gravity

A large quantity of sand is often produced from a well when backsurging is used to clean debris from the perforations. Sand flow tends to increase the effective pressure gradient of the fluid in the well bore because the sand is momentarily suspended by the produced fluid.

When multiple pressure recorders are used to record the pressure response of a backsurge, it is possible to calculate the effective fluid gradient from the pressure differential between gauges. Data from the Gulf of Mexico indicates that the hydrostatic gradient of well bore fluid can be as high as 1.0 psi/ft during backsurge operations. Such a gradient is significantly greater than the gradient of either completion fluid in the well or the gradient of the produced oil.

The presence of sand in the produced fluids makes it difficult to determine the effective hydrostatic fluid gradient during the backsurge. It is therefore Important to understand the Influence of produced fluid gravity on the closed

chamber well test response.

Produced fluid gravity was varied from −25 to 40 degrees API. Table **6.2** presents the pressure gradient of the fluid densities tested.

TABLE 6.2: FLUID GRADIENTS OF DENSITIES TESTED

API Gravity	lbm/gal	psi/ft
40	6.88	0.375
25	7.54	0.391
10	**8.34**	**0,433**
0	8.97	0.466
-25	11.08	0.575

Figure 6.1 presents the pressure response data generated using the superposition model. Figure 6.2 is an enlargement of Figure 6.1 which emphasizes the influence of fluid gravity. As expected the pressure rise is **more** abrupt **for** heaver fluid.

Figure 6.3 presents the early time dimensionless plot of the pressure data. Fluid gravity causes **a** change in the early time curve shape. Comparison of Figure **6.3** and Figure **3.5** indicates confusion may occur if the early time format were to be used for type curve skin determination when the produced fluid gravity **is** also unknown.

Figure 6.4 illustrates that fluid gravity variation has little effect on the late time dimensionless plot. **It** is therefore not necessary to accurately measure the produced fluid gravity **if** the late time curve is used for the type curve analysis of field data. This is also expected because the late time pressure rise **Is** governed **by** the gas compression.

Figures 6.5 and 6.6 are included to illustrate that using t_D / C_D **as** the abscissa to collapse the dimensionless curves is ineffective. Practical use of the type curve technique **of** history matching requires that t_D be divided **by** a

constant value of C_D. Division of dimensionless time by the changing value of dimensionless well bore storage may collapse the curves, but the resulting graph would be useless for field data evaluation.

In Figure ***6.5*** t_D is divided by dimensionless well bore storage calculated from well bore storage resulting from the rising fluid level alone. Note that this plot is successful in collapsing the early time response. During this period the effect of gas compression is not significant, and the response is equivalent to a slug test. But as expected, at late time, when the gas compression becomes important, the curves separate due to the changing value of well bore storage.

Figure **6.6** illustrates that including storage due to initial gas compression in the constant value of C_D by which t_D is divided does not improve the curve collapsing effect of using $t \sim C_D$ as the abscissa.

6.2: Effect of Chamber Gas Gravity

The basecase gas gravity was varied from ***0.5*** to **1.6** (relative to air) to test the influence of chamber gas gravity on the closed chamber well test pressure response. Figure **6.7** illustrates that gas gravity does ot significantly effect the Isothermal pressure response.

6.3: Effect of Initial Fluid Level

Well bore storage resulting from a rising fluid level is dependent upon the cross sectional area of the liquid interface and the density of the well bore liquid. As a result, the slug test dimensionless response is independent of the initial fluid level. To investigate the significance of initial fluid level on the closed chamber response, the basecase initial fluid level of **100** ft was varied between 0 and 500 ft.

Figure ***6.8*** illustrates how initial fluid level influences the pressure versus time plot. Figures **6.9** and **6.10** illustrate that the influence of fluid level on the

dimensionless plots is more significant in the late time data. Both Figures **6.9** and **6.10** indicate that a smaller initial chamber gas volume, due to a longer initial fluid column, results in an earlier rise in the chamber pressure. **If** slug test type curves were to be used to evaluate a closed chamber well test, a lower initial fluid level would result in a greater portion of the data matching with the early time slug test type curve.

To further illustrate the ineffectiveness **of** using t_D / C_D **as** the abscissa, when C_D is a function **of** fluid level rise only, Figures **6.11** and **6.12** are included. Note that as the initial fluid column length is increased the curves separate earlier. This is because the well bore storage change occurs earlier due to the chamber pressure rise which is a result **of** the smaller initial gas volume. Less fluid influx is required before the volumetric compression ratio of the gas governs the bottom hole pressure response.

6.4: Effect of initial Chamber Pressure

The initial gas pressure in a closed chamber test is usually ambient atmospheric pressure. **If** either a tool joint **or** one **of** the surge valves leaks during the run in of the test assembly the fluid level inside the chamber may rise resulting in premature compression of the chamber gas. **It** is therefore Important to understand the influence of initial chamber pressure.

Figure **6.13** shows how a higher initial chamber pressure tends to smooth the pressure response. This **is** expected because less compression of the gas is required before the gas pressure governs the bottom hole pressure.

Figure **6.14** illustrates that increasing the initial chamber pressure shifts the early time dimensionless plot to the left and causes an earlier increase in $(1 - p_D)$. **If** slug test type curves were to be used to evaluate the early time closed chamber response an initial atmospheric chamber pressure should be main-

tained. Even a chamber pressure of 30 psig causes a time shift to the left that would cause permeability determined by the slug test type curve match point to be artificially low.

Figure 6.15 indicates that the late time format of data plotting is not as significantly influenced by the initial chamber pressure. As with Figures 6.13 and 6.14 the response is smoothed by an increase in chamber pressure, but no significant time shift occurs.

Figures 6.16 and 6.17 illustrate these points on traditional slug test coordinates. But as with the other cases presented, the closed chamber curves cannot be reduced to a single type curve by plotting on slug test coordinates.

6.5: Effect of Total Chamber Length

When well control problems are anticipated, safety dictates that the upper surge valve be placed deep enough that if the chamber pipe should part and create an upward piston action the tool assembly remain heavy. This requirement often limits the chamber length which can be used to surge shallow high pressure sands. To Investigate the effect of total chamber length the basecase length of 1000 ft as varied to *500* and 2000 *ft.*

Figure 6.18 indicates that the abrupt pressure rise due to chamber gas compression can be delayed by utilizing a longer chamber. This idea is supported by Figure 6.19 which shows that a longer chamber results in more of the response being similar to the slug test. This effect is also expected because a slug test can be thought of as a closed chamber test with an infinite chamber length.

Figure 6.20 illustrates that the late time format response is also delayed by use of a longer chamber. Such a delay would allow pressure recording with a less accurate device. Closed chamber tests are usually of such short duration that traditional mechanical pressure recorders lack sufficient sensitivity to record the

true pressure response. Thus it appears beneficial to use as long of chamber length as possible.

6.6: Effect *of* Chamber Diameter

A similar effect can be obtained by increasing the chamber diameter. This increases the portion of well bore storage attributable to the rising fluid level. More fluid influx is required before the gas compression becomes significant, resulting in a time shift to the right. Because the flow period is longer a larger portion of the formation is investigated.

Figure 6.21 shows how the abrupt pressure rise is delayed by increasing the chamber diameter. Figure 6.22 and 6.23 illustrate the dimensionless time shift to the right caused by increasing the internal tool diameter.

Analogous to the tool length increase, an increase in chamber diameter would decrease the pressure recorder sensitivity required to accurately record the closed chamber pressure response. But unlike increasing the chamber length, increasing the chamber diameter does not decrease the safety of the test.

6.7: Effect *of* Reservoir Sand Thickness

Reservoir sand thickness also causes a time shift in the dimensionless plots. A thicker sand increases the ability of the formation to quickly fill the chamber. Early chamber gas compression occurs as a result, and the abrubt rise in the bottom hole pressure occurs sooner.

Figure 6.24 shows the influence of reservoir sand thickness on the pressure versus time plot. Figure 6.25 and 6.26 illustrate the time shift which occurs on dimensionless coordinates.

Type curve generation by the superposition model requires estimation of the reservoir sand thickness. Dimensionless time does not contain sand thickness so the time match of field data will yield only $(\frac{k}{\mu})$. But because the dimensionless

curves shift with respect to time as sand thickness varies the same transmissibility, $(\frac{kh}{\mu})$, should result from the field data match regardless of the initial sand thickness estimate. This occurs because reservoirs of equal transmissibility will yield equivalent pressure responses, if all other parameters are equal.

6.8: Effect of Initial Reservoir Pressure

The flow period **of** a closed chamber test is usually **of** very short duration. **As** a result the bottom hole pressure **of** the well quickly returns to the Initial static reservoir pressure. **If** the tool assembly is not quickly removed from the well a good estimation of static reservoir pressure is obtained from the final pressure recording prior to release of the temporary packer. Yet unlike the slug test response, the closed chamber dimensionless plots are effected by the reservoir pressure.

Figure ***6.27*** illustrates how initial reservoir pressure effects the pressure vs time response. The increase in the final pressure trend **of** the closed chamber test response is expected. **Also** note that the period of rapid pressure rise due to gas compression occurs earlier for higher pressured formations. This occurs as a result of the increased flow rate due to greater pressure differential at the sand face.

Figure 6.28 again illustrates a difference between slug and closed chamber tests. At very early time, when the closed chamber test behaves as a slug test, initial reservoir pressure does not influence the dimensionless plot. But at latter time the influence **of** initial reservoir pressure becomes significant as emphasised in Figure 6.29.

6.9: Effect **of** Chamber Gas Temperature

As discussed in Section **3.4,** the thermodynamic path of gas compression is **not** known. **To** simplify the mathematical model isothermal gas compression was

assumed. Figure **6.30** illustrates that the temperature at which the isothermal gas compression occurs does not influence the pressure response. **If** the gas compression occurs adiabatically the gas temperature will increase as the pressure increases. Based on the results of Figure **6.30, it** *is* probable that adiabatic gas compression will not significantly alter the isothermal bottom hole pressure response. Further studies should confirm this concept.

6.10: Effect of Assuming **Ideal Gas** Behavior

An assumption of ideal gas behavior would greatly simplify the partial differential equations which govern the closed chamber pressure response. **To** investigate the error induced by assuming ideal gas behavior the superposition model was modified with the gas deviation factor set equal to unity.

Figure **6.31** illustrates that for the typical reservoir temperature and pressure values **of** the basecase, the assumption of ideal gas behavior does **not** effect the pressure response. **For** reservoir pressures approaching **10,000** psig the affect may **be** more significant.

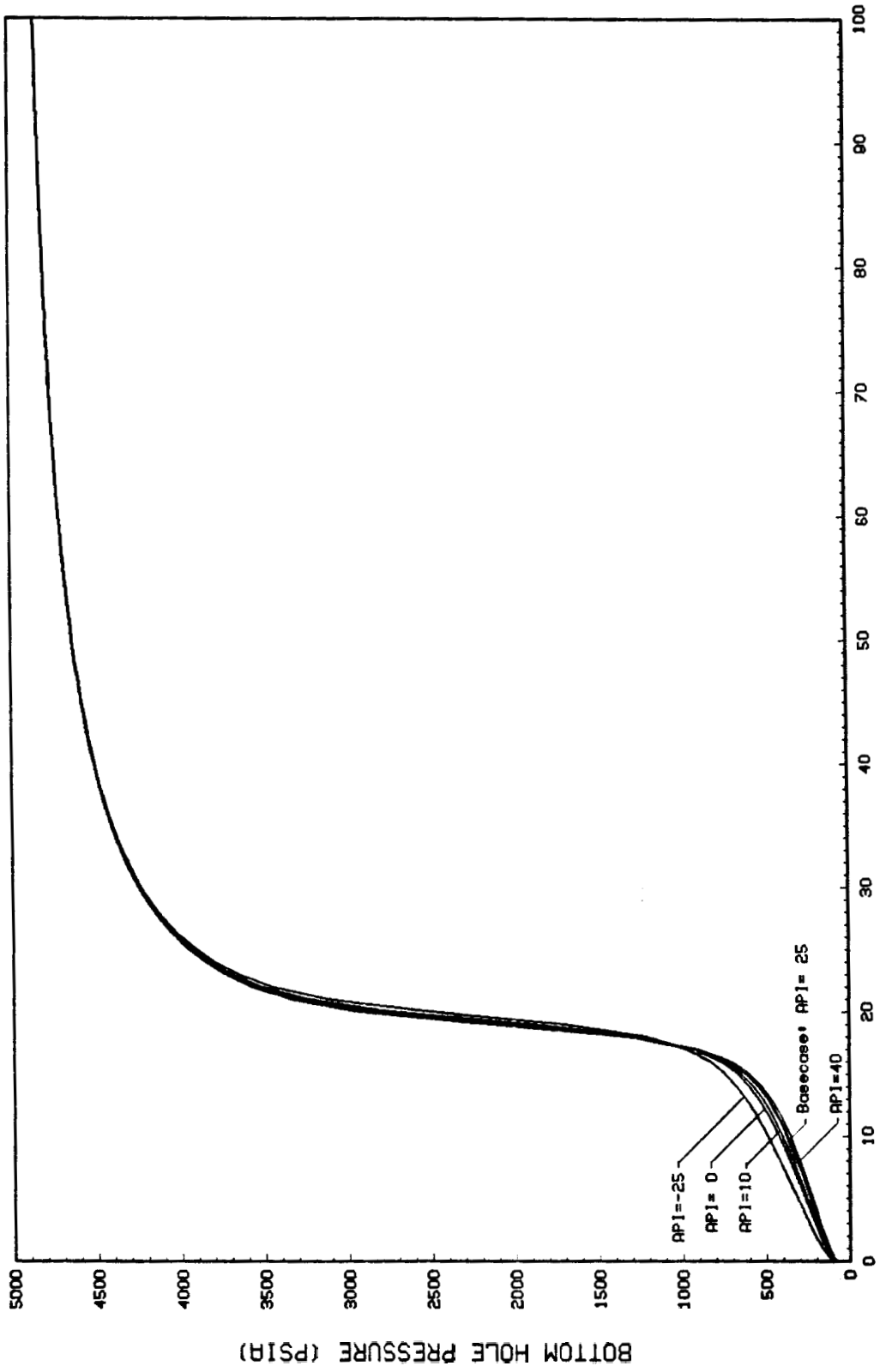

Figure 6.1 Pwf vs Time: (Effect of Produced Fluid Gravity)

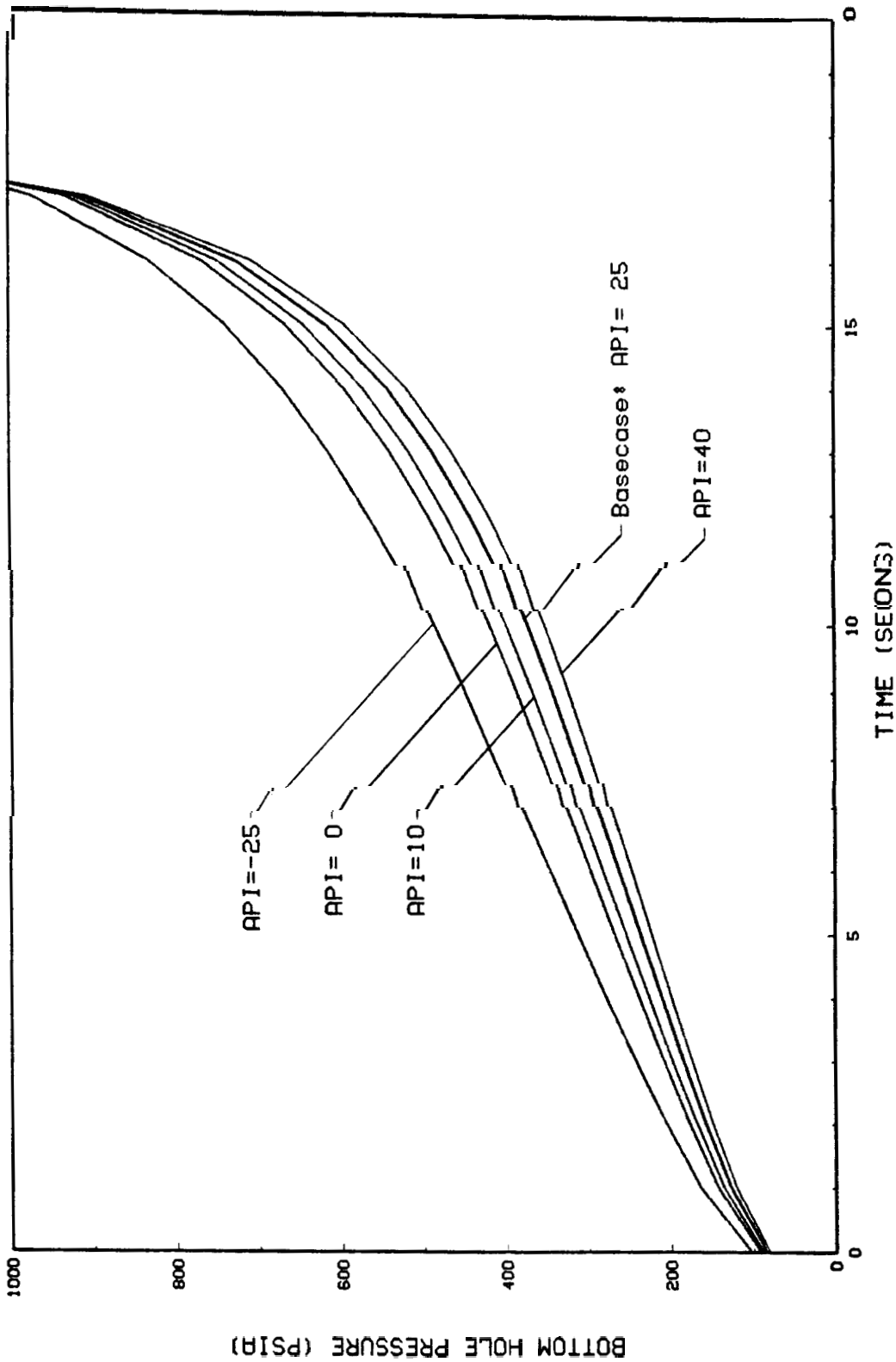

Figure 6.2 Pwf vs Time: (Effect of Produced Fluid Gravity)

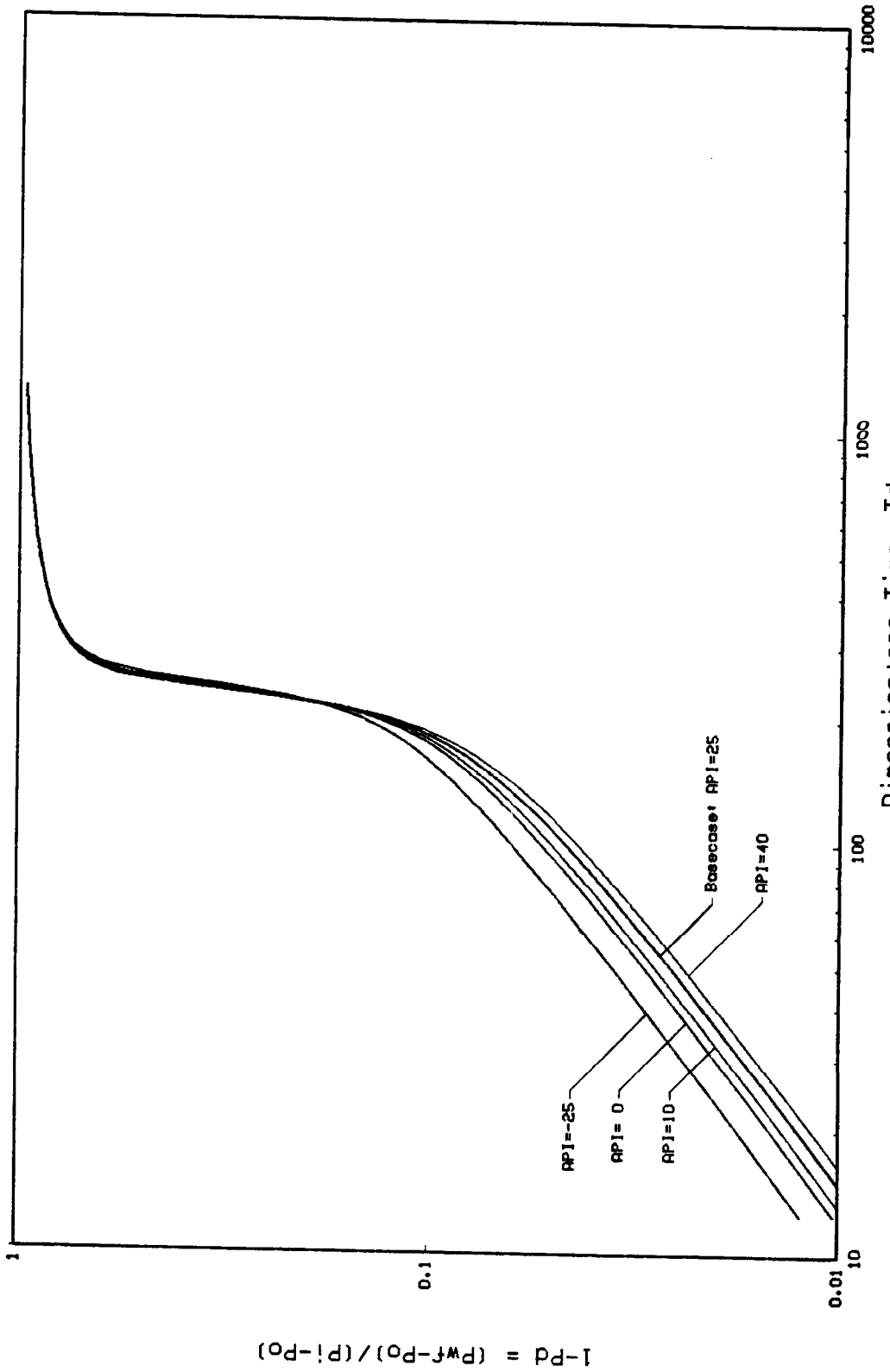

Figure 6.3 Early Time Plots (Effect of produced Fluid Gravity)

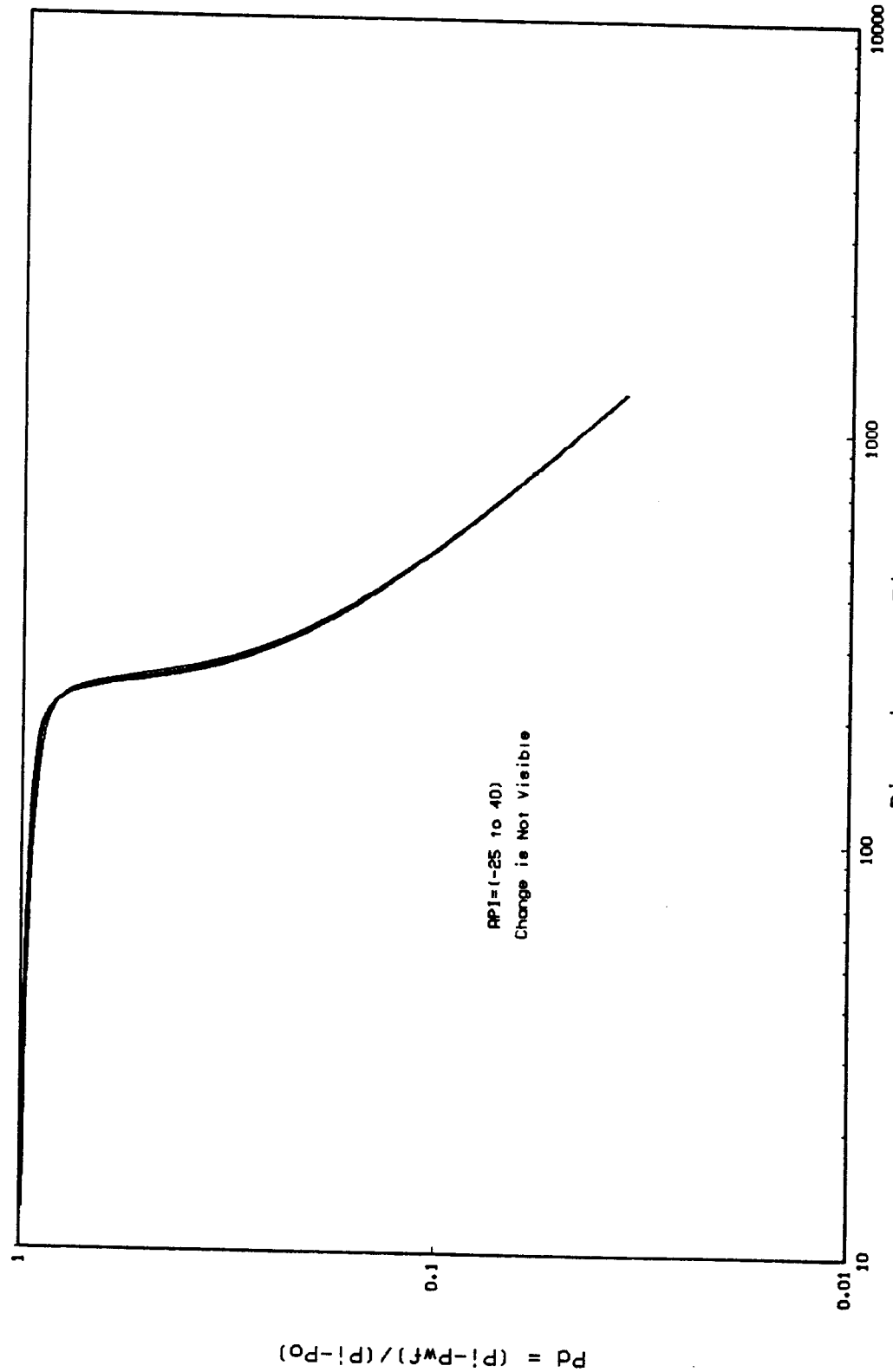

Figure 6.4 Late Time Plots (Effect of Fluid Gravity)

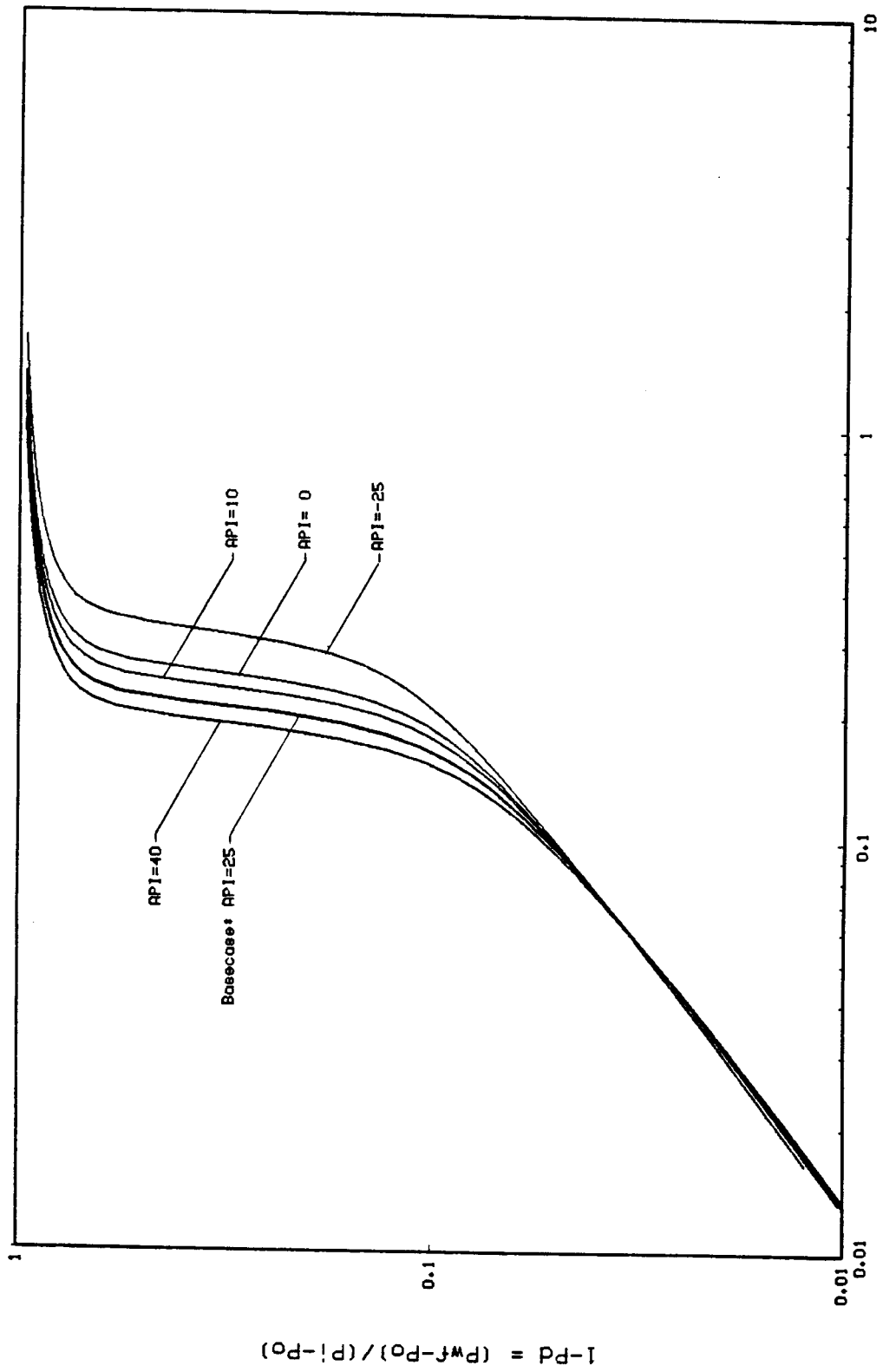

Figure 6.5 Early Time Plots (Effect of Produced Fluid Gravity)

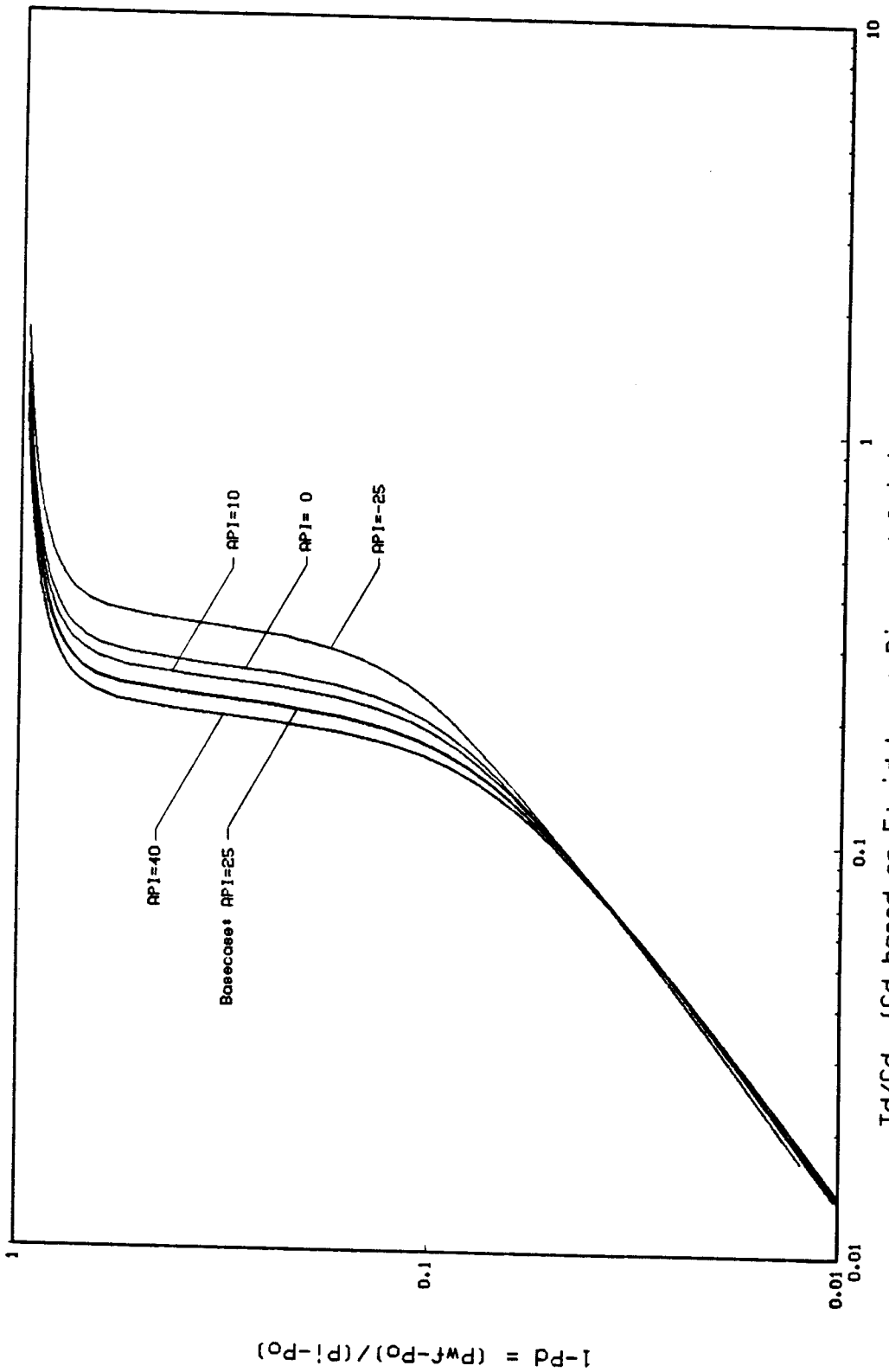

Figure 6.6 Early Time Plots (Effect of Produced Fluid Gravity)

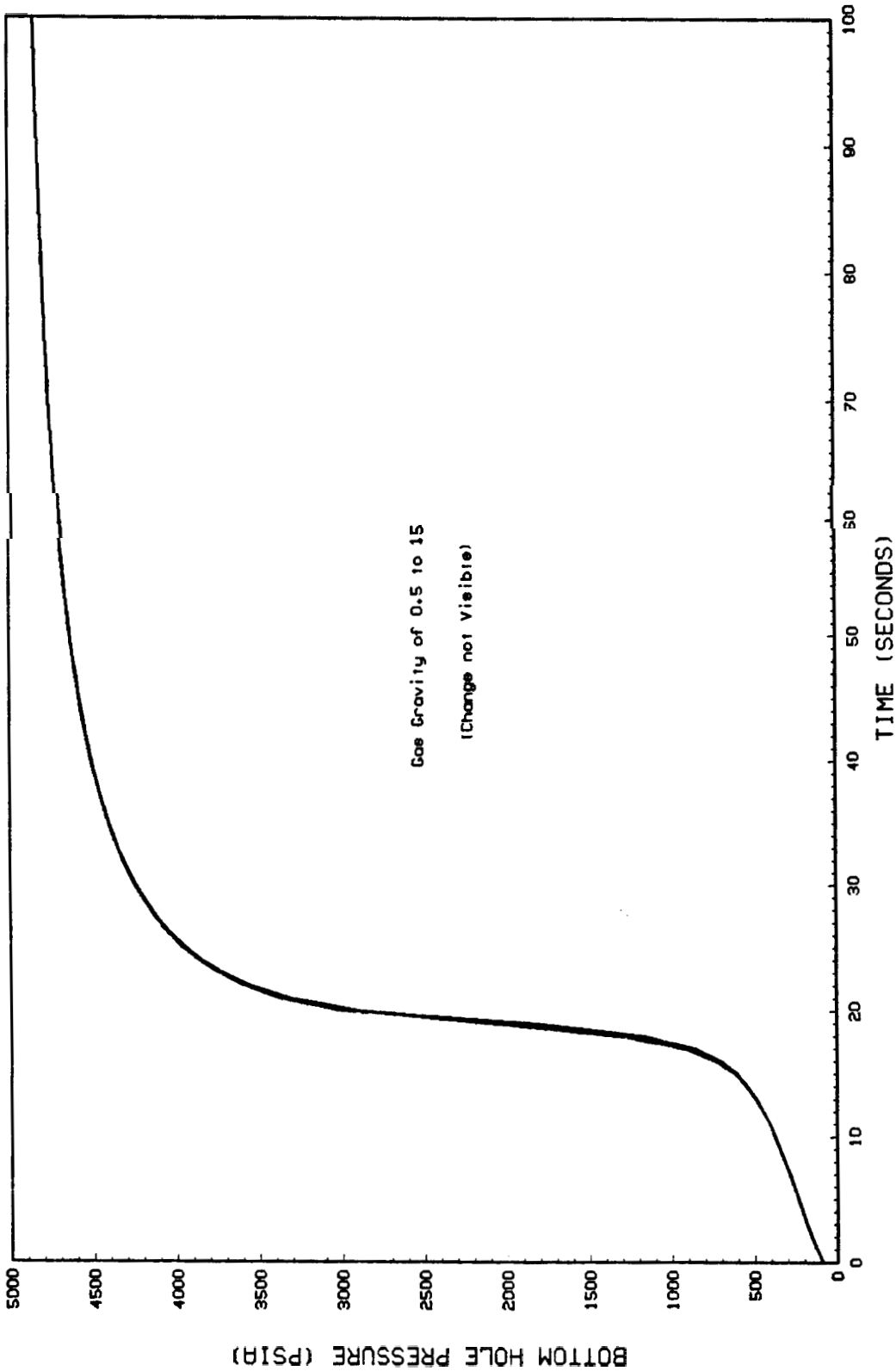

Figure 6.7 Pwf vs Time (Effect of Chamber Gas Gravity)

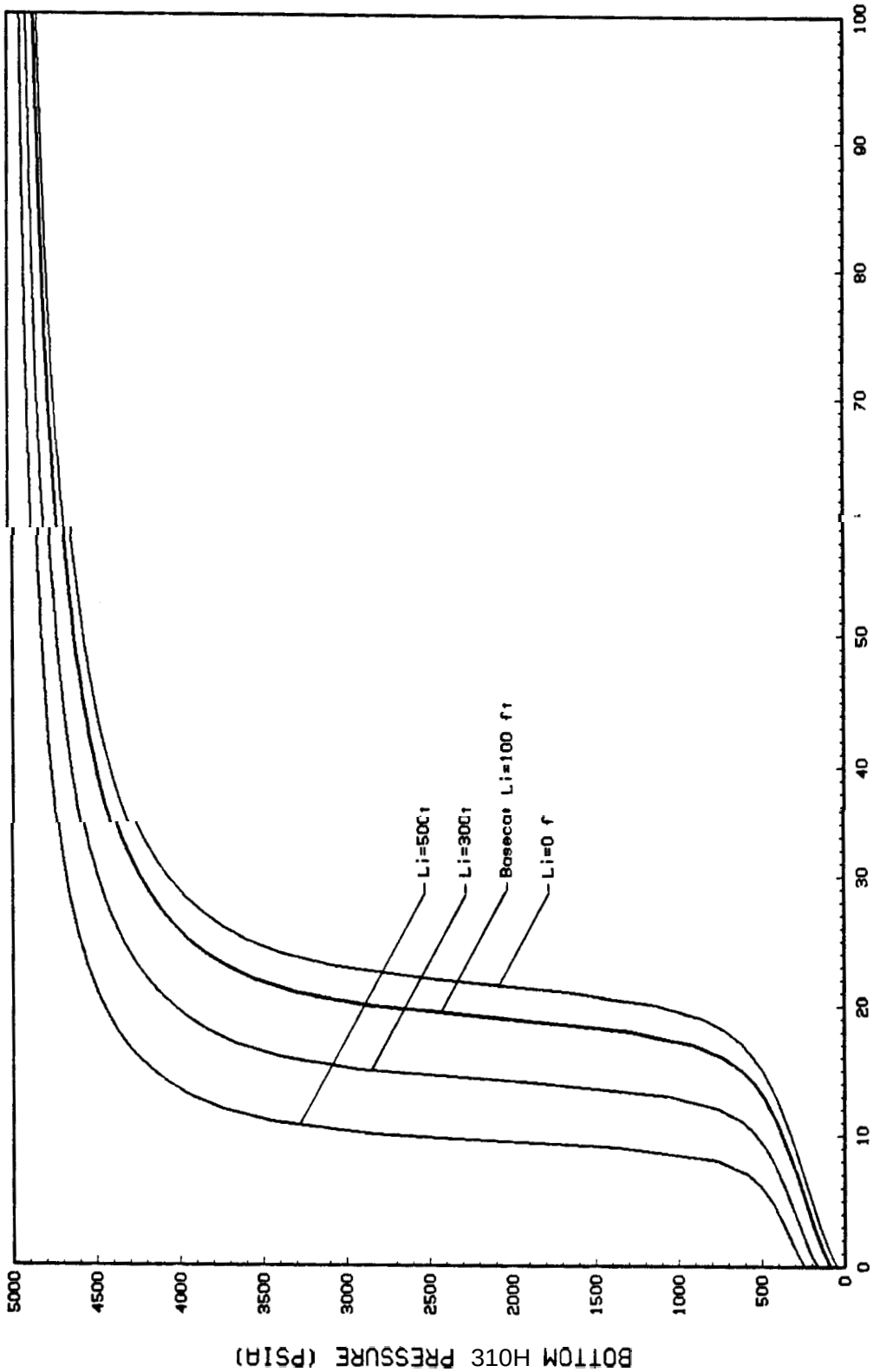

Figure 6.8 Pwf vs Time (Effect of Initial Fluid Level)

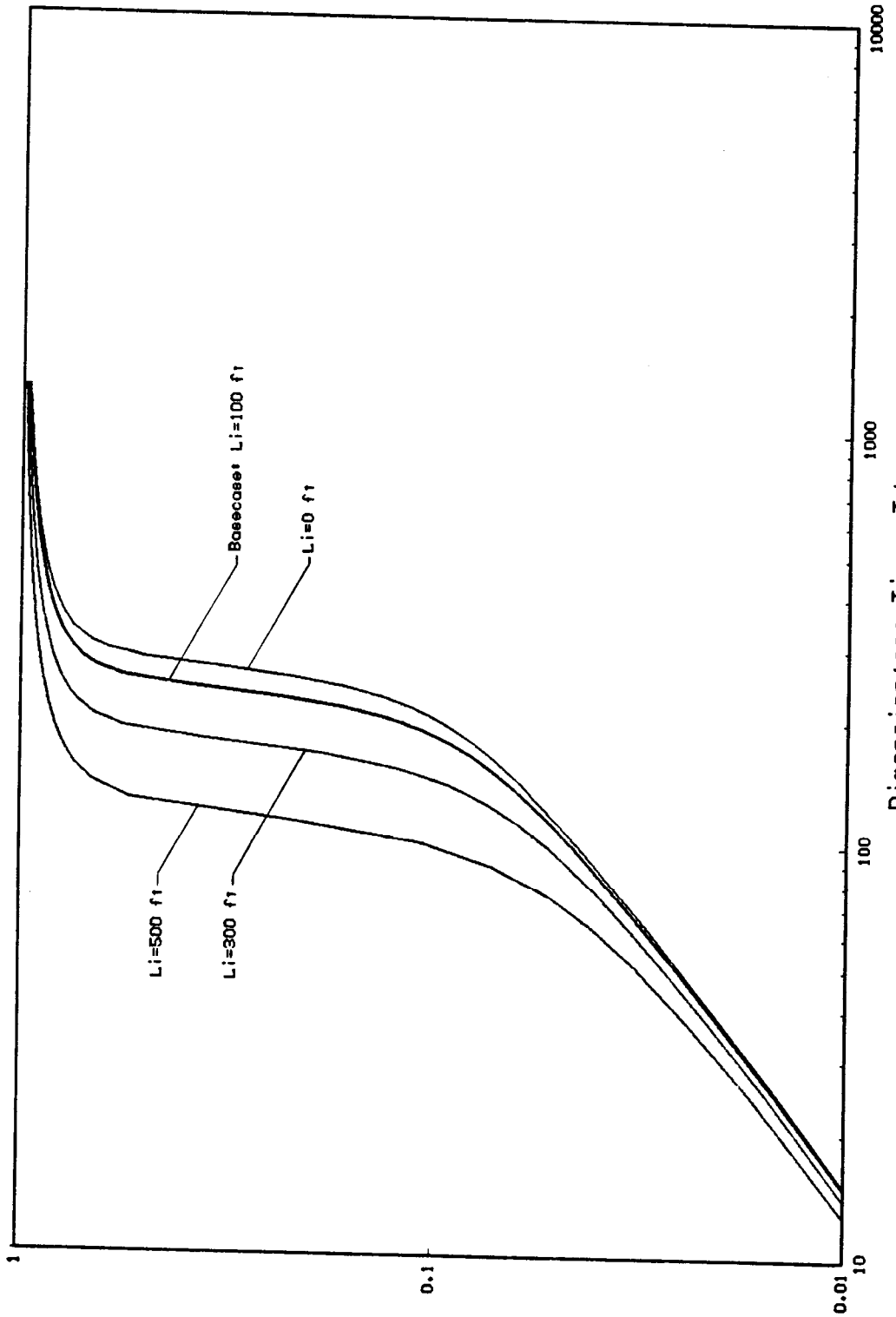

Figure 6.9 Early Time Plots (Effect of Initial Fluid Level)

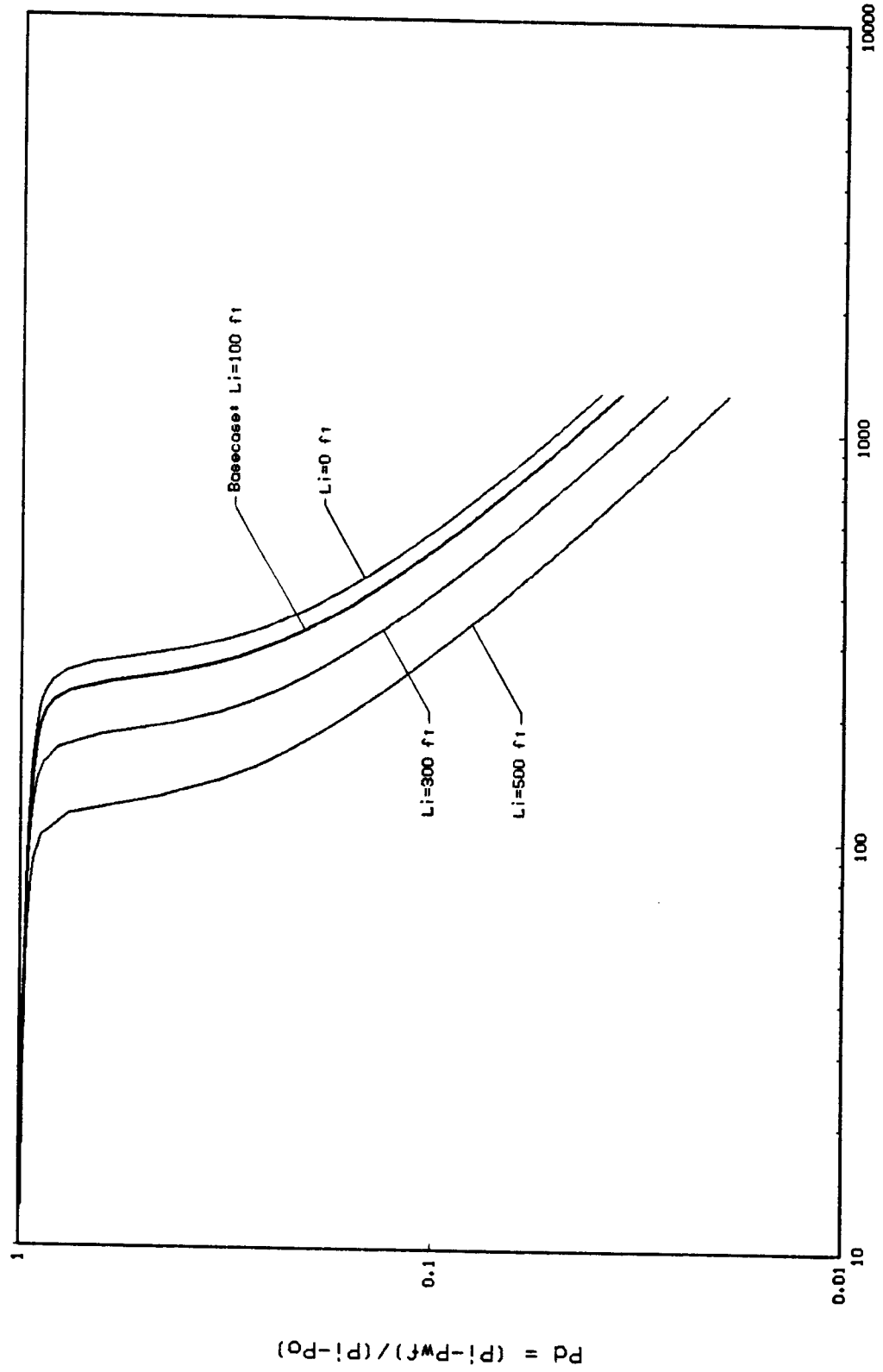

Figure 6.10 Late Time Plots (Effect of Initial Fluid Level)

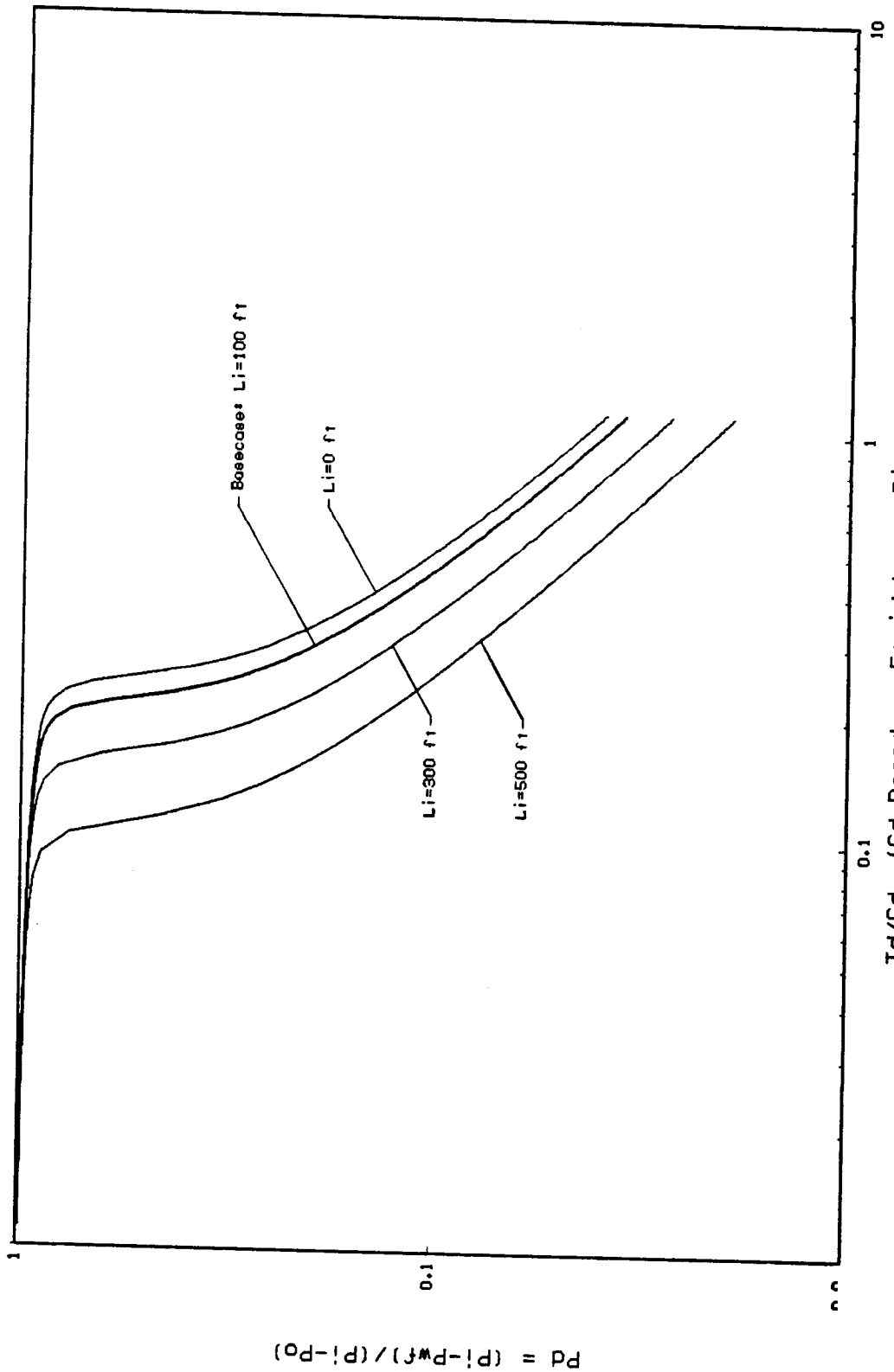

Figure 6.11 Late Time Plots (Effect of Initial Fluid Level)

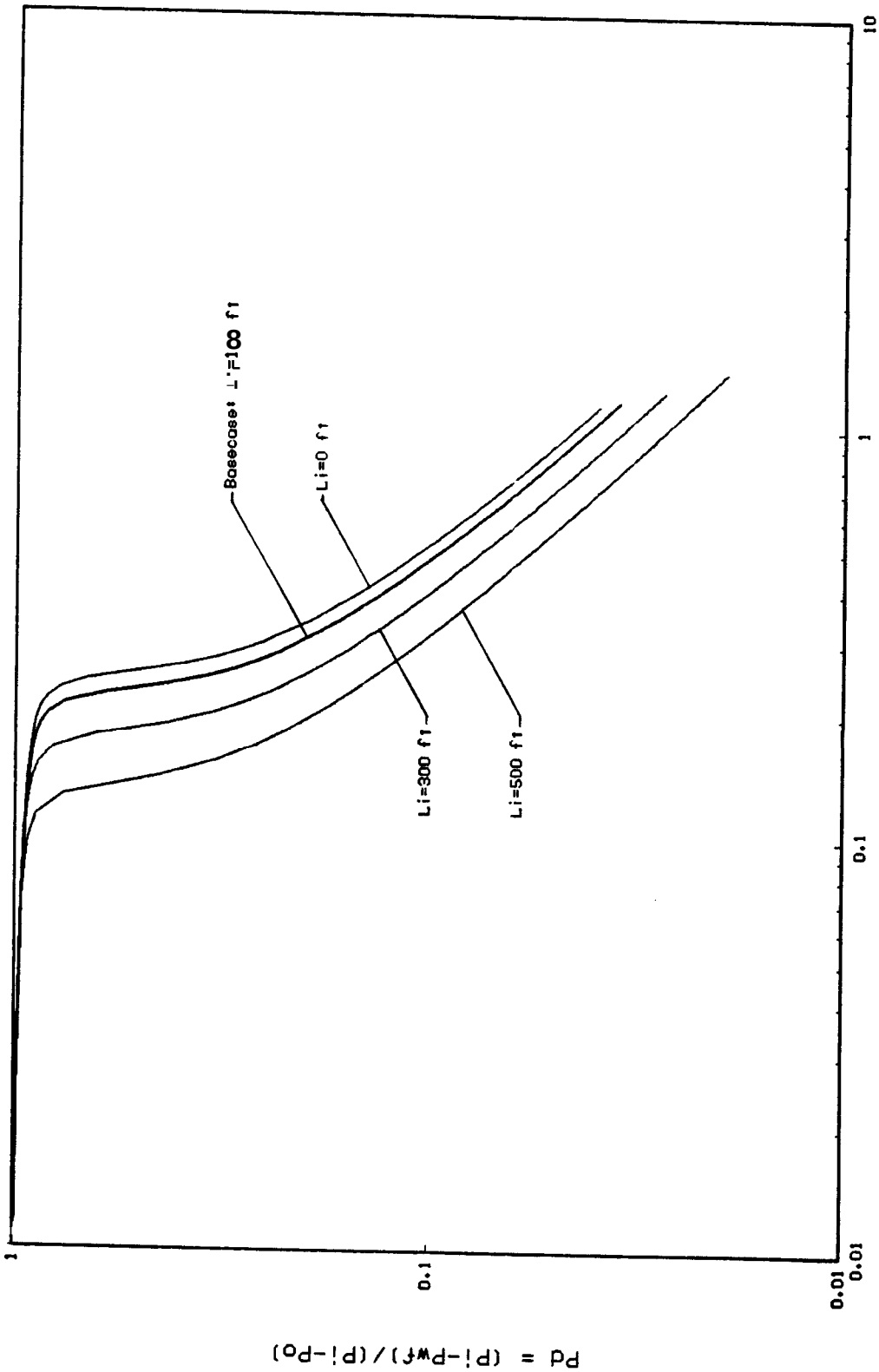

Figure 6.12 Late Time Plots (Effect of Initial Fluid Level)

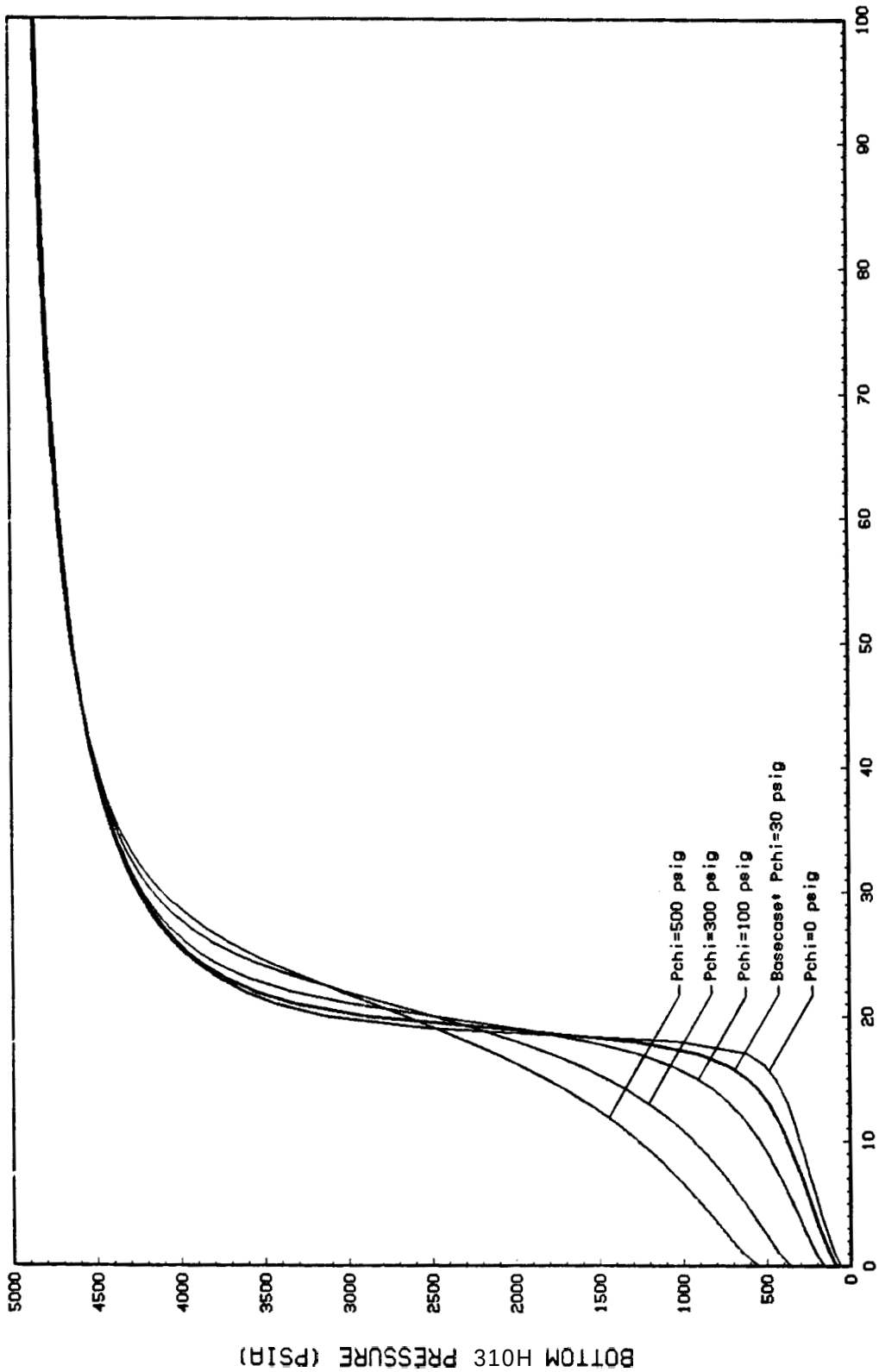

Figure 6.13 Pwf vs Time: (Effect of Initial Chamber Pressure)

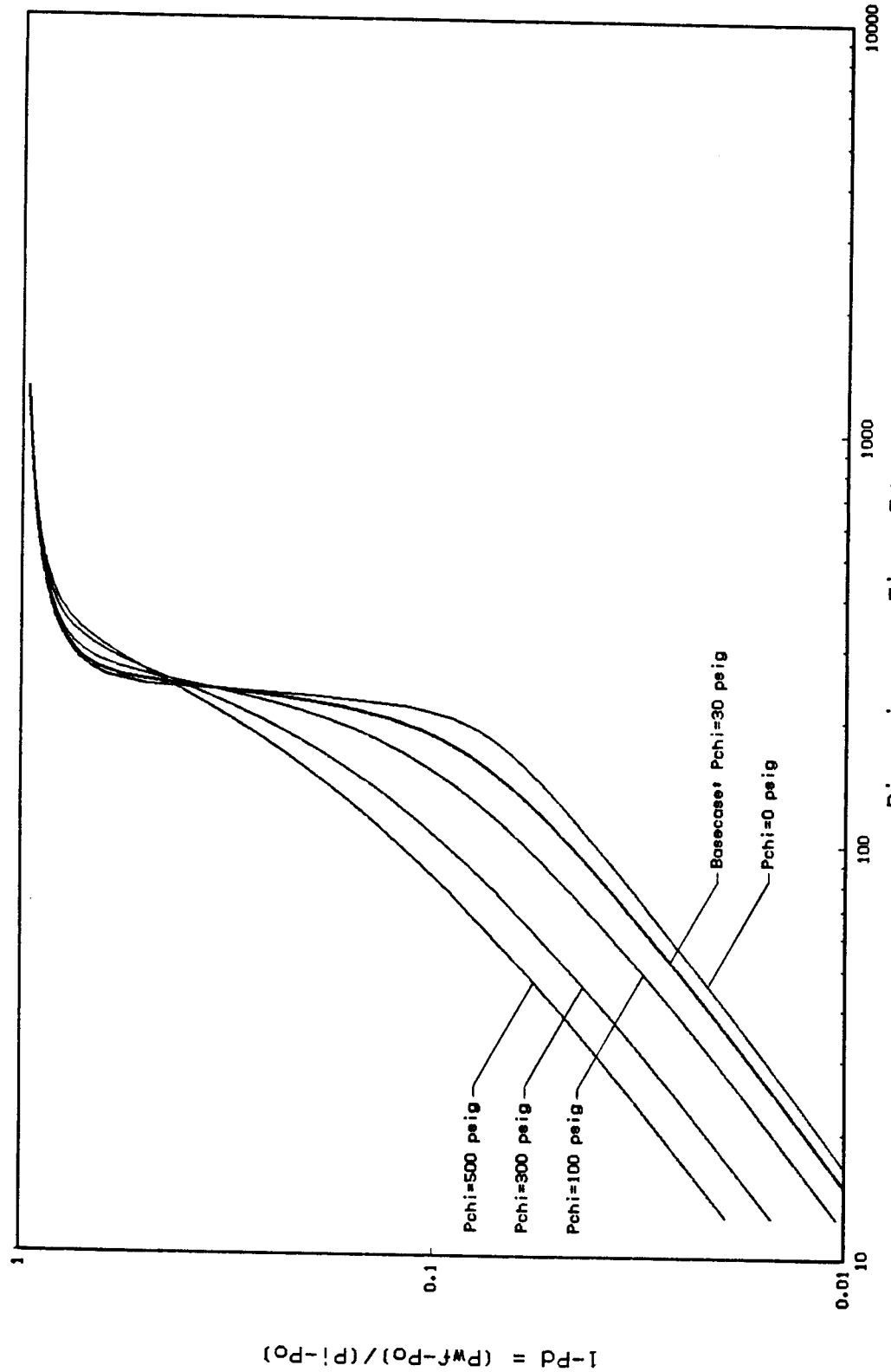

Figure 6.14 Early Time Plots (Effect of Initial Chamber Pressure)

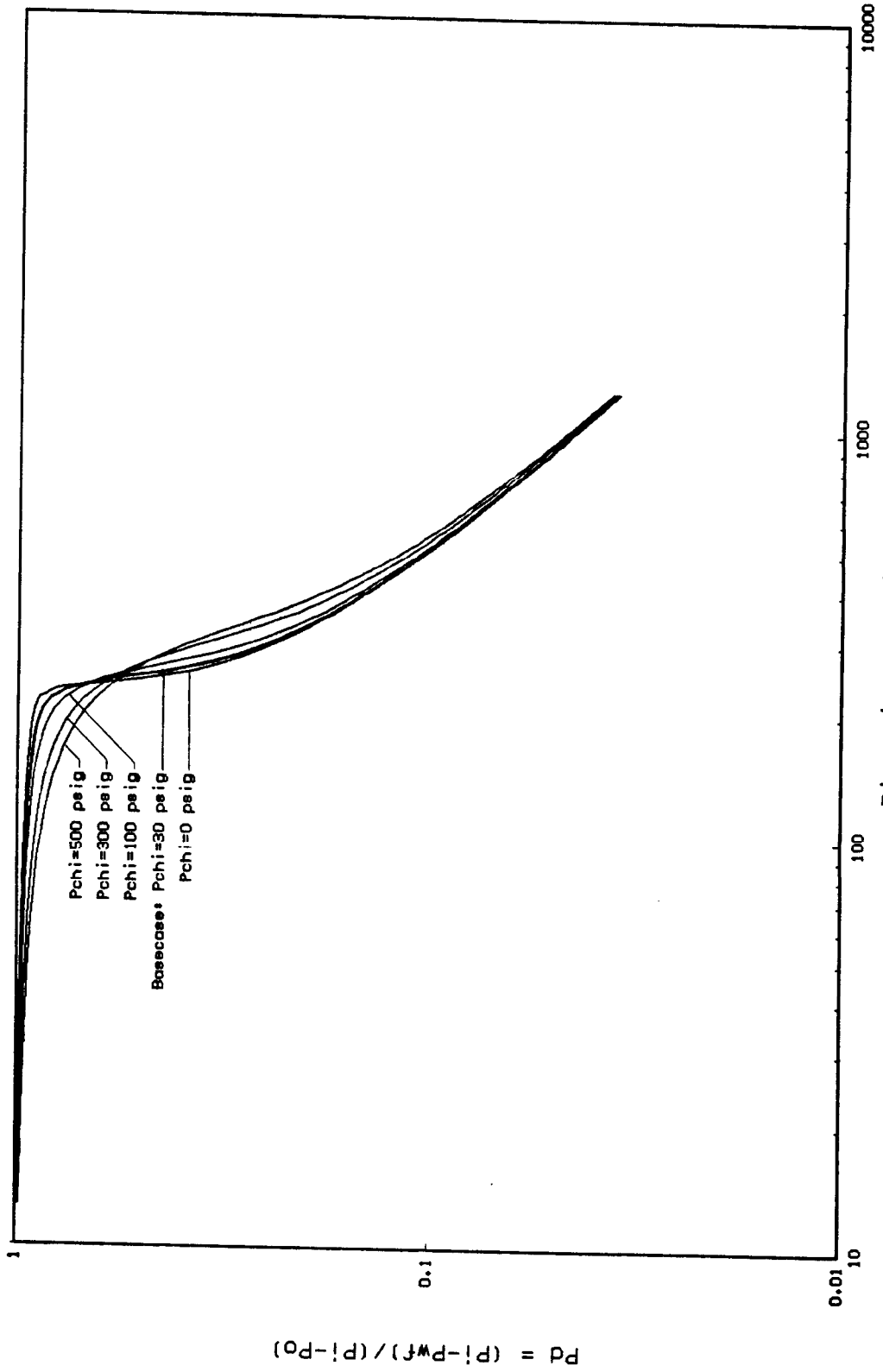

Figure 6.15 Log-Log Plots (Effect of Initial Chamber Pressure)

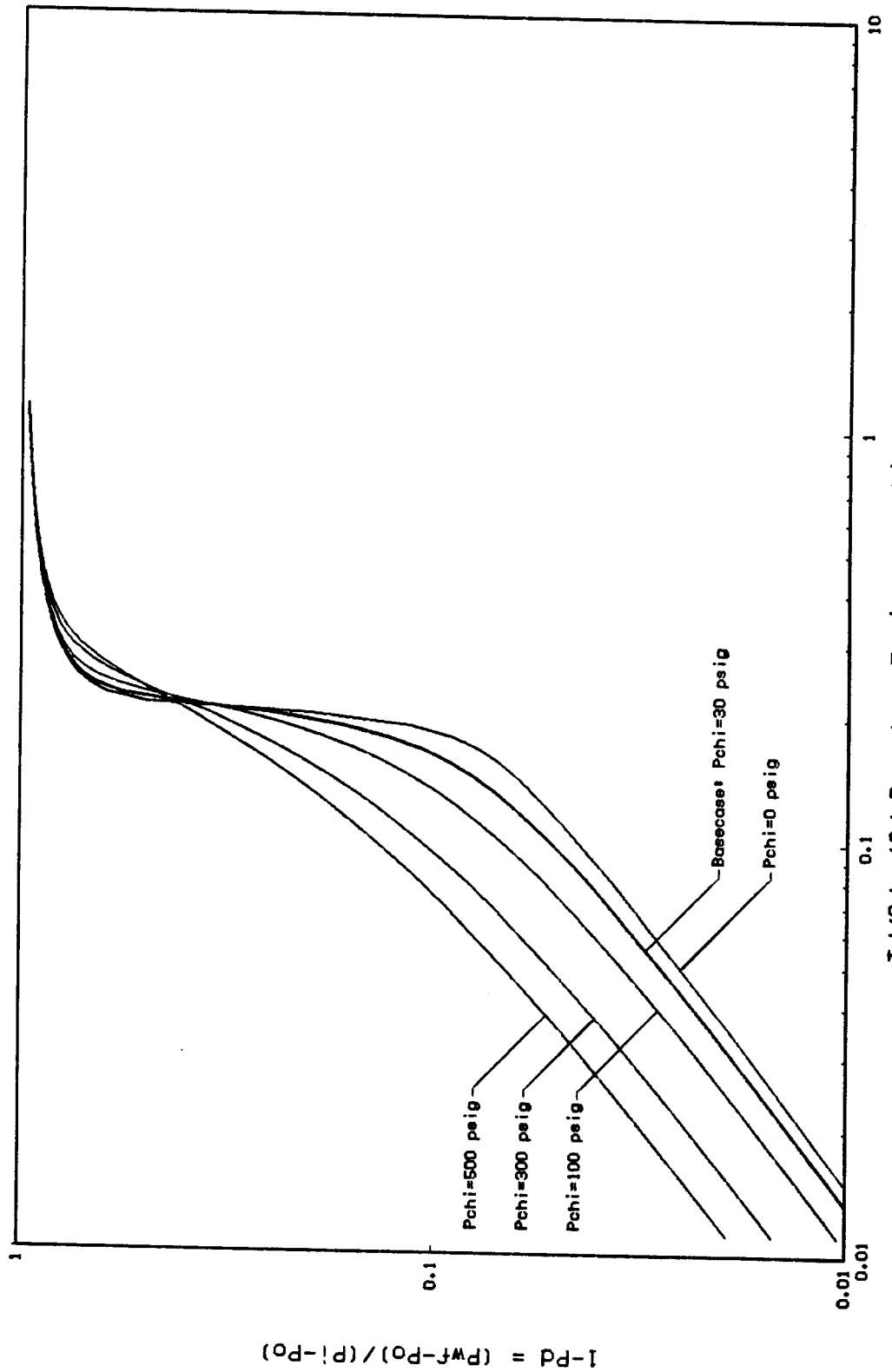

Figure 6.16 Early Time Plots (Effect of Initial Chamber Pressure)

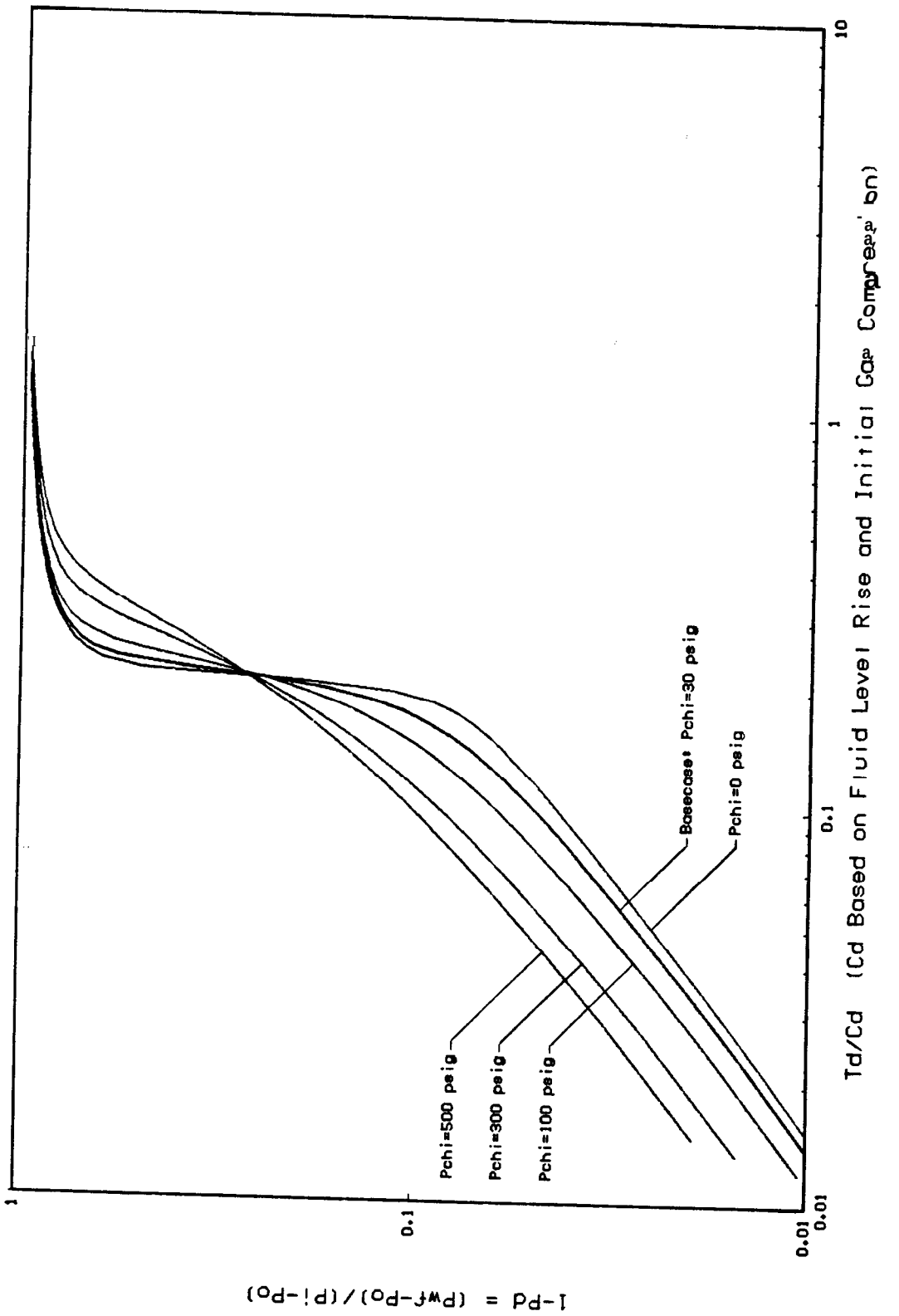

Figure 6.17 Early Time Plots (Effect of Initial Chamber Pressure)

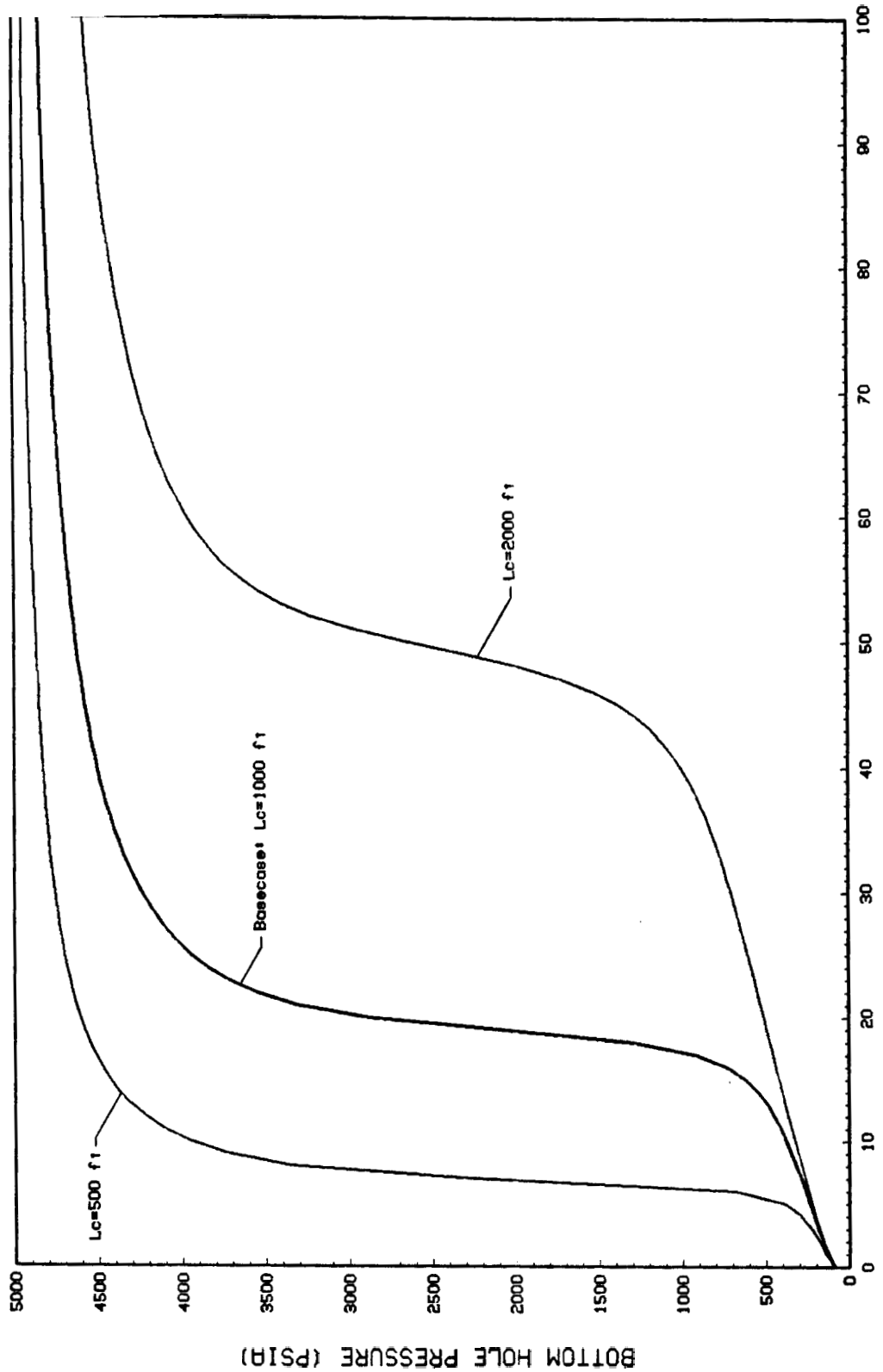

Figure 6.18 Pwf vs Time: (Effect of Total Chamber Length)

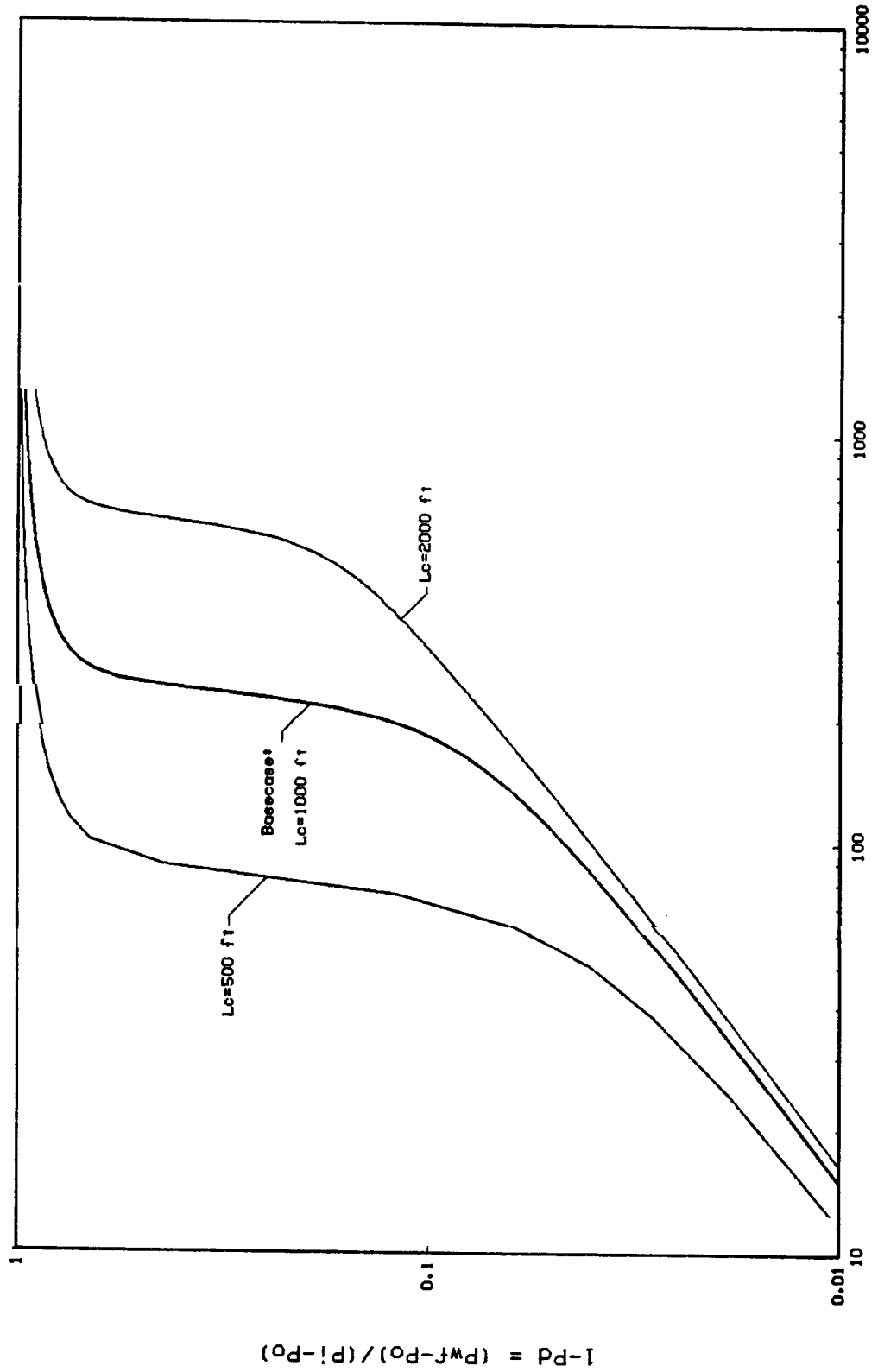

Figure 6.19 Early Time Plots (Effect of Total Chamber Length)

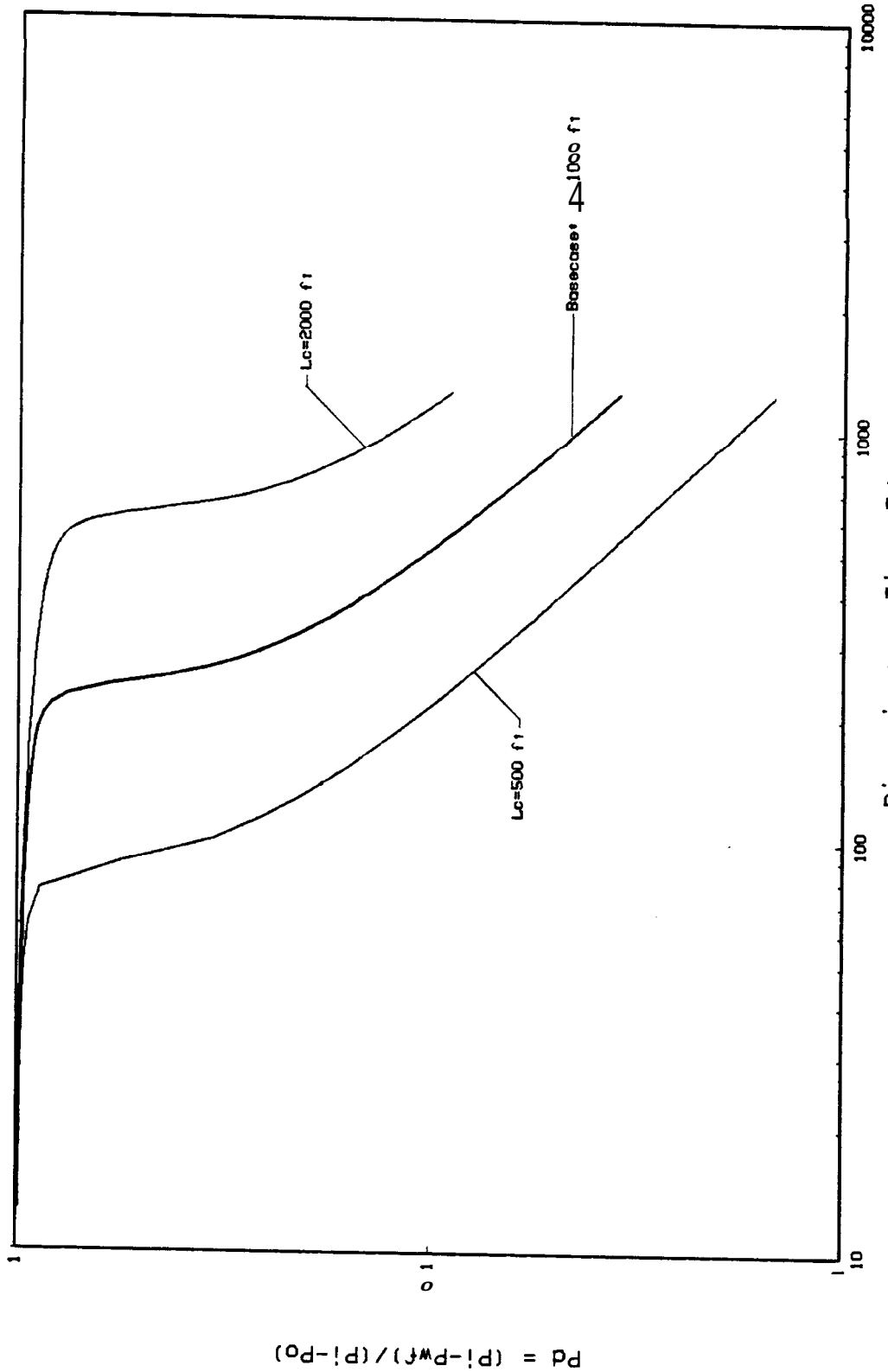

Figure 6.20 Late Time Plots (Effect of Total Chamber Length)

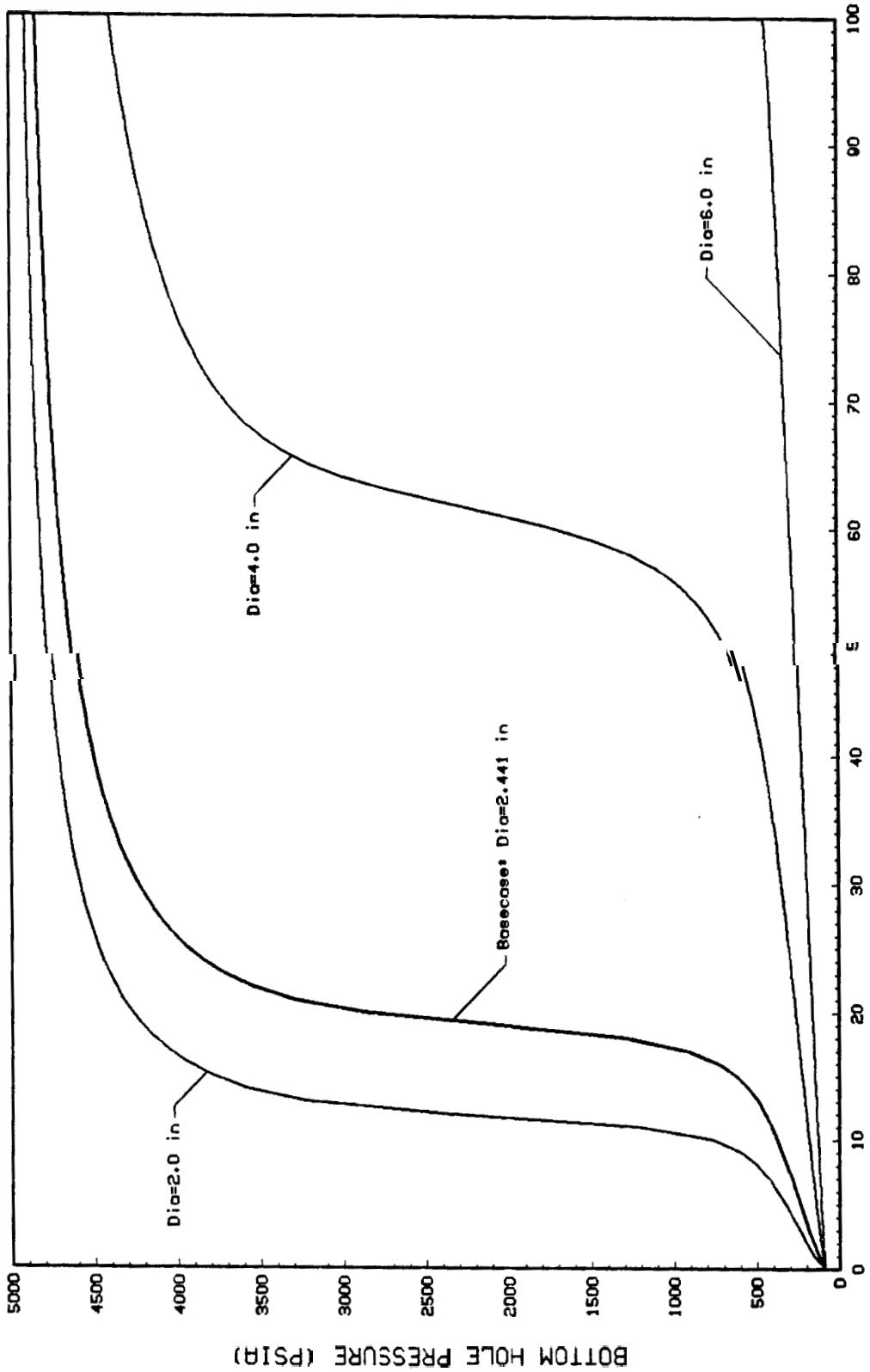

Figure 6.21 Pwf vs Time (Effect of Chamber Diameter)

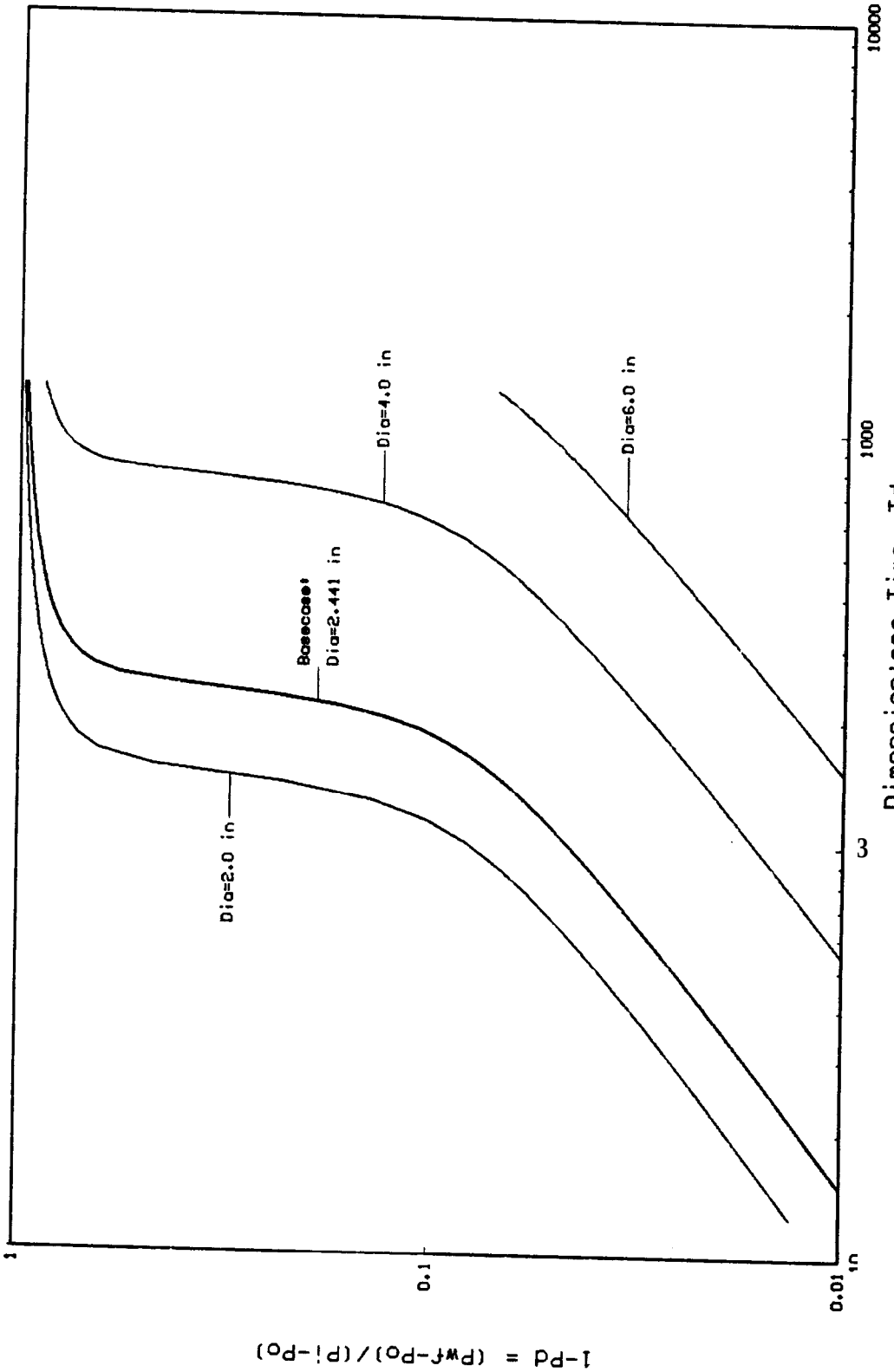

Figure 6.22 Early Time Plots (Effect of Chamber Diameter)

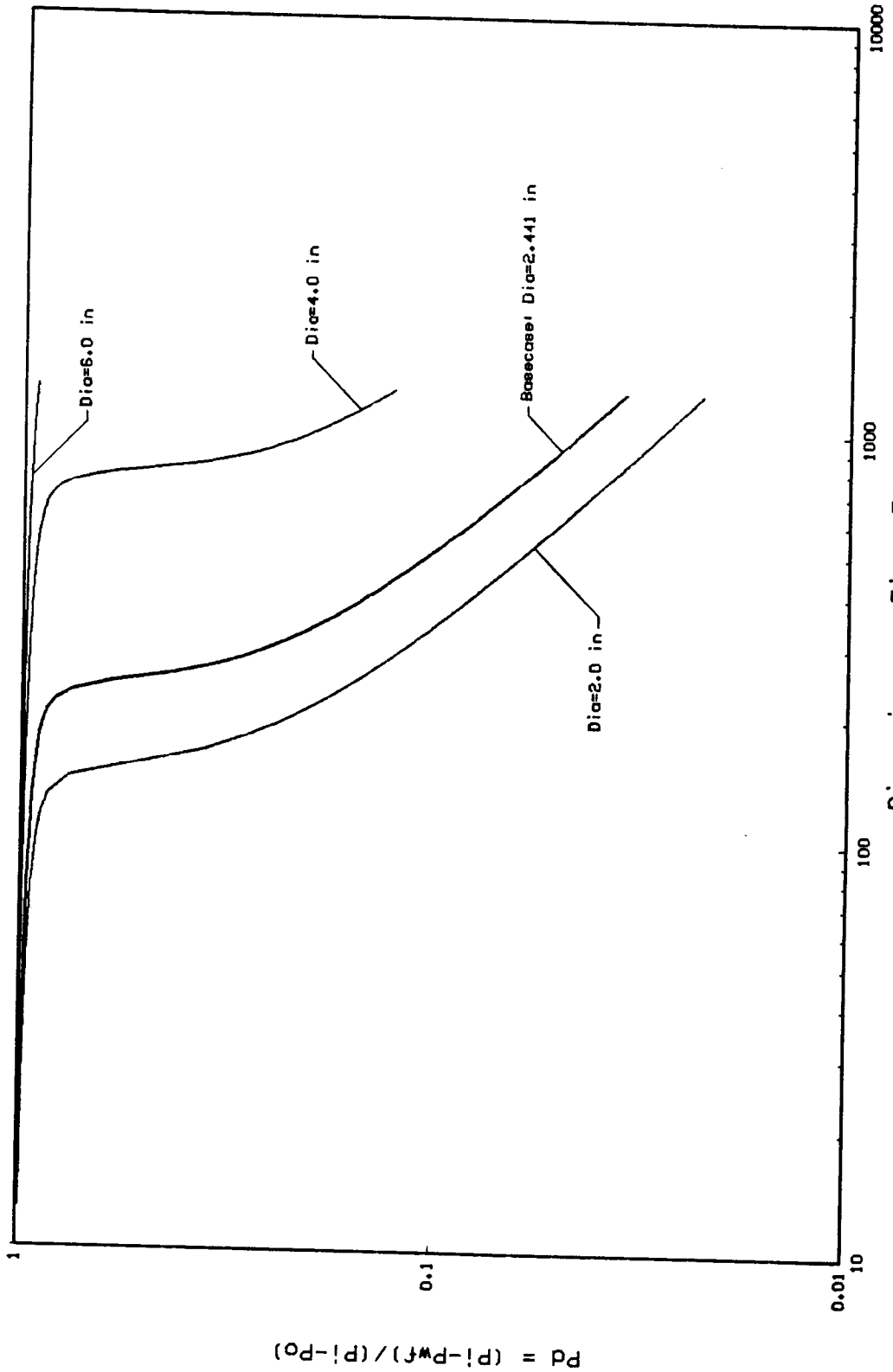

Figure 6.23 Log Time Plots (Effect of Chamber Diameter)

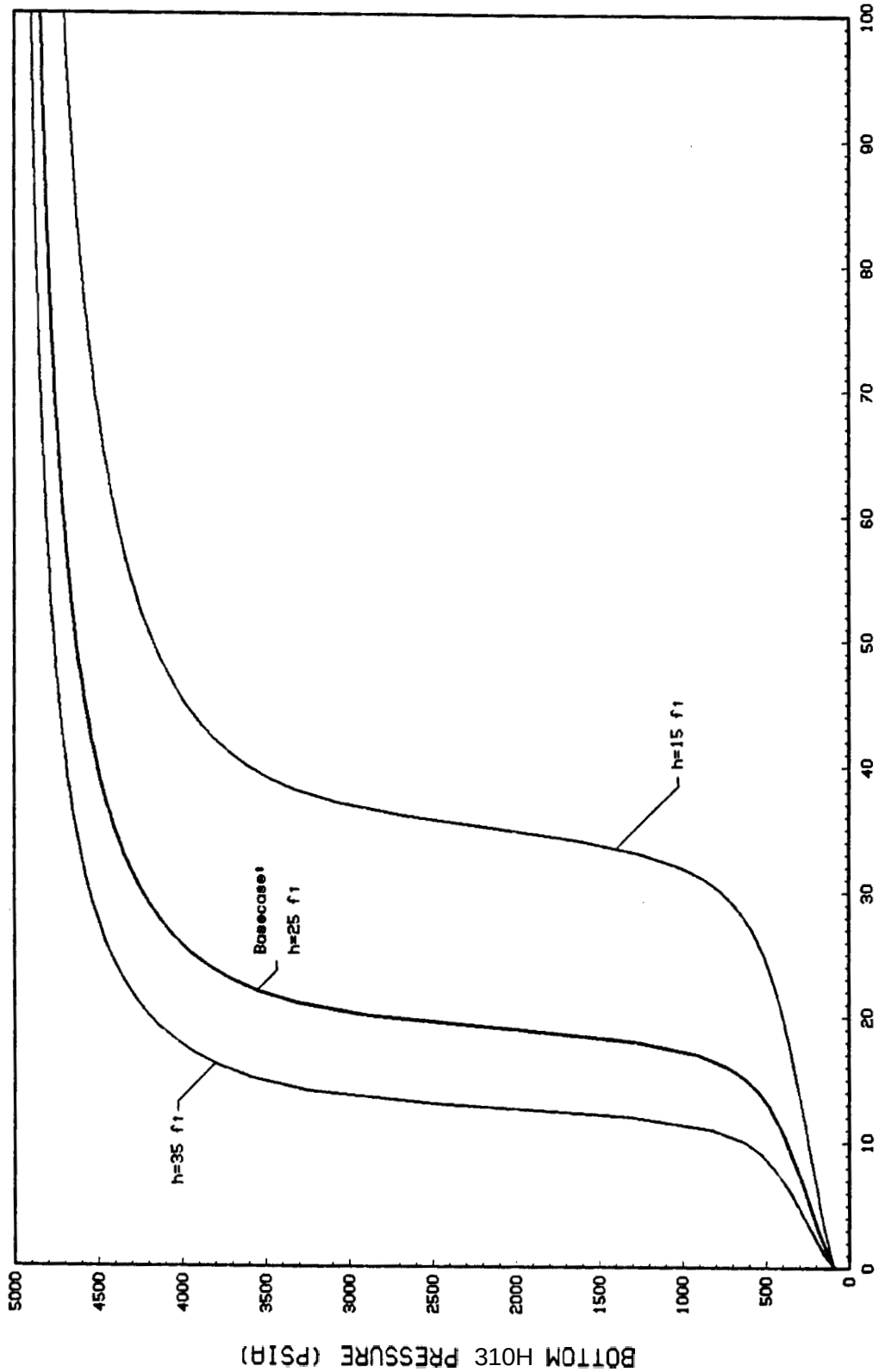

Figure 6.24 Pwf vs Time: (Effect of Reservoir Sand Thickness)

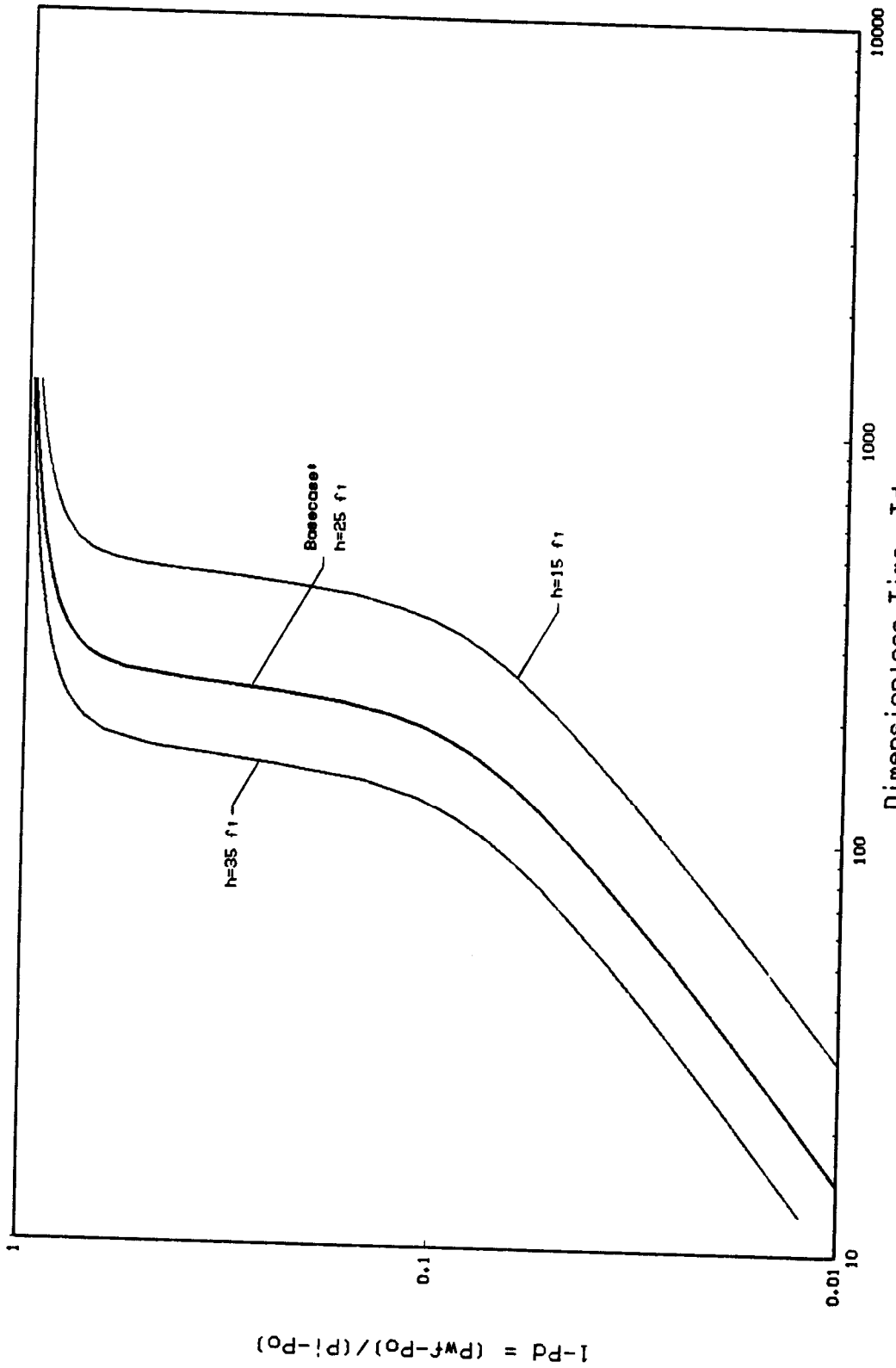

Figure 6.25 Early Time Plots (Effect of Reservoir Sand Thickness)

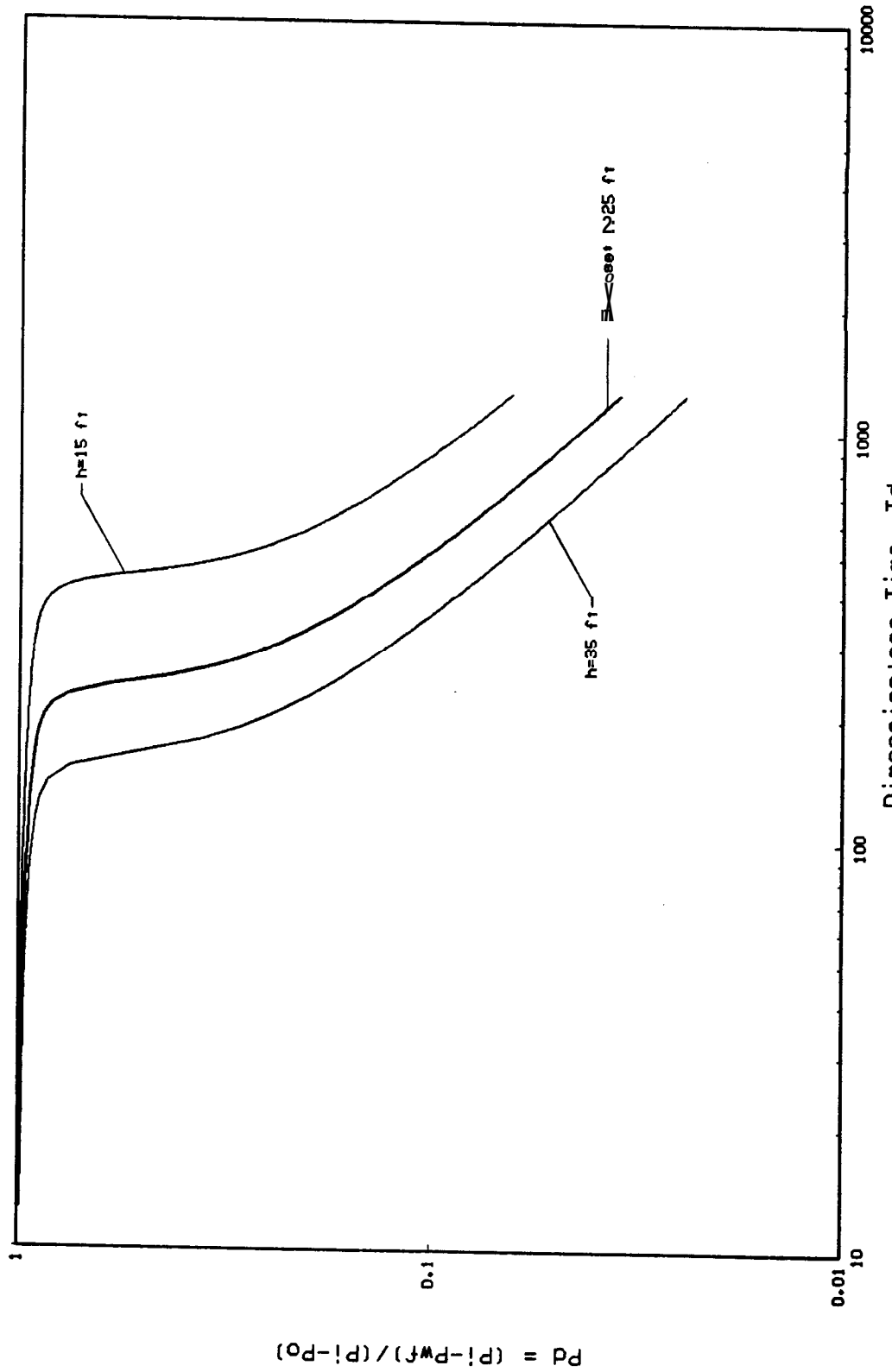

Figure 6.26 Late Time Plots (Effect of Reservoir Sand Thickness)

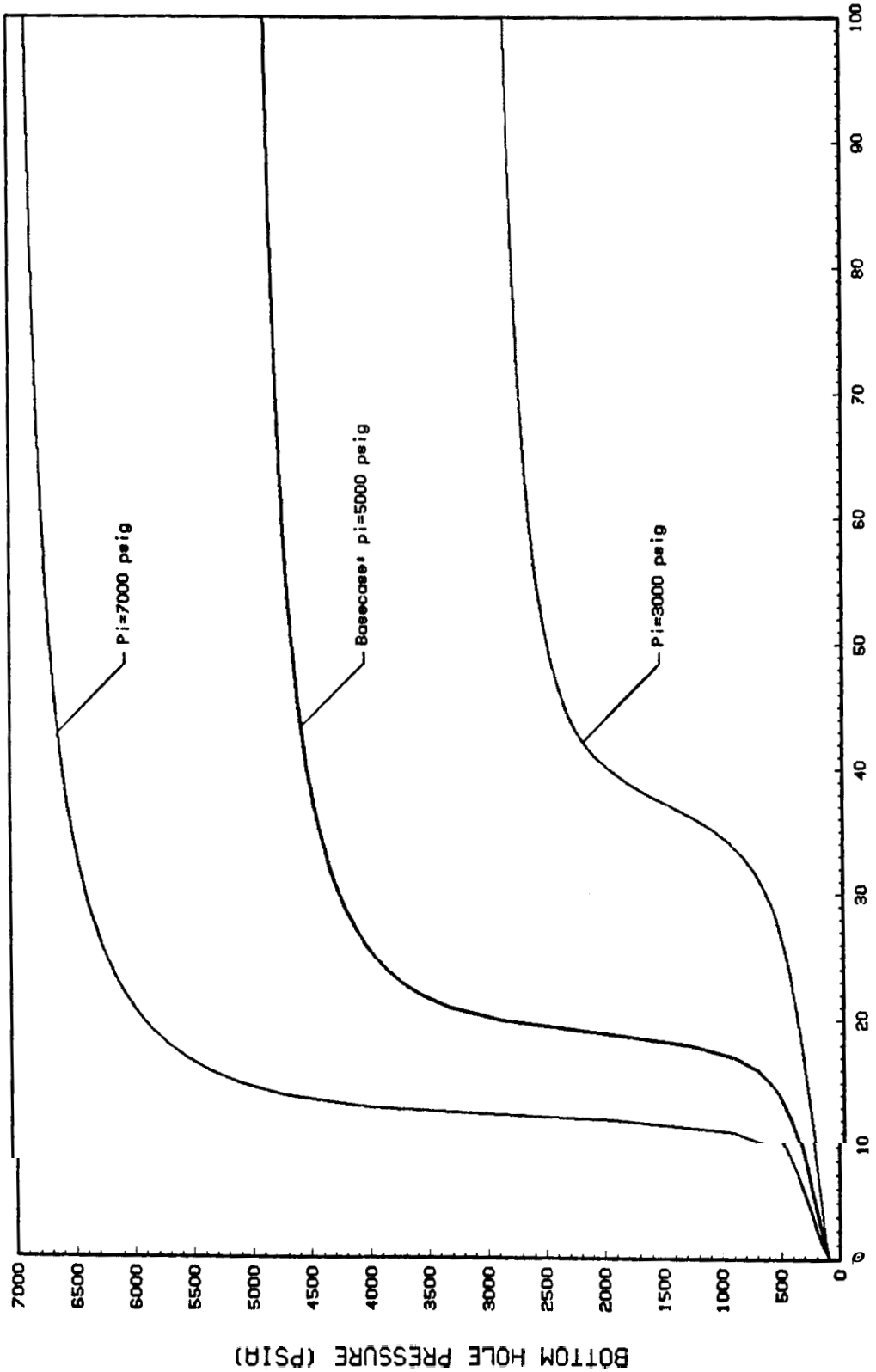

Figure 6.27 Pwf vs Time (Effect of Initial Reservoir Pressure)

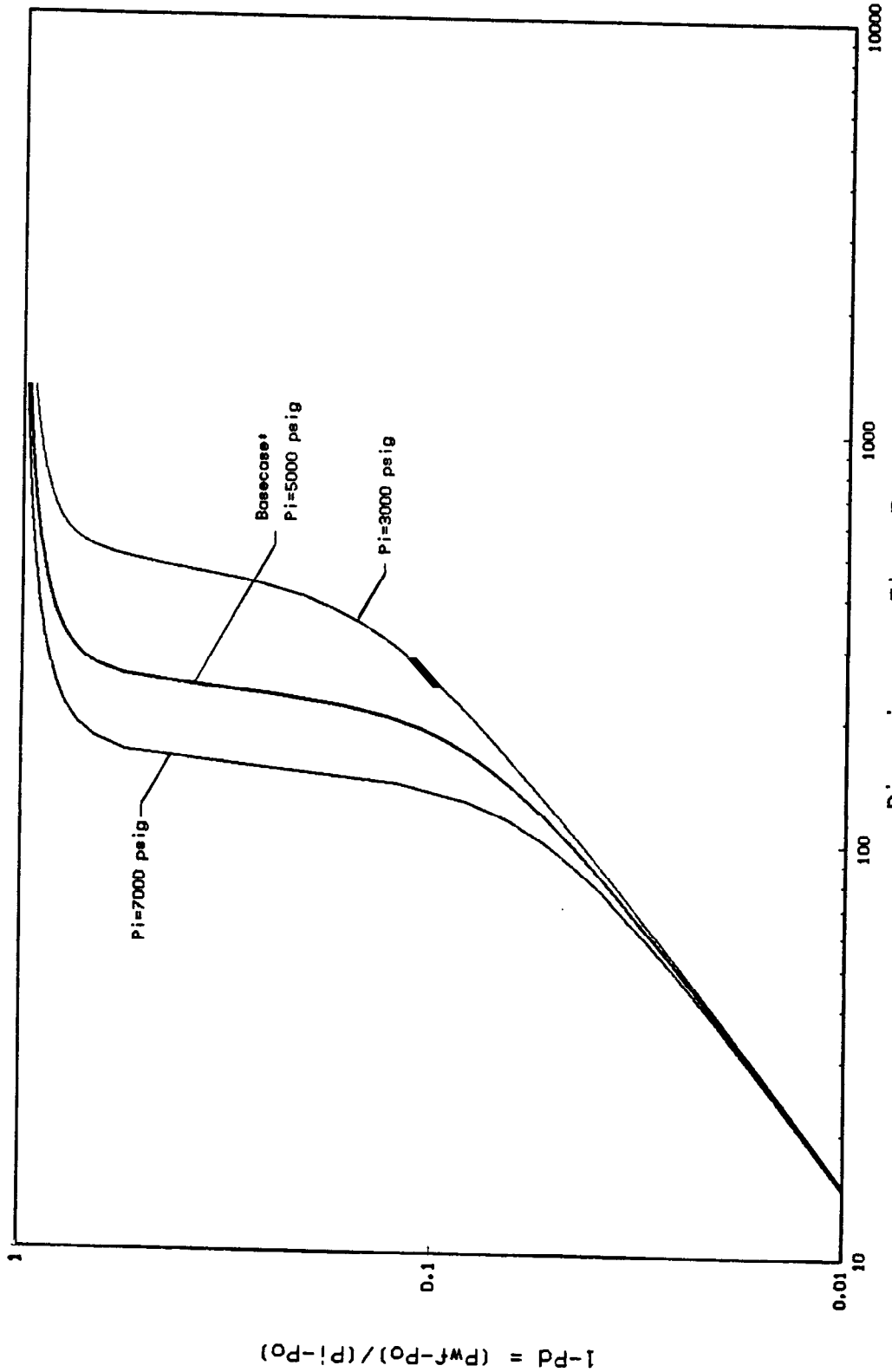

Figure 6.28 Early Time Plots (Effect of Initial Reservoir Pressure)

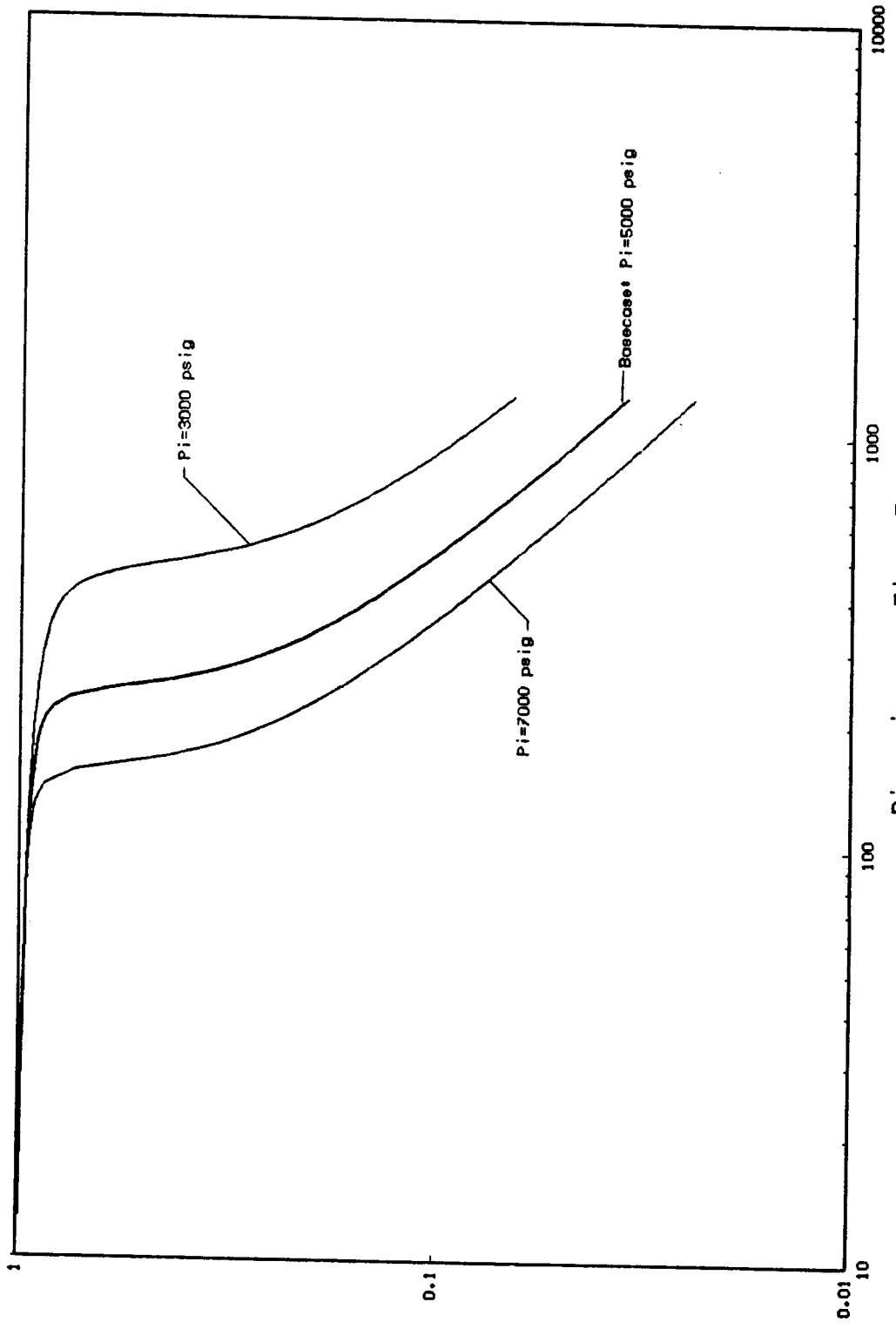

Figure 6.29 Log-Log Type Plots (Effect of Initial Reservoir Pressure)

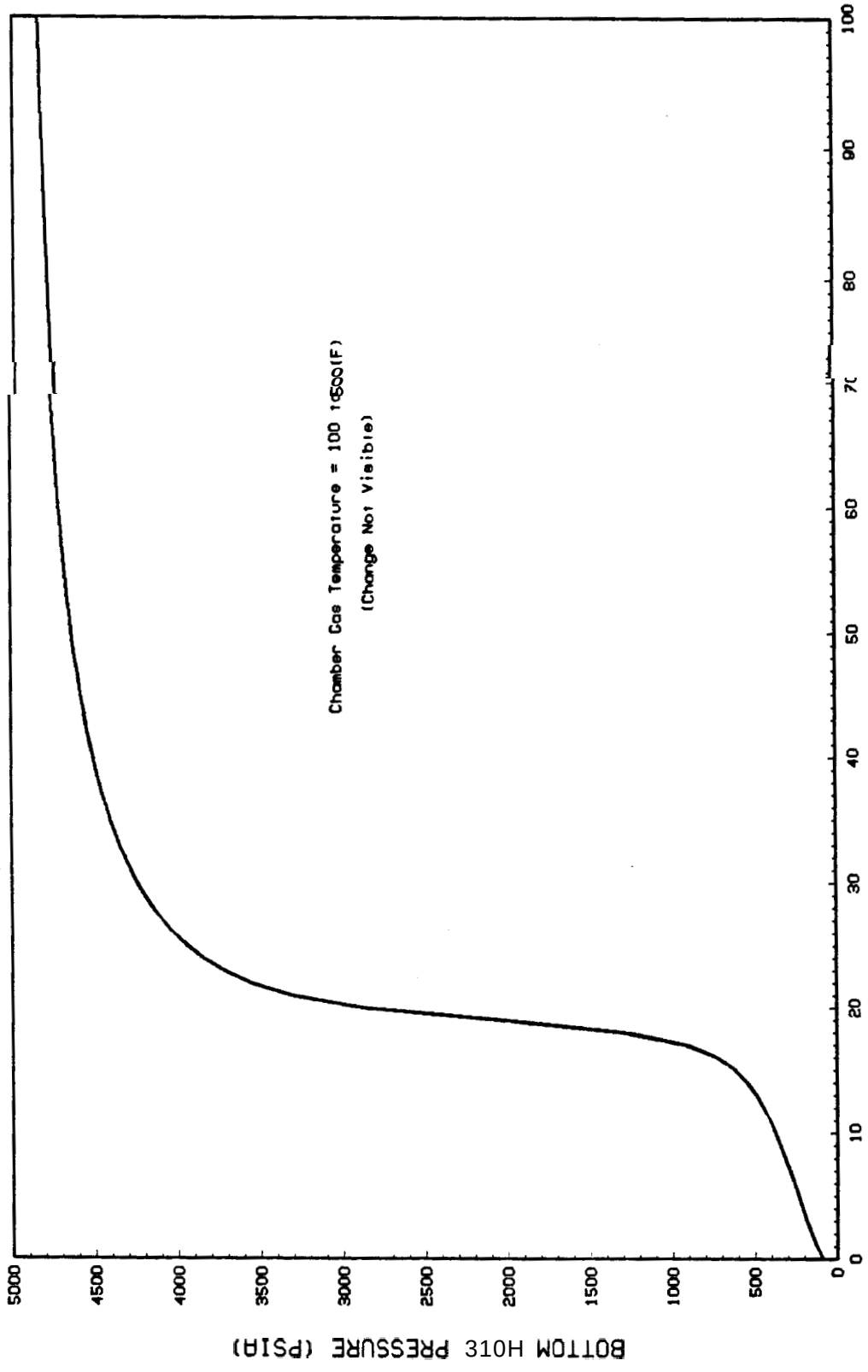

Figure 6.30 Pwf vs Time: (Effect of Chamber Gas Temperature)

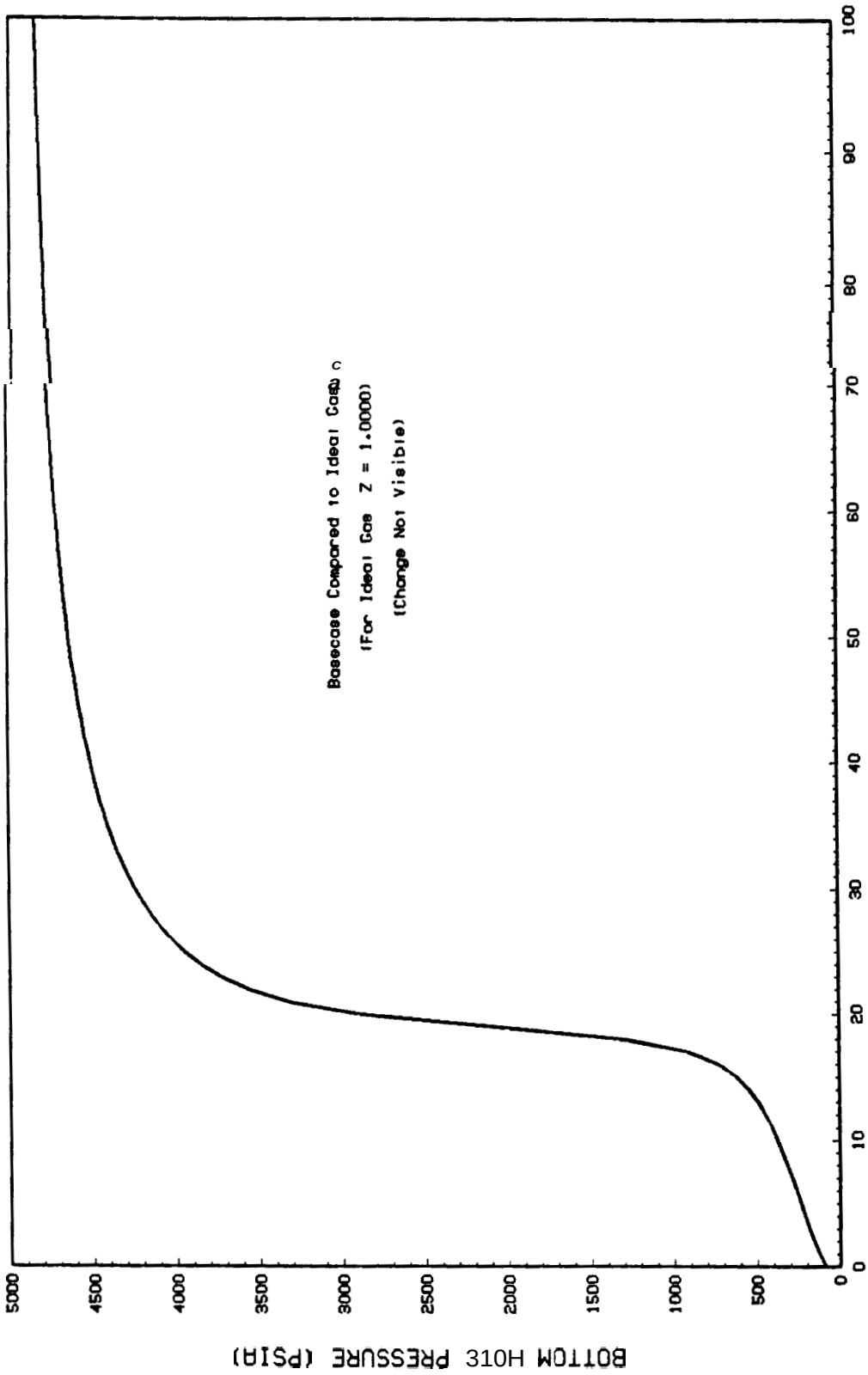

Figure 6.31 Pwf vs Time (Effect of Assuming Ideal Chamber Gas Behavior)

7: CONCLUSIONS AND RECOMMENDATIONS

A computer model was developed to simulate the pressure response of a closed chamber well test. Superposition of the constant pressure, cumulative influx solution to the radial diffusivity equation was used in the model to avoid the direct solution *of* the governing non-linear partial differential equations. Although real gas compressibility effects were included in the model, the effects of friction and momentum were not. Chamber **gas** compression was assumed isothermal in the mathematical model development.

The proposed superposition model was tested for ability to reproduce the **slug** test solution of Ramey, Agarwal, and Martin **(1875).** Agreement was found to be within ***0.7 X*** **for** values of t_D / C_D less than ***20.*** The percent deviation was shown **to** increase with respect to t_D / C_D. The deviation is believed a result of the cumulative error present in both solutions.

The superposition model provided illustration of differences between the **slug** test and closed chamber test. Initially the closed chamber test behaves **as** a slug test. Compression of the chamber gas causes the well bore storage to decrease during the test resulting in **a** dimensionless curve change on the **slug** test coordinates **of** Ramey et. al.. The final portion of the dimensionless curve ***is*** shifted on logarithmic coordinates **an** amount proportional to the ratio **or** the initial to final well bore storage. Because well bore storage changes during the test, there is no advantage to using t_D / C_D as the abscissa, **as** is an effective curve collapsing technique for the slug test.

The superposition model was used to generate dimensionless response curves for varying values of Hurst skin effect. The late time slug test format, with t_D as the abscissa, yields the greatest resolution to skin.

A sensitivity study was conducted to evaluate the influence of nine reservoir and tool parameters on the closed chamber pressure response. For a reservoir pressure of 5000 psig the effect of non-ideal gas behavior was shown insignificant. As a result, the pressure response is independent of gas gravity. Chamber gas temperature also was shown to have little effect on the bottom hole pressure response of the closed chamber test. In addition to yielding the greatest resolution to skin effect, the late time format of dimensionless plot was shown to be the least influenced by produced fluid gravity, which is often not known.

A greater portion of the closed chamber test response was shown to behave as a slug test as the chamber length and chamber diameter are increased. Similarly, maintaining an initial chamber pressure near atmospheric is required to produce slug test behavior during the early portion of the closed chamber test. Thus proper test tool design would allow a greater portion of the closed chamber test response to be analyzed using the slug test type curves of Ramey, Agarwal, and Martin (1975).

The results of the sensitivity study indicate that many variables, such as initial fluid column length, influence the closed chamber test pressure response. Because the solution approach was not analytic the dimensionless groups required to generalize the closed chamber test response were not derived. But the similar effect of chamber diameter and reservoir sand thickness suggest the existence of such groups.

Generation of closed chamber type curves for a particular test situation, by the superposition model, will require improvements in the efficiency of the model. An algorithm utilizing a variable time step composed of multiple increments of a

basic unit of time is suggested. Such a routine may require an iterative pressure calculation. It is believed that the improved model would require an order of magnitude less computer time due to the repetitive nature of the superposition calculation.

The greatest contribution of the model developed is the creation of a foundation for future analytic approaches to the closed chamber governing partial differential equations. The sensitivity study has shown that for typical reservoir pressures the chamber gas deviation from real gas behavior can be neglected. This result should facilitate development of the dimensionless groups needed to generalize the closed chamber test response.

Future studies should consider the effect of adiabatic chamber gas compression. Momentum and friction effects need also to be considered in the model. Data from backsurges performed in the Gulf of Mexico indicate limited occurrence of an oscillating fluid level resulting form the effects of momentum and friction.

Summary

1) A Superposition model was developed for the closed chamber test which neglects momentum and friction but includes real gas behavior.

2) The superposition model is capable of reproducing the slug test results of Ramey, Agarwal, and Martin (1975), which also neglected momentum and friction effects.

3) Closed chamber test deviation from the slug test was illustrated. The shift on logarithmic coordinates of the late time dimensionless closed chamber pressure response is proportional to the ratio of the initial to final well bore storage.

4) For the closed chamber well test, the late time slug test format of Ramey et. al. (1975), yields the greatest resolution to skin effect. The late time format

also has the advantage of being the least influenced by the produced fluid gravity, which is often unknown.

5) For moderate reservoir pressure, *(5000* psig), non-ideal chamber gas behavior does not affect the bottom hole pressure response of the closed chamber test. As a result, chamber gas gravity is insignificant.

6) Over a range of 100 to 500 (F), the temperature at which the isothermal compression of the chamber gas occurs does not influence the bottom hole pressure response of the closed chamber test.

7) A greater portion of the closed chamber test response wiii be equivalent to a slug test, and thus suitable for slug test type curve analysis, if the effect of the chamber gas compression is minimized during the test. The sensitivity study indicates that increasing the chamber length, increasing the chamber diameter, and decreasing the initial fluid column length will decrease the effect of chamber gas compression. An initial chamber gas pressure near atmospheric is required to avoid deviation from the equivalent early time slug test response.

Recommendations for Future Study

1) Return to governing partial differential equations and attempt to define dimensionless groups to generalize the closed chamber solution. The results of this study indicate it is reasonable to assume ideal gas behavior and thus neglect the real gas deviation factor in the deviation.

2) Improve the Superposition model with a variable time step.

3) Consider the effect of adiabatic chamber gas compression.

4) Determine the influence of momentum and friction on the closed chamber well test.

8: NOMENCLATURE

A_{ch} = Cross sectional area of chamber (ft^2)

C_D = Dimensionless well bore storage

C_t = Total formation compressibility (psi^{-1})

g = Acceleration of gravity constant ($32.2 \frac{ft}{sec^2}$)

h = Formation sand thickness (ft)

k = Reservoir permeability (milli-darcy)

k_{max} = Maximum anticipated reservoir permeability (milli-darcy)

K_0 = Modified Bessel function of second kind, first order

K_1 = Modified Bessel function of second kind, second order

L_c = Total chamber length as illustrated in figure 3.3 (ft)

L_i = Initial chamber length as illustrated in figure 3.3 (ft)

N = Time step index

N_p = Cumulative liquid production (ft^3)

p_{ch} = Chamber pressure (psia)

p_{ch_i} = initial chamber pressure (psia)

p_f = Formation pressure on the formation side of skin (psia)

p_{f_D} = Dimensionless pressure drop on the formation side of skin

p_{wf} = Flowing pressure in the well bore (psia)

p_{wf_D} = Dimensionless pressure drop within the well bore

p_i = Static initial reservoir pressure (psia)

p_o = Minimum well bore pressure achieved during test (psia)

$\bar{q}_D$ = Laplace Dimensionless rate of influx

Q = Cumulative influx (ft^3)

$\bar{Q}_D$ = Laplace Dimensionless cumulative influx

Q_D = Dimensionless cumulative influx

r_w = Well bore radius (ft)

r_D = Dimensionless radius

s = Laplace variable

S = Dimensionless skin factor

t = Time (seconds)

Δt = Time step (seconds)

t_D = Dimensionless time

Δt_D = Dimensionless time step

V_{ch} = Chamber gas volume (ft^3)

V_{ch_i} = Initial chamber gas volume (ft^3)

X = Dynamic fluid level as illustrated in figure 3.3 (ft)

ΔX = Fluid level change per time step (ft)

Z = Real gas deviation factor of chamber gas

Z_i = Initial real gas deviation factor of chamber gas

β = Influx constant as defined in equation 3.17 ($\frac{ft^3}{psi}$)

μ = Fluid viscosity (centi Poise)

φ = Formation porosity (fraction)

ρ_f = Fluid density ($\frac{lbm}{ft^3}$)

Subscripts

ch = Chamber conditions

D = Dimensionless

o = Minimum during test

p = Produced

t = Total

wf = Bottom hole flowing conditions

REFERENCES

Alexander, L. G. :"Theory and Practice of the Closed Chamber Drillstem Test Method," *Soc. Pet. Eng. J.* (December 1977), p. 1539.

Brill, J. P. and Beggs, H. D., University of Tulsa : "Two Phase Flow in Pipes," INTER-COMP Course, The Hague, 1974.

Dake, L. P: Fundamentals of Reservoir Enaineerina, Elservier Scientific Publishing Company, Amsterdam, The Hague, 1974.

Da Prat, G: "Well Test Analysis for Naturally Fractured Reservoirs," Ph.D. Dissertation, Stanford University, July 1981.

Mateen, K.: "Slug Test Data Analysis in Reservoirs with Double Porosity Behavior," M.S. Report, Stanford University, September 1983.

Ramey, H. J., Agarwal, R. G., and Martin, I.: "Analysis of Slug Test or DST Flow Period Data," *Can Pet. J.* (July 1975).

Saldana, M.: "Flow Phenomenon of Drill Stem Test With Inertial and Frictional Wellbore Effects," Ph.D. Dissertation, Stanford university, October 1983.

Shinohara, K.: "A Study of Inertial Effect in the Wellbore in Pressure Transient Well Testing," Ph.D. Dissertation, Stanford University, April 1980.

Stehfest, H: "Algoritm 368, Numerical Inversion of Laplace Transforms," *Communications of the ACM*, D-5 (January 1970) 13, No. 1, 47-49

Standing, M. B.: Volumetric and Phase Behavior of Oil Field Hydrocarbon Svstems , Millet the Printer, Inc., Dallas Texas 1981, p. 122

Suman, G. O., Jr., Ellis, R. C, and Snyder, R. E: Sand Control Handbook, Gulf Publishing Company, Houston Texas, 1983, 30-31.

APPENDIX A

COMPUTER PROGRAM

```
C     ************************************************************************
C     *                                                                      *
C     *          CLOSED CHAMBER WELL TEST RESPONSE SIMULATOR                 *
C     *                                                                      *
C     ************************************************************************
C     *                                                                      *
C     *  This program generates a pressure as a function of time             *
C     *  response for a Closed Chamber Drill Stem test. The method of        *
C     *  solution is a well bore material balance of the fluids              *
C     *  produced.  Fluid influx is evaluated by superposition of the        *
C     *  constant pressure cumulative influx solution.                       *
C     *                                                                      *
C     *  The program is written for interactive input of run parameters      *
C     *  at execution time.  The output file name is also specified at       *
C     *  execution time.                                                     *
C     *                                                                      *
C     *  Veriable Definitions:                                               *
C     *                                                                      *
C     *    ALC =    Total Chamber Length as shown in figure 3.3 (ft)        *
C     *    ALI =    Initial Fluid Column Length (ft)                        *
C     *    API =    Produced Liquid Gravity (Degrees API)                   *
C     *    B =      Influx Constant ((ft**3)/psi)                           *
C     *    CL =     Fluid Column Length within chamber (ft)                 *
C     *    CT =     Total Formation Compressibiltlty (psi**(-1))            *
C     *    D =      Internial Chamber Diameter (in) ---> (ft)               *
C     *    DB =     Lower Surge Valve Depth (ft)                            *
C     *    DF =     Mid-Perforation Depth (ft)                              *
C     *    DT =     Time Step (seconds)                                     *
C     *    DTD =    Dimensionless Time Step                                 *
C     *    DU =     Upper Surge Valve Depth (ft)                            *
C     *    DW =     Well Bore Diameter (in)                                 *
C     *    DZ =     Change in Z during one iteration                        *
C     *    FP =     Cumulative Liquid Produced (ft**3)                      *
C     *    GG =     Chamber Gas Gravity (relative to air)                   *
C     *    H =      Formation Sand Thickness (ft)                           *
C     *    IFLAG =  Flag Veriable for Iterative Z factor Calculation:       *
C     *               0 = Convergence Achieved                               *
C     *               1 = No Convergence                                     *
C     *    MMBSK0 = Modified Bessel Function of the Second Kind, Order-0     *
C     *    MMBSK1 = Modified Bessel Function of the Second Kind, Order=1     *
C     *    N =      Time Step Index                                         *
C     *    NAME =   Output File Name                                        *
C     *    NDP =    Number of Output Data points                            *
C     *    NOUT =   Number of Time Steps between output data points         *
C     *    P =      Bottom Hole Flowlng Pressure Array (psia)               *
C     *    PCH =    Chamber Gas Pressure (psia)                             *
C     *    PCHI =   Initial Chamber Gas Pressure (psig) ---> (psia)         *
C     *    PERM =   Formation Permeability (milli-darcy)                    *
C     *    PHI =    Formation Porosity (fraction)                           *
C     *    PI =     Initial Reservoir Static Pressure (psig) ---> (psia)    *
C     *    PR =     Pseudo Reduced Pressure                                 *
C     *    Q =      Dimensionless Cumulatlve Fluid Influx Array             *
C     *    RW =     Well Bore Radius (ft)                                   *
C     *    SFG =    Specific Liquld Gravity (relative to water)             *
C     *    SKN =    Hurst Skin Factor                                       *
C     *    T =      Time Elapsed Array (seconds)                            *
C     *    TEMP =   Chamber Gas Temperature (F) ---> (R)                    *
C     *    TR =     Pseudo Reduced Temperature                              *
C     *    UF =     Produced Liquid Viscosity (cP)                          *
C     *    X =      Fluld Level measured from Mid-Perferatlons (ft)         *
C     *    Z =      Chamber Real Gas Deviation Factor                       *
C     *    ZI =     Initial Chamber Real Gas Deviation Factor               *
C
```

```
C     *  NOTE:  Input variable units are "field units" and converted to *
C     *         absolute units during execution.  In the above variable *
C     *         listing this change in units in denoted as:             *
C     *                                                                 *
C     *                 (input unit) --->(output unit)                  *
C     *                                                                 *
C     *  SUBROUTINES:                                                   *
C     *    GPC =   Pseudo Critical Temperature and Pressure Calculation *
C     *            for hydrocarbon gas.                                 *
C     *    GZ  =   Real Gas Deviation Factor Calculation for Hydrocarbon*
C     *            gas.                                                 *
C     *  FUNCTIONS:                                                     *
C     *    OD  =   Dimensionless Influx from Dimensionless Time and Skin*
C     *    PWD =   The Stehfest Algorithm                               *
C     *    PWDL =  LaPlace Influx Solution called by Stehfest Algoritym *
C     *  EXTERNAL FUNCTIONS: (IMSL Library Routines Used)               *
C     *    MMBSK0 = Modified Bessel Function: Second Kind, Zero Order   *
C     *    MMBSK1 = Modified Bessel Function: Second Kind, First Order  *
C     *                                                                 *
C     *  Jeff Simmons                                  February 1984    *
C     *******************************************************************
C
      IMPLICIT REAL*8(A-H,O-Z)
      DOUBLE PRECISION MMBSK0, MMBSK1
      DIMENSION T(100001), P(100001), Q(100001)
      CHARACTER NAME*10
C     *******************************************************************
C                              INPUT RUN DATA
C     *******************************************************************
C
      WRITE(6,990)
  990 FORMAT(///,'CLOSED CHAMBER WELL TEST SIMULATOR',/,80('*'))
C
      WRITE(6,995)
  995 FORMAT(///,'OUTPUT FILE NAME FOR THIS RUN ? (10 CHAR. MAX.)')
      READ(5,*)NAME
C
      WRITE(6,1000)
 1000 FORMAT(///,'INPUT TOOL PARAMETERS',/,70('*'),/)
C
      WRITE(6,1010)
 1010 FORMAT('CHAMBER DIAMETER ? (INCHES)')
      READ(5,*)D
C
      WRITE(6,1020)
 1020 FORMAT('LOWER SURGE VALVE DEPTH ? (FEET)')
      READ(5,*)DB
C
      WRITE(6,1030)
 1030 FORMAT('UPPER SURGE VALVE DEPTH ? (FEET)')
      READ(5,*)DU
C
      WRITE(6,1040)
```

```
 1040 FORMAT('MID-PERFORATION DEPTH ? (FEET)',
      READ(5,*)DF
C
      WRITE(6,1050)
 1050 FORMAT('FLUID CUSHION LENGTH ? (FEET)')
      READ(5,*)CL
C
      WRITE(6,1060)
 1060 FORMAT('INITIAL CHAMBER PRESSURE ? (PSIG)')
      READ(5,*)PCHI
C
      WRITE(6,1070)
 1070 FORMAT('CHAMBER GAS GRAVITY ? (AIR=1.0)')
      READ(5,*)GG
C
      WRITE(6,1080)
 1080 FORMAT(/,'INPUT RESERVOIR PARAMETERS',/,70('*'),/)
C
      WRITE(6,1090)
 1090 FORMAT('RESERVOIR TEMPERATURE ? (DEG F)')
      READ(5,*)TEMP
C
      WRITE(6,1095)
 1095 FORMAT('INITIAL RESERVOIR PRESSURE ? (PSIG)')
      READ(5,*)PI
C
C
      WRITE(6,1100)
 1100 FORMAT('POROSITY ? (FRACTION)')
      READ(5,*)PHI
C
      WRITE(6,1110)
 1110 FORMAT('PERMEABILITY ? (MD)')
      READ(5,*)PERM
C
      WRITE(6,1115)
 1115 FORMAT('SKIN ?')
      READ(5,*)SKN
C
      WRITE(6,1120)
 1120 FORMAT('WELL DIAMETER ? (INCHES)')
      READ(5,*)DW
C
      WRITE(6,1130)
 1130 FORMAT('FORMATION THICKNESS ? (FEET)')
      READ(5,*)H
C
      WRITE(6,1140)
 1140 FORMAT('TOTAL FORMATION COMPRESSIBILITY ? (1/PSI)')
      READ(5,*)CT
C
      WRITE(6,1150)
 1150 FORMAT('PRODUCED FLUID GRAVITY ? (API)')
      READ(5,*)API
C
      WRITE(6,1155)
 1155 FORMAT('PRODUCED FLUID VISCOSITY ? (CP)')
      READ(5,*)UF
C
      WRITE(6,1160)
 1160 FORMAT(/,'INPUT TEST TIME PARAMETERS',/,70('*'),/)
C
      WRITE(6,1170)
 1170 FORMAT('TOTAL ELAPSED TIME OF TEST ? (SECONDS)')
```

```
      READ(5,*)TT
C
      WRITE(6.1180)
 1180 FORMAT('TIME INCREMENT ? (SECONDS)')
      READ(5,*)DT
C
      N = TT/DT
C
      WRITE(6,1190)N
 1190 FORMAT('NUMBER OF TXME STEPS = ',I10,//,
     &'NUMBER  OF OUTPUT DATA POINTS ?')
      READ(5,*)NDP
C
C     ************************************************************************
C                          CORRECT UNITS TO USEABLE FORM
C     ************************************************************************
C
      D = D/12.
C
      ALC = DF - DU
C
      ALI = DF - DB + CL
C
      PCHI = PCHI + 14.696
      PI = PI + 14.696
C
      TEMP = TEMP + 460
C
      RW = DW/24
C
      SGF = 141.5/(131.5+API)
C
C     ************************************************************************
C               CALCULATE THE INITIAL CONDITIONS AND CONSTANTS
C     ************************************************************************
C
      CALL GPC(GG,TC,PC)
C
      TR = TEMP/TC
      PR = PCHI/PC
C
      CALL GZ(TR,PR,ZI)
C
      T(1) = O.b
      P(1) = PCHI + 0.4333*ALI*SGF
C
      B = 1.119*PHI*CT*(RW**2)*H
C
      DTD = 73.25E-9 *PERM*DT/(PHI*UF*CT*(RW**2))
C
      NOUT = N/NDP
C
C     ************************************************************************
C                             OUTPUT THE DATA CHECK
C     ************************************************************************
C
      OPEN(1,FILE=NAME)
C
      WRITE(1,3000)
 3000 FORMAT('CLOSED CHAMBER WELL TEST',/,80('*'),///,
     &'INPUT DATA AS FOLLOWS:',//)
C
      WRITE(1,3005)NAME
 3005 FORMAT('OUTPUT FILE NAME = ',T49,A10,/)
```

```
C
      WRITE(1,3010)D
 3010 FORMAT('CHAMBER DIAMETER = ',T47,F6.3,' (FEET)')
C
      WRITE(1,3020)ALC
 3020 FORMAT('TOTAL CHAMBER LENGTH FROM PERFORATIONS = ',
     &T45,F8.2,' (FEET)')
C
      WRITE(1,3030)ALI
 3030 FORMAT('INITIAL FLUID COLUMN LENGTH = ',T45,F8.2,' (FEET)')
C
      WRITE(1,3040)PCHI
 3040 FORMAT('INITIAL CHAMBER PRESSURE = ',T45,F8.2,' (PSIA)')
C
      WRITE(1,3045)GG
 3045 FORMAT('CHAMBER GAS GRAVITY = ',T47,F6.4,' (AIR=1.0)',/)
C
      WRITE(1,3050)PI
 3050 FORMAT('INITIAL RESERVOIR PRESSURE = ',T45,F8.2,' (PSIA)')
C
      WRITE(1,3060)TEMP
 3060 FORMAT('RESERVOIR TEMPERATURE = ',T45,F8.2,' (R)')
C
      WRITE(1,3070)SGF
 3070 FORMAT('PRODUCED FLUID SPECIFIC GRAVITY = 'T47,F6.4)
C
      WRITE(1,3075)UF
 3075 FORMAT('PRODUCED FLUID VISCOSITY = ',T47,F6.3,' (CP)')
C
      WRITE(1,3080)PHI
 3080 FORMAT('RESERVOIR POROSITY = ',T47,F6.4)
C
      WRITE(1,3090)PERM
 3090 FORMAT('RESERVOIR PERMEABILITY = ',T45,F8.2,' (MD)')
C
      WRITE(1,3095)SKN
 3095 FORMAT('SKIN = ',T45,F8.3)
C
      WRITE(1,3100)DW/12
 3100 FORMAT('WELL DIAMETER = ',T47,F6.4,' (FEET)')
C
      WRITE(1,3110)CT
 3110 FORMAT('FORMATION TOTAL COMPRESSIBILITY = ',
     &T43,E10.4,' (1/PSI)')
C
      WRITE(1,3120)H
 3120 FORMAT('FORMATION THICKNESS = ',T45,F8.2,' (FEET)'.)
C
      WRITE(1,3125)TT,DT,N,NDP
 3125 FORMAT(/,'TOTAL TEST TIME = ',T43,F10.4,' (SECONDS)',/,
     &'TIME INCREMENT = ',T43,F10.5,' (SECONDS)',/,
     &'NUMBER OF TIME STEPS = ',T43,I10,/,
     &'NUMBER OF DATA POINTS = ',T43,I10)
C
C
      WRITE(1,3130)
 3130 FORMAT(///,'PRESSURE VS TIME DATA:',/,80('*'),//,
     &5X,'TIME',T17,'Pwf',T25,'FLD PRD',T37,'X',T47,
     &'Pch',T57,'Z',T68,'IFLAG',/,T3,'(SECONDS)',
     &T15,'(PSIA)',T26,'(BBLS)',T35.'(FEET)',T45,
     &'(PSIA)',/)
C
      WRITE(1,3200)0,P(1),0,ALI,PCHI,ZI,0
C
```

```
C     ***********************************************************************
C                        CALCULATE THE PRESSURE RESPONSE
C     ***********************************************************************
C
C     ********Calculate the Cumulative Dimensionless Influx**************
C
      DO 5 M=1,N
        TD = M*DTD
        Q(M) = QD(TD,SKN,M)
    5 CONTINUE
C
      Z = ZI
C
C     ********************** Top of Time Step Loop **********************
C
      DO 10 I=1,N
C
C     ******* Superposition to Determine Cumulative Fluid Influx ********
C
        IFLAG=0
        T(I+1) = I*DT
        FP = B*(PI-P(1))*Q(I)
        IF(I.EQ.1)GO TO 25
C
        DO 20 J=2,I
          M = (I-J+1)
          FP = FP - B*(P(J)-P(J-1))*Q(M)
   20   CONTINUE
C
   25   CONTINUE
        X = ALI + (FP*5.615)/((3.1415926)*(D**2)/4)

C
C     ************** Iterative Calculation of PCH and Z *****************
C
        DO 30 L=1,500
          PCH = PCHI*(ALC-ALI)*Z/((ALC-X)*ZI)
          PR = PCH/PC
          CALL GZ(TR,PR,ZN)
          DZ=SQRT((ZN-Z)**2)
          Z=ZN
          IF(DZ.LT.0.00001)GO TO 35
   30   CONTINUE
C
        IFLAG = 1
   35   CONTINUE
C
C     *********** Bottom Hole Pressure Form Hydrostatics ***************
C
        P(I+1) = PCH + 0.4333*SGF*X
C
C     ******************** Selective Data Output ************************
C
        RI = I
        AA = RI/NOUT
        NA = AA
        BB = NA
        IF(AA.NE.BB)GO TO 10
C
        WRITE(1,3200)T(I+1),P(I+1),FP,X,PCH,Z,IFLAG
 3200   FORMAT(F10.5,F10.2,F10.4,2F10.2,F10.4,I10)
C
   10 CONTINUE
C
```

```
C
C
C
C
C
      STOP
      END
C
C
C
C
C     ************************************************************************
C
      SUBROUTINE GPC(GG,TC,PC)
C
C     ************************************************************************
C
C     THIS ROUTINE CALCULATES THE PSEUDOCRITICAL
C     TEMPERATURE AND PRESSURE FOR CONDENSATE WELL
C     FLUIDS, GIVEN THE GAS GRAVITY. THE EQUATIONS
C     USED ARE THOSE GIVEN BY STANDING.
C
C     ************************************************************************
C
      IMPLICIT REAL*8(A-H,O-Z)
C
      PC = 706. - 51.7*GG - 11.1*(GG**2)
C
      TC = 187 + 330*GG - 71.5*(GG**2)
C
      RETURN
      END
C
C
C
C
C     ************************************************************************
C
      SUBROUTINE GZ(TR,PR,Z)
C
C     ************************************************************************
C
C     THIS ROUTINE CALCULATES THE GAS DEVIATION
C     FACTOR FOP A NATURAL GAS GIVEN THE REDUCED
C     PSEUDOCRITICALS.  THE EQUATIONS USED ARE
C     CURVE FIT RELATIONS FROM THE STANDING KATZ
C     CHART GIVEN BY BRILL AND BEGGS.
C
C     ************************************************************************
C
      IMPLICIT REAL*8(A-H,O-Z)
C
      A = 1.39*SQRT(TR-0.92) - 0.36*TR - 0.101
C
      B = (0.62 - 0.23*TR)*PR
     &+ (0.066/(TR-0.86) - 0.037)*(PR**2)
     &+ (0.32/(10**(9*(TR-1))))*(PR**6)
C
      C = (0.132 - 0.32*DLOG10(TR))
C
      D =10.**(0.3106 - 0.49*TR +0.1824*(TR**2))
C
      Z = A + (1-A)/(2.718281828**B) + C*(PR**D)
C
```

```
      RETURN
      END
C
C
CCC   ****************************************************************************
C
      FUNCTION QD(TD,SKN,ISKP)
C     ****************************************************************************
C
C     THIS FUNCTION CALCULATES THE DIMENSIONLESS
C     CUMULATIVE FLUID INFLUX GIVEN DIMENSIONLESS
C     TIME AND SKIN.
C
C     ****************************************************************************
C
      IMPLICIT REAL*8(A-H,O-Z)
      DOUBLE PRECISION MMBSKØ, MMBSK1
      IF(ISKP.NE.1)GO TO 10
      N=10
      M=777
   1Ø CONTINUE
      QD = PWD(TD,N,M,SKN)
      RETURN
      END
C
C
C
C
C     ****************************************************************************
C
      FUNCTION PWDL(S,I,SKN)
C     ****************************************************************************
C
C     THIS FUNCTION IS CALLED BY THE STEFEST ROUTINE AND
C     CONTAINS THE LAPLACE SPACE SOLUTION TO THE CUMULATIVE
C     INFLUX CONSTANT PRESSURE PROBLEM.
C
C     ****************************************************************************
C
      IMPLICIT REAL*8(A-H,O-Z)
      DOUBLE PRECISION MMBSKØ, MMBSK1
      IOPT=1
      RS = S**Ø.5
      A0 = MMBSKØ(IOPT,RS,IER)
      A1 = MMBSK1(IOPT,RS,IER)
      PWDL = (RS*A1)/((S**2)*(AØ + SKN*RS*A1))
      RETURN
      END
C
C
C
C
C     ****************************************************************************
C     *                                                                          *
C     *                      THE STEHFEST ALGORITHM                              *
C     *                                                                          *
C     ****************************************************************************
C
      FUNCTION PWD(TD,N,M,SKN)
C
```

```
C     ************************************************************************
C
C     THIS FUNTION COMPUTES NUMERICALLY THE LAPLACE TRNSFORM
C     INVERSE OF F(S).  THE ROUTINE WAS WRITTEN BY DR. A. SAGEEV
C     OF STANFORD UNIVERSITY.
C
C     ************************************************************************
C
      IMPLICIT REAL*8 (A-H,O-Z)
      DIMENSION G(50),V(50),H(25)
C
C*****NOW IF THE ARRAY V(I) WAS COMPUTED BEFORE THE PROGRAM
C     GOES DIRECTLY TO THE END Of THE SUBROUTINE TO CALCULATE
C     F(S).
C
      IF (N.EQ.M) GO TO 17
      M=N
      DLOGTW=0.693147180559
      NH=N/2
C
C*****THE FACTORIALS OF 1 TO N ARE CALCULATED INTO ARRAY G.
C
      G(1)=1
      DO 1 I-2,N
      G(I)=G(I-1)*I
1     CONTINUE
C
C*****TERMS WITH K ONLY ARE CALCULATED INTO ARRAY H.
C
      H(1)=2./G(NH-1)
      DO 6 I-2,NH
      FI=I
      IF(I-NH) 4,5,6
4     H(I)=FI**NH*G(2*I)/(G(NH-I)*G(I)*G(I-1))
      GO TO 6
5     H(I)=FI**NH*G(2*I)/(G(I)*G(I-1))
6     CONT1NUE
C
C*****THE TERMS (-1)**NH+1 ARE CALCULATED.
C     FIRST THE TERM FOR I=1
C
      SN=2*(NH-NH/2*2)-1
C
C*****THE REST OF THE SN'S ARE CALCULATED IN THE MAIN ROUTINE.
C
C
C
C*****THE ARRAY V(I) IS CALCULATED.
C
      DO 7 I=1,N
C
C*****FIRST SET V(I)=0
C
      V(I)=0.
C
C*****THE LIMITS FOR K ARE ESTABLISHED.
C     THE LOWER LIMIT IS K1=INTEG((I+1/2))
C
      K1=(I+1)/2
C
C*****THE UPPER LIMIT IS K2=MIN(I,N/2)
C
      K2=I
      IF (K2-NH) 8,8,9
```

```
9     K2=NH
C
C*****THE SUMMATION TERM IN V(I) IS CALCULATED.
C
8     DO 10 K=K1,K2
      IF (2*K-I) 12,13,12
12    IF (I-K) 11,14,11
11    V(I)=V(I)+H(K)/(G(I-K)*G(2*K-I))
      GO TO 10
13    V(I)=V(I)+H(K)/G(I-K)
      GO TO 10
14    V(I)=V(I)+H(K)/G(2*K-I)
10    CONTINUE
C
C*****THE V(I) ARRAY IS FINALLY CALCULATED BY WEIGHTING
C     ACCORDING TO SN.
C
      V(I)=SN*V(I)
C
C*****THE TERM SN CHANGES ITS SIGN EACH ITERATION.
C
      SN=-SN
7     CONTINUE
C
C*****THE NUMERICAL APPROXIMATION IS CALCULATED.
C
17    PWD=Ø.
      A=DLOGTW/TD
      DO 15 I=1,N
      ARG=A*I
      PWD=PWD+V(I)*PWDL(ARG,I,SKN)
15    CONTINUE
      PWD=PWD*A
18    RETURN
      END
```

APPENDIX B

BASECASE NUMERICAL VALUES

CLOSED CHAMBER WELL TEST

INPUT DATA AS FOLLOWS:

OUTPUT FILE NAME =	basecase	
CHAMBER DIAMETER =	0.283	(FEET)
TOTAL CHAMBER LENGTH FROM PERFORATIONS =	1000.00	(FEET)
INITIAL FLUSD COLUMN LENGTH =	100.00	(FEET)
INITIAL CHAMBER PRESSURE =	44.70	(PSIA)
CHAMBER GAS GRAVITY =	0.6500	(AIR=1.0)
INITIAL RESERVOIR PRESSURE =	5014.70	(PSIA)
CHAMBER GAS TEMPERATURE =	635.00	(R)
PRODUCED FLUID SPECIFIC GRAVITY =	0.9042	
PRODUCED FLUID VISCOSITY =	1.250	(CP)
RESERVOIR POROSITY =	0.2700	
RESERVOIR PERMEABILITY =	100.00	(MD)
SKIN =	0.	
WELL DIAMETER =	0.8333	(FEET)
FORMATION TOTAL COMPRESSIBILITY =	0.1000e-04	(1/PSI)
FORMATION THICKNESS =	25.06	(FEET)
TOTAL TEST TIME =	100.0000	(SECONDS)
TIME IVCREMENT =	0.01086	(SECONDS)
NUMBER OF TIME STEPS =	10000	
NUMBER OF DATA POINTS =	100	

PRESSURE VS TIME DATA:

TIME (SECONDS)	Pwf (PSIA)	FLD PRD (BBLS)	X (FEET)	Pch (PSIA)	Z	IFLAG
0.	83.87	0.	100.80	44.70	0.9964	0
1.00300	127.11	0.5595	196.68	50.05	0.9959	0
2.00300	156.78	0.9335	261.29	54.41	0.9956	0
3.00800	184.05	1.2684	319.15	59.01	0.9952	0
4.00300	210.25	1.5808	373.12	64.07	0.9948	0
5.00800	236.02	1.8776	424.41	69.75	0.9943	0
6.00300	261.79	2.1625	473.64	76.23	0.9938	0
7.00300	287.94	2.4378	521.19	83.75	0.9932	0
8.00300	314.87	2.7048	567.33	92.61	0.9925	0
9.00200	343.09	2.9646	612.22	103.24	0.9916	0
10.00300	373.24	3.2179	655.98	116.25	0.9906	0
11.00300	406.27	3.4650	698.68	132.55	0.9892	0
12.00800	443.61	3.7063	740.36	153.56	0.9875	0
13.00300	487.62	3.9416	781.02	181.64	0.9852	0
14.00800	542.43	4.1705	820.57	220.96	0.9820	0
15.00300	615.96	4.3921	858.85	279.49	0.9771	0
16.00300	725.16	4.6041	895.48	374.34	0.9692	0
17.00300	911.59	4.8015	929.59	547.48	0.9546	0
18.00800	1287.68	4.9728	959.05	911.95	0.9249	0
19.00300	2055.68	5.0866	978.85	1672.19	0.8760	0
2J3.00.800	2879.14	5.1289	986.16	2492.79	0.8545	0
21.00800	3312.87	5.1405	988.17	2925.73	0.8575	0
22.00300	3557.09	5.1454	989.01	3169.63	0.8632	0
23.00300	3722.23	5.1482	989.49	3334.58	0,8685	0
24.00300	3845.56	5.1508	989.80	3457.79	0.8732	0

25.00000	3343.06	5.1514	990.04	3555.20	0.0774	0
26.00300	4023.00	5.1524	990.22	3635.06	0.8810	0
27.00300	4090.22	5.1532	990.36	3702.23	0.8843	0
28.00 a00	4147.84	5.1539	990.47	3759.80	0.8872	0
29.00300	4197.95	5.1544	990.57	3809.88	0.8898	0
38.00300	4242.06	5.1549	990.65	3853.95	0.8921	0
31.00800	4281.25	5.1553	990.73	3893.11	0.8943	0
32.00300	4316.37	5.1557	990.79	3928.21	0.8963	0
33.00300	4348.05	5.1568	990.84	3959.87	0.8981	0
34.00800	4376.81	5.1563	990.89	3988.60	0.8997	0
35.00300	4403.05	5.1566	990.94	4014.83	0.9013	0
36.00800	4427.10	5.1568	990.98	4038.87	0.9027	0
37.00300	4449.25	5.1570	991.01	4061.00	0.9040	0
38.00 a00	4469.72	5.1572	991.05	4081.45	0.9052	0
39.00300	4488.69	5.1574	991.08	4100.42	0.9064	0
48.00 a00	4506.34	5.1575	991.10	4118.06	0.9075	0
41.00300	4522.80	5.1577	991.13	4134.51	0.9085	0
42.00300	4538.20	5.1578	991.15	4149.90	0.9095	0
43.00300	4552.63	5.1579	991.17	4164.32	0.9104	0
44.00300	4566.19	5.1581	991.19	4177.87	0.9112	0
45.00800	4578.95	5.1582	991.21	4190.62	0.9120	0
46.00800	4590.99	5.1583	991.23	4202.65	0.9128	0
47.00300	4602.36	5.1584	991.25	4214.02	0.9135	0
48.00300	4613.13	5.1585	991.26	4224.78	0.9142	0
49.00300	4623.33	5.1585	991.28	4234.98	0.9149	0
511.00300	4633.02	5.1586	991.29	4244.66	0.9155	0
51.00300	4642.23	5.1587	991.31	4253.87	0.9161	0
52.00200	4651.00	5.1588	991.32	4262.63	0.9167	0
53.00800	4659.36	5.1588	991.33	4270.99	0.9172	0
54.00300	4667.34	5.1589	991.34	4278.96	0.9178	0
55.00200	4674.96	5.1598	991.35	4286.58	0.9183	0
56.00300	4682.25	5.1598	991.36	4293.86	0.9187	0
57.00300	4689.22	5.1591	991.37	4300.83	0.9192	0
58.00300	4695.91	5.1591	991.38	4307.52	0.9196	0
59.00.800	4702.32	5.1592	991.39	4313.93	0.9201	0
68.00 a00	4708.48	5.1592	991.40	4320.08	0.9205	0
61.00100	4714.40	5.1593	991.41	4325.99	0.9209	0
62.00300	4720.08	5.1593	991.41	4331.68	0.9213	0
63.00300	4725.56	5.1594	991.42	4337.15	0.9216	0
64.00300	4730.83	5.1594	991.43	4342.42	0.9220	0
65.00300	4735.91	5.1594	991.43	4347.50	0.9223	0
66.00300	4740.82	5.1595	991.44	4352.48	0.9226	0
67.00300	4745.55	5.1595	991.45	4357.13	0.9230	0
68.00200	4750.11	5.1596	991.45	4361.69	0.9233	0
69.00300	4754.53	5.1596	991.46	4366.10	0.9236	0
70.00800	4758.80	5.1596	991.47	4370.37	0.9239	0
71.00300	4762.93	5.1597	991.47	4374.50	0.9241	0
72.00300	4766.92	5.1597	991.48	4378.49	0.9244	0
73.00300	4770.79	5.1597	991.48	4382.36	0.9247	0
74.00300	4774.54	5.1597	991.49	4386.11	0.9249	0
75.00300	4778.18	5.1596	991.49	4389.74	0.9252	0
76.00300	4781.71	5.1598	991.50	4393.27	0.9254	0
77.00300	4785.13	5.1598	991.50	4396.69	0.9257	0
78.00300	4788.45	5.1598	991.50	4400.01	0.9259	0
79.00300	4791.68	5.1599	991.51	4403.24	0.9261	0
811.00 a00	4794.81	5.1599	991.51	4406.37	0.9263	0
81.00300	4797.86	5.1599	991.52	4409.42	0.9265	0
82.00300	4800.83	5.1599	991.52	4412.38	0.9267	0
83.00100	4803.71	5.1608	991.52	4415.26	0.9269	0
84.00300	4806.52	5.1608	991.53	4418.07	0.9271	0
85.00300	4809.25	5.1608	991.53	4420.80	0.9273	0
86.00300	4811.91	5.1608	991.53	4423.46	0.9275	0
87.00300	4814.51	5.1600	991.54	4426.05	0.9277	0
88.00300	4817.03	5.1601	991.54	4428.58	0,9278	0

89.00600	4819.50	5.1601	991.54	4431.04	0.9280	0
90.00800	4821.90	5.1601	991.55	4433.44	0.9282	0
91.00808	4824.24	5.1601	991.55	4435.78	0.9283	0
92.00300	4826.53	5.1601	991.55	4438.07	0.9285	0
93.00108	4828.76	5.1601	991.56	4440.38	0.9287	0
94.00800	4830.94	5.1602	991.56	4442.48	0.9288	0
95.00300	4833.07	5.1602	991.56	4444.61	0.9289	0
96.00300	4835.15	5.168'2	991.56	4446.69	0.9291	0
97.00300	4837.19	5.1602	991.57	4448.72	0.9292	0
98.00800	4839.18	5.1602	991.57	4450.71	0.9294	0
99.00108	4841.12	5.160'2	991.57	4452.65	0.9295	0
100.00300	4843.02	5.1603	991.57	4454.55	0.9296	0